FEBRUARY 1990

ENVIRONMENTAL PROGRESS

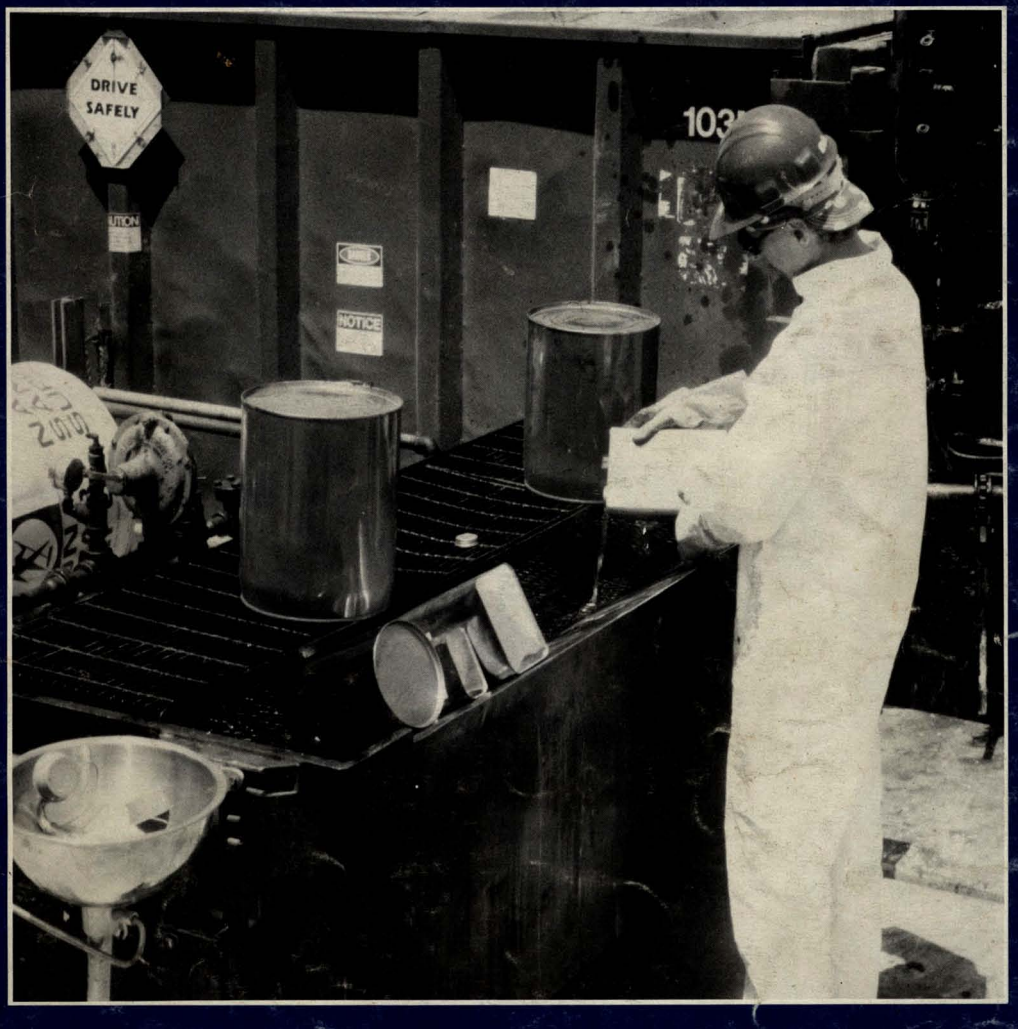

Pouring oil for recycling (see article on page 30).
Photo courtesy of M.J. Boortz, Chevron Research Corp., Richmond, CA.

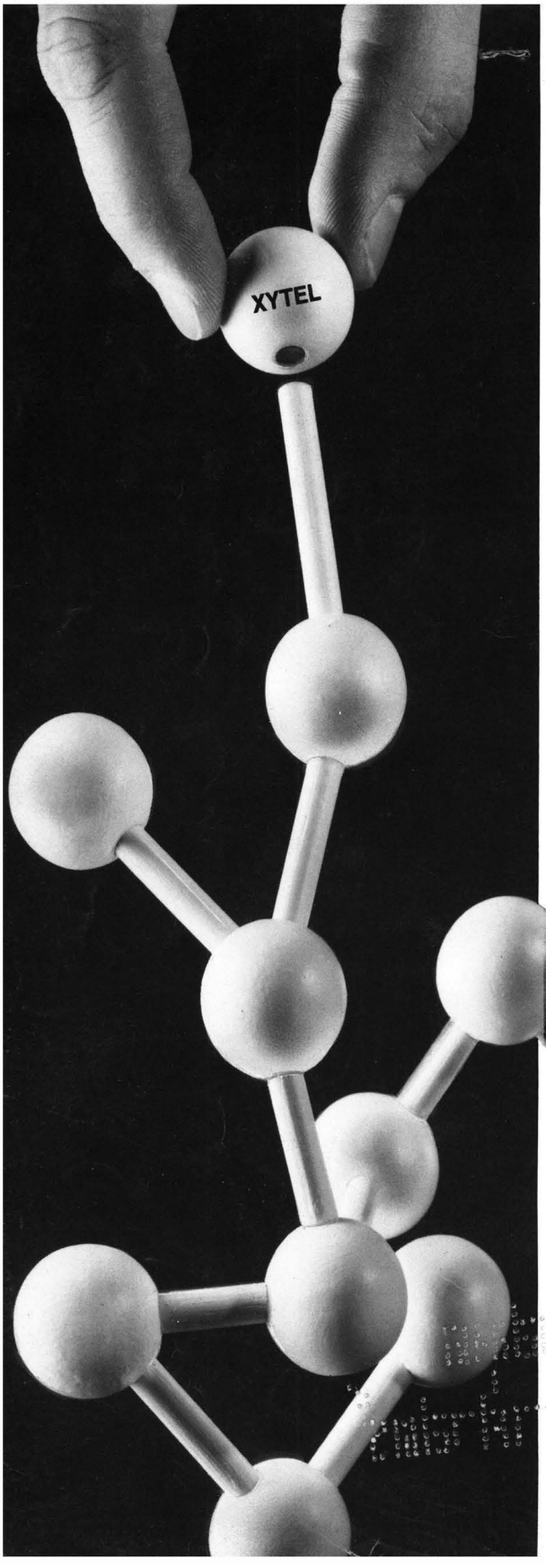

Get More Out Of Your Pilot Plant By Putting Xytel In.

More than 120 customers around the world have used Xytel's pilot plant expertise to gain additional dividends from their research investments.

During the past decade, Xytel has completed 350 pilot plants, many in the realm of threshold technology. Our experience inventory includes 137 different products for the petroleum, chemical, food, and pharmaceutical industries.

We have worked with all conventional processes, as well as exotic new technologies such as liquid-liquid extraction, adsorption-desorption, supercritical extraction, and membrane separation.

Our modular design and construction practices give you lower costs and shorter delivery times. Sophisticated Xytel computer control systems automate your pilot plant for totally unattended operation, and enable you to collect large quantities of useful, accurate data.

Whatever your product or process of interest, Xytel has the technology to translate your requirements into a working pilot plant. Call or write for our brochure.

The pilot plant company . . . putting technology to the test

xytel

Xytel Corporation
801 Business Center Drive
Mt. Prospect, Illinois 60056, USA
(708) 299-9200, Telex 270672

Xytel Europe b.v.
Wegtersweg 30,
7556 BR Hengelo (O)
The Netherlands
31.74.913576, Telex 44882

ENVIRONMENTAL PROGRESS

Environmental Progress is a publication of the American Institute of Chemical Engineers. It will deal with multi-faceted aspects of the pollution problem. It will provide thorough coverage of abatement, control, and containment of effluents and emissions within compliance standards. Papers will cover all aspects including water, air, liquid and solid wastes. Progress and technological advances vital to the environmental engineer will be reported.

Published four times a year (February, May, August and November) by the American Institute of Chemical Engineers, 345 East 47 St., New York, N.Y., 10017. (ISSN 0278-4491). Manuscripts should be submitted to the Manuscript Center. American Institute of Chemical Engineers, 345 East 47 St., New York, N.Y. 10017. Statements and opinions in *Environmental Progress* are those of the contributors, and the American Institute of Chemical Engineers assumes no responsibility for them. Subscription price per year: $53. AIChE Environmental Division Members: $19 included in dues. Outside the U.S. please add $6 per subscription for postage and handling. Single copies $18. Outside the U.S. please add $2 for postage and handling. Payment must be made in U.S. dollars. Second-class postage paid at New York, N.Y. and additional mailing offices.

Volume 9 Number 1

Contents

Environmental Progress fee code: 0278-4491/90 $2.00. Postmaster: Please send change of addresses to *Environmental Progress*, AIChE, 345 East 47 Street, New York, N.Y. 10017.

Let's *Really* Support Recycling

Gary F. Bennett

Disposal of hazardous materials, especially to land, is becoming increasingly difficult. However, in spite of this trend, the options for handling metal sludges are increasing. New pyrometallurgical and hydrometallurgical processes are being developed to economically compete with chemical solidification and land disposal of hazardous metal-bearing sludges.

Currently, Best Demonstrated Available Technology (BDAT) for certain U.S. EPA-designated F, K and D series wastes is chemical stabilization, which can be accomplished by adding cement kiln dust to the sludges. Many factors influenced the U.S. EPA to establish these BDAT regulations. However, it does not make political or economic sense to increase the volume and weight of metal sludges using chemical stabilization. Also, the country's limited and decreasing hazardous waste landfill capacity should be utilized for wastes that cannot be economically reclaimed.

Both domestic and foreign smelters are being utilized to reclaim metals. However, costs are sometimes excessive and the generator does not receive value for metals recovered. Restrictions are being placed on these smelters in terms of trace metal contaminants.

Recent advances in pyrometallurgical technology have been made. Using patented processes, purified metal alloys can be produced economically by even small generators (above 50 tons/yr). Slag depleted of valuable metals is a by-product of the treatment processes, and it has multiple uses in the construction trades.

Generators should contact their TSD facility and encourage them to consider installing a recycle process for metal wastes. A recycle process will lower processing costs through sales of metal alloys and slags. However, perhaps the most significant factor to the generator is the elimination of future RCRA liability.

Generators can install a pyrometallurgical process in their own plant depending upon waste characteristics and waste loads. Due to the high capital cost for hydrometallurgical processes, these processes may only be economical at large central reclaim facilities. The downside of central reclaim facilities is that generators still have the transportation costs and the generator is not rewarded for metals reclaimed.

The U.S. EPA is committed to recycling in accordance with their Pollution Prevention Policy published in the Federal Register dated Jan. 26, 1989 and with the mandates of RCRA (*Resource Conservation and Recovery Act*). Both Federal and State regulatory agencies must become pro-active to reduce regulatory red tape for legitimate recycling processes. But being pro-active does not mean promulgation of further stultifying regulations such as case by case determination of the process regulatory status. This situation significantly retarded the use of transportable incinerators. A blanket approval of the technology is needed. "Case by case" decisions on legitimate recycling technologies simply present another moving target for industry.

Recycle processes are available today. Certain recycle processes are less expensive than landfilling. Insist that your feedstock (formally considered hazardous wastes) be recycled either in the producing plant or at the receiving TDS facility.

Gary F. Bennett, PhD, P. Eng., DEE, is editor of Environmental Progress. *He is also editor of the* Journal of Hazardous Materials *and is Professor of Chemical and Biochemical Engineering at the University of Toledo.*

Washington Environmental Newsletter

Department of Defense Takes on "Environmental Battle"

Defense Secretary Dick Cheney has committed DOD to lead the administration's battle against pollutants, by ensuring all facilities, including military bases meet environmental standards.

"I want every command to be an environmental standard by which federal agencies are judged," Cheney said.

Given the widespread view that DOD is not only the most polluting but also the most environmentally insensitive of any federal agency, Cheney's initiative reflects a personal commitment to clean up more than just the Pentagon's image.

By mid-February, DOD Deputy Secretary Donald Atwood is expected to issue a detailed guidance to Cheney's memo which orders service secretaries to integrate and budget environmental considerations into their activities and operations. The initiative has already been backed with money—an additional $101 million this year for the Pentagon's estimated $1.2 billion environmental funds and another increase slated for 1991. The R&D portion is now at $27 million.

Deputy Secretary of Defense (Environment) is William Parker III who is calling for open communications in the Pentagon and the recognition of a "new ethic." The key words for environmental leadership are compliance, adequate budget and people—getting them trained. Parker also believes that under current legislation, DOD will have time to implement cost-effective programs. As an engineer, Parker is concerned about the "emotionalism" environmental issues generate. DOD will turn to outside contractors for help in setting and meeting priority activities.

Bill Calls for Report on Environment

DOD's actions dovetail with a bill introduced by Sen. John Warner (R., Va.) that would require the president to make an annual report to Congress on "National Environmental Strategy," similar to the "National Security Strategy" report first required by Warner-introduced legislation in 1987. The bill is designed to put environmental concerns on a par with national security as a U.S. strategic interest. A member of the Senate's Environment and Public Works Committee said that both Congress and the private sector need an annual update to meet the environmental challenges of the future.

Under the terms of the proposal, the President would provide a comprehensive discussion of all federal policy, plans and programs as well as an equally comprehensive description of national and global environmental problems. The report should include the integration of environmental strategy with national strategies for science and technology, energy, education and technology transfer.

CWRT Progress

As the new AIChE Center for Waste Reduction Technologies gets organized and into operation, this column will report on CWRT's progress and its interactions with government efforts in pollution prevention.

This material was prepared by AIChE's Washington Representative, Siegel • Houston & Associates, Inc. Suite 333,1707 L Street, N.W., Washington, D.C. 20036. Tel. (202) 223-0650

Environmental Shorts

Coalition Superfund Names New Chairman

Lee M. Thomas, Administrator of the Environmental Protection Agency (EPA) from 1985 to 1989, has recently been appointed chairman of the Coalition on Superfund.

Thomas is the chief executive officer of Law Environmental, Inc., a national environmental engineering and policy firm. Law Environmental specializes in solving hazardous waste problems, specifically those found at Superfund sites.

"I look upon this position with the Coalition as an exciting opportunity to reinforce the Superfund goals for hazardous site cleanup," Thomas said. "The Coalition intends to continue to rigorously and impartially examine the current Superfund program."

The Coalition on Superfund was founded in 1987 under the leadership of William D. Ruckelshaus and Charles E. Walker, to encourage and conduct objective research on the nature and implementation of the Superfund law. The Coalition is comprised of major manufacturing, chemical processing, insurance and waste management companies that support the goals of the Superfund program. In 1989, it funded and released the results of four interrelated research projects that focused on the law and its implementation.

Ruckelshaus, who served as the first chairman of the Coalition, is currently chief executive officer of Browning-Ferris Industries, Inc., a member company of the Coalition. Under Thomas' direction, the management of Coalition activities will be shared by Charles E. Walker Associates and the Environmental Policy Center, a Washington, D.C. office of Law Environmental, Inc.

"Lee Thomas has unequaled knowledge of the Superfund program and the issues surrounding it, a result of his experience in both the public and private sectors. I think he is exactly the right person to head the Coalition's effort, and believe that he will be an important voice in the evolving environmental public policy discussions," William D. Ruckelshaus said.

Thomas has served as a presidential appointee in two key environmental policy positions. Prior to being EPA Administrator, he headed the Agency's hazardous and solid waste program, which includes Superfund. He managed the program's day-to-day operations and established policy direction in its early days. From 1984 to 1986, he was the principal architect of Administration Superfund policy during the reauthorization process.

"Lee Thomas brings extensive, hands-on environmental policy experience to the Coalition," Ruckelshaus said, "He has detailed knowledge of the intricacies of the Superfund program, sought to integrate this law with other laws under EPA's jurisdiction, and has worked closely with environmental groups, state officials and private companies on major Superfund issues."

The Coalition-sponsored research projects, and other projects, including recently released EPA and congressional oversight studies, have identified obstacles to effective implementation of Superfund.

"As the Coalition moves forward, we will continue to both encourage and conduct objective research on the current Superfund program," Thomas said. "In addition, we will focus research on methods to achieve the goals of Superfund."

Thomas also noted that he has spent many years dealing with Superfund issues. "I want the law to work," he said. "If research indicates that there are policy alternatives that could improve Superfund, I hope we can get other groups to give them serious consideration and a fair hearing."

The Coalition is currently reviewing possible research projects.

MIT Group to Hold Conference on Incineration

The MIT Hazardous Substances Management Program, an environmental research and action program, will hold a one-day conference, "Incinerator Monitoring: Techniques for Assuring Performance and Building Public Trust," beginning at 8:00 a.m. on Wednesday, June 6, 1990, at Kresge Little Theater at the MIT Campus in Cambridge, Massachusetts. The conference is sponsored by the U.S. EPA as part of a national effort to encourage sound waste management practices.

The purpose of the conference is two-fold. First, speakers will define the "state of the art" of incinerator monitoring. They will present papers on federal and state monitoring requirements and incinerator operators' experience complying with these requirements. Second, speakers will consider how current practice could be improved to ensure regulatory compliance and to build public confidence in incineration. Emerging monitoring techniques will be described, such as continuous emissions monitoring.

Conference organizers have invited speakers from government, industry, and environmental groups to ensure that a broad range of perspectives is represented.

The conference is part of the activities of the EPA Northeast Hazardous Substances Research Center, a consortium of the New Jersey Institute of Technology, MIT, and Tufts University.

Cost of registration is $100 for representatives for industry and $35 for representatives from government and private non-profit organizations. This cost includes a copy of conference proceedings. Scholarships are available.

For more information, call Jennifer Nash at the Hazardous Substances Management Program at (617) 253-0902.

Academy of Environmental Engineers Names Officers

David M. Benforado, P.E., DEE was installed as President and Joseph F. Lagnese, Jr., P.E., DEE was installed as President-Elect for 1989-90 at the Annual Meeting of the American Academy of Environmental Engineers held November 4 to November 5, 1989 in Boston.

David M. Benforado is a Senior Environmental Specialist in the Environmental Engineering and Pollution Control Division at 3M where he has been employed since 1969. He represents 3M on key business associations such as The Business Roundtable, and Environment Task Force Staff Services Committee. Mr. Benforado is a past president of the Air and Waste Management Association. A chemical engineering graduate from Columbia University, he is active in AIChE and the National Governor's Association.

Joseph F. Lagnese, Jr. is a consultant and Adjunct Professor serving the University of North Carolina, Carnegie-Mellon University and the University of Pittsburgh. Previously, he founded and developed Duncan, Lagnese and Associates of Pittsburgh, an environmental consulting firm. He was President of the Water Pollution Control Federation in 1972.

Also elected for a one-year term as Vice President was Jerome B. Gilbert, P.E., DEE and as Treasurer, Charles A. Willis, P.E., DEE. Mr. Gilbert is the General Manager of East Bay Municipal Utility District headquartered in Oakland, California. Mr. Willis is President of Willis Engineers of Charlotte, North Carolina.

The American Academy of Environmental Engineers is a specialty certification board for environmental engineers that is dedicated to improving the quality of environmental engineering practice. Headquartered in Annapolis, MD, it certifies environmental engineers of proven quality from around the world in one or more of seven specialties of environmental engineering practice. The Academy's program, unusual in the engineering profession, has been in existence for over 30 years and requires professional engineering registration as a prerequisite for certification along with at least eight years of experience and a bachelor's degree in engineering.

Book Reviews

Dust Control Handbook, by Vinit Mody and Raj Jakhete, Noyes Data Corporation, Park Ridge, NJ, 1988, 203 pages, U.S. List Price: $39.00.

Dust control in the mining and minerals processing industry is of importance in reducing worker exposure and assuring compliance with environmental standards. This book addresses dust control in the above industry as it relates to occupational health and safety.

The subject document is a reprint of a technical report prepared under contract to the U.S. Bureau of Mines. As such, there is no new information contained in the book which consists simply of a compilation of data from standard reference texts and published literature. It does, however, bring together a good deal of information for use by persons unfamiliar with the subject area. In such cases, the book can be useful as a starting place for additional investigation. The following summarizes the nine chapters of the book.

In the subject document, Chapter 1 provides a general background on the characteristics of respirable dust, the associated health hazards, and general dust control methods. In Chapters 2 and 3, control of dust emissions through the use of preventive measures, equipment design, wet suppression, and ventilated capture systems, are described. This information includes general guidelines as well as illustrations of typical system applications.

Next, Chapter 4 outlines the various types of wet and dry dust collectors which can be used in the above systems along with guidance on the selection of ancillary equipment such as fans and motors. Removal of dust from the collector and subsequent disposal are also briefly discussed. Specific illustrations of dust capture and collection systems for representative industrial operations are provided in Chapter 5.

Of interest in Chapter 6 is the estimation of costs associated with dust capture and collection systems. The various cost elements associated with the major operating equipment are provided. Chapter 7 provides guidance on various administrative measures (e.g., housekeeping) which can be used to assist in proper dust control on a plant-wide basis.

With respect to testing, Chapters 8 and 9 provide information on the determination of personnel exposure and performance of dust control systems. This information includes the type of test equipment to be used and samples to be collected. Finally, the book concludes with a bibliography of references which can be consulted for additional, more detailed information on the various topics associated with actual system design.

John S. Kinsey, Ph.D.
Principal Environmental Scientist
Midwest Research Institute
425 Volker Boulevard
Kansas City, MO 64110

Flocculation, Sedimentation & Consolidation, by Brij M. Moudgil and P. Somasundaran, American Institute of Chemical Engineers (AIChE), New York, NY, 1986, 633 pages, U.S. List Price: $70.

Flocculation, coagulation, sedimentation, and consolidation phenomena are extremely important for the fields of chemical, mineral, environmental, and coastal engineering. They are likewise important for applications such as wastewater treatment, coal liquefaction, tar sand processing, and electrophoresis. This textbook presents state-of-the-art reviews and recent advances in the areas of flocculation, settling, and consolidation of fine suspensions in aqueous and nonaqueous media. The book is based upon research papers which were presented at the Engineering Foundation Conference, held at Sea Island, Georgia, on January 27-February 1, 1985. All the papers included in this volume were accepted for inclusion, based upon a formal peer review process.

The book, containing 42 chapters, is divided into five major sections. The sections include plenary lectures, flocculation, sedimentation, consolidation, and research needs. The individual chapters are written by leading authorities in the field. The book describes such areas as the flocculating action of polymeric flocculants, aggregate breakage, floc characteristics, charge stabilization, equipment design, sedimentation theory, thickening and dewatering, and effects of chemical additives. Results are presented from many research studies, as well as from pilot plant and field studies. The references are relevant and current (through the time of the publication).

This book represents a welcome addition to the field of flocculation and coalescence phenomena. The book serves as a useful reference for those professionals involved in water and wastewater treatment, environmental engineers, coastal engineers, and those people concerned with the quality of their water supplies.

Robert W. Peters, Ph.D., P.E.
Energy Systems Division
Argonne National Laboratory
9700 South Cass Avenue
Argonne, IL 60439

Red Book on Transportation of Hazardous Materials, 2nd Edition, by Lawrence W. Bierlein, Van Nostrand Reinhold Company, New York, NY, 1988, 1203 pages, U.S. List Price: $104.95.

Due to new developments and regulations governing the transportation of hazardous materials, the U.S. Department of Transportation (DOT) has revised many of the regulations. This second edition of the Red Book on Transportation of Hazardous Materials represents an update of the material contained in the first edition, published in 1976. These books are intended to serve as

guides for the transportation of hazardous materials, including hazardous substances and hazardous wastes designated by EPA.

Federal safety regulations are written with the legal enforcement of the regulations in mind, rather than with the user or subject in mind. This book is not intended as a substitute for the regulations, but rather is used in conjunction with the regulations; frequent reference back and forth between the Red Book and the applicable EPA and DOT regulations is intended. The book contains 32 chapters and 4 appendices. Topics covered include hazardous materials transportation regulations; DOT–regulated hazardous materials; determination of proper DOT shipping name, hazardous materials packaging, marking, and labeling; shipping requirements, placarding of vehicles and containers; shipping requirements; inspection and enforcement; liability associated with shipment and transport; and various regulations associated with hazardous materials transportation. The book has as its goal to simplify the process of compliance with the regulations.

The book provides important information for those companies and personnel responsible for the shipment and transport of hazardous materials.

Robert W. Peters, Ph.D., P.E.
Energy & Environmental Systems Division
Argonne National Laboratory
9700 South Cass Avenue
Argonne, IL 60439

TESTAir: A Program for Air Pollution Reference Testing Methods

Ashok Kumar and Sushant Agarwal
Department of Civil Engineering, The University of Toledo, Toledo, OH 43606

Environmental Engineers involved in air pollution testing and monitoring are required to perform various calculations using field observations. Some of these calculations are easy while others are lengthy and tedious. Help is now available from Dawn Graphics, 19 Edge Hill Road, Winchester, MA 01890 (Telephone No. (617) 721-0456). They have developed a spreadsheet "template" program using Lotus 1-2-3. The package costs $330 and a demonstration diskette is available for $20.

The program can be run on an IBM compatible PC/AT/XT/PC Jr using a Lotus (or look alike) spreadsheet. The procedure used in the program is in accordance with the calculations given in the Title 40 of the Code of Federal Regulations (United States of America), Part 60, Appendix A (40 CFR 60, Appendix A).

The TESTAir diskettes contain 76 files, consisting of various air pollution sampling spreadsheets for reference methods 1 to 27. The following areas are covered in these spreadsheets:

1. Flow measurement techniques
2. Particulate sampling and analysis
3. Gas sampling, eg. SO_2, NO_2, H_2S, etc.
4. Organic emissions and leaks
5. Calibration of instruments

Data can be entered and stored for future reference, thus simplifying the procedure of creating and filling out forms needed to record data. The files are labeled systematically according to the method and units of measurement used.

The program comes with a manual [*1*], which is divided into five sections. The introduction section describes the procedure for entering data and loading the program files. The subsequent sections describe the printing, saving and other operating procedures. A hardcopy of all the 76 files, which facilitates data entry, is given in the last section of the manual. The manual is easy to understand.

In order to test the package, six spreadsheets were tried using actual field data. The results obtained were satisfactory in most cases. No difficulty was encountered using the spreadsheets or printing the results from diskettes. Use of the menus was straightforward and travel across the data form posed no problem. It is also possible to customize one's own forms.

Minor problems were encountered during the testing of the package. For example, the final result form is not displayed directly after data entry, but has to be searched for in the subsequent columns and rows. If the data entered do not satisfy the assumptions used in the equations, results may not be satisfactory. In order to use the program effectively, the user should be quite familiar with the various terms encountered in sampling calculations [*2, 3*].

The package is a useful tool for environmental scientists using the United States Environmental Protection Agency (USEPA) methods for air sampling activities at their plants. The use of the program will save time and will reduce calculation errors in field data. Moreover, it will reduce training time for new field personnel involved in sampling.

LITERATURE CITED

1. TESTAir User's Manual, Dawn Graphics Company, 1988.
2. APTI Course 435, Atmospheric Sampling Student Manual, USEPA 450/2-80-004, June 1983.
3. Paul N. Cheremisinoff and Angelo C. Monesi, *Air Pollution Sampling & Analysis*, Ann Arbor Science, Ann Arbor, MI, 1981.

[NOTE: People interested in submitting software for review should contact Dr. Kumar.]

EDITOR'S NOTE: The November, 1989 column featured waste reduction achieved by a large chemical company. DuPont's Sabine River Works billion pound/year ethylene plant eliminated 10 million pounds/year of waste oil with a cost savings of $2 million per year. The column below describes how a smaller company, Sterling Chemicals, Inc., initiated a waste minimization program, highlights the requirements and methodology of waste minimization, and indicates how the program was put in place.

R. Lee Byers
editor of
Pollution Prevention/Waste Minimization section

Development of a Waste Minimization Program at Sterling Chemicals in Texas City, Texas

Stephen W. Moncla
Sterling Chemicals, P.O. Box 1311, Texas City, Texas 77592-1311
Thomas P. Nelson
Radian Corporation, P.O. Box 201088, Austin, Texas 78720-1088

More than two years ago, Sterling Chemicals, Inc. (Sterling) in Texas City, Texas identified the need and began planning for an effective waste minimization program. This program was to be in effect by the end of calendar year 1990 and would become part of the company's Environmental Long Range Plan. Sterling needed an overall waste management program that would focus on waste reduction, recycling, and recovery to respond to regulatory requirements and to reduce the costs associated with managing wastes generated at its Texas City petrochemical plant.

The Texas City plant is the only site owned and operated by Sterling. Located on a 250-acre site bordering Galveston Bay, approximately 45 miles southeast of Houston, the facility employs about 950 people and produces acrylonitrile, styrene, ethylbenzene, acetic acid, plastizers, tertiary butyl amine, sodium cyanide, and lactic acid. To support the manufacturing operations, the site has utility boilers, raw water treatment, wastewater treatment, laboratories and maintenance functions. Up till now, Sterling has managed its wastes using both on-site and off-site treatment and disposal methods.

Sterling's goal was to develop a waste minimization program that would apply to all plant manufacturing and service groups and that would address the air, waste, and solid (multi-media) waste categories. Sterling first assembled an in-house team to begin developing the methodologies for waste minimization. At different times in the process, members of the team represented manufacturing, technical services, engineering, accounting, environmental affairs, and quality facilitation. The Environmental Affairs Department, having direct responsibility for meeting federal and state permitting and reporting requirements, developed the agenda and plan to implement the waste minimization program. The initial outline of the agenda covered project identification, ranking, approval, execution, feasibility, tracking, and reporting.

At first there was a general resistance to adding another "Environmental Affairs" program. The Environmental Affairs Department pointed out the benefits of a waste minimization program: 1) Sterling's potential for saving two million dollars a year in disposal costs, 2) an improved ability to comply with state and federal regulations, and 3) the ability to maintain excellent relations with Sterling's Texas City Neighbors. Concern was also voiced by some plant groups that already had informal waste reduction programs in place. These groups were afraid that a formal program would force them into duplicating their efforts. They were shown that by using the ranking and tracking features of a formal waste minimization methodology that each group could elect to include existing projects into any part of the new program without significantly detracting from their existing efforts.

Sterling's second step was to engage a consulting firm to help develop the program. The consulting firm's experience with other companies' waste minimization efforts provided an independent review of the program developed at Sterling and provided ready-made tools for implementing the program. Radian Corporation was hired to develop a customized waste minimization program and manual and then to test the procedures described in the manual by spearheading a waste minimization survey of the ethyl benzene/styrene plant. A major thrust of the manual development work was to integrate the waste minimization program with existing Sterling procedures. It was felt the most successful approach would be to incorporate existing engineering, accounting, and reporting procedures into the new waste minimization program. Concepts of waste minimization, such as use of a survey team, a project champion, and effective brainstorming, were applied specifically to Sterling's program. The final waste minimization manual includes seven chapters ranging from survey methodology through feasibility assessment and reporting, fourteen worksheets, and nine tutorial examples for implementing the procedures.

As the manual was being developed, Sterling's Environmental Affairs Department worked with plant and corporate management to obtain and document a commitment to the waste minimization program. The use of existing quality and engineering procedures was instrumental in gaining the support of Sterling's managers. Another strong selling point was the fact that the waste minimization program supports Sterling's commitment to the Chemical Manufacturers Association's Responsible Care program. A final key to the program was Sterling's Board of Directors approval of a corporate policy statement on waste minimization.

To test the waste minimization manual and the procedures it embodies, Sterling and Radian performed an initial waste minimization survey in the ethyl benzene/styrene area of the plant. The survey identified over 200 potential activities within the facility where waste minimization could be practiced. Sterling has proceeded with some of these projects to reduce air emissions from the facility. Other opportunities for source reduction were identified that would help define the scope of Sterling's Organic Toxicity Characteristic Compliance Project. In a similar manner, Sterling expects that a waste minimization survey will be completed in each of the manufacturing and service areas within the next three years. After the initial survey in each area, an audit will be conducted at least once every three years.

In summary, the results of the program to date include a corporate commitment to minimizing waste generation at Sterling and a written manual of structured concepts, procedures, and formats. Sterling is now performing waste minimization surveys, developing and ranking waste minimization alternatives, and implementing waste minimization as each area of the facility initiates the program. The procedures for the waste minimization program are based on Sterling's current evaluation framework for routine capital investment with the facility. In addition, and more importantly, Sterling now has a database documenting waste minimization activities for compliance and other reporting requirements. The overall program results are expected to significantly continue improvement of the quality of life for Sterling's employees and Sterling's neighbors and to greatly reduce the cost of waste management.

EMERGENCY RELIEF SYSTEM DESIGN

developed by AIChE's Design Institute for Emergency Relief Systems (DIERS)

SAFIRE COMPUTER PROGRAM & DOCUMENTATION

The *Systems Analysis for Integrated Relief Evaluation* (SAFIRE) computer program and accompanying manuals are useful for designing emergency relief systems for runaway reactions or fire exposure. Engineers can utilize this tool to estimate the pressure/temperature/time history for selected relief devices in a variety of applications and situations.

Your have a choice of one of two formats: Computer Tape for use with an IBM, VAX or UNIVAC Mainframe Computer.....or.....diskette for IBM Compatible Personal Computers.

Purchase of a single copy entitles a company to worldwide use of both versions of this computer program.

Pub# B-1 Computer Tape and/or PC Floppy Disk *plus* One set of 7 Manuals (782 pp) $7500

EMERGENCY RELIEF SYSTEMS FOR RUNAWAY CHEMICAL REACTIONS & STORAGE VESSELS: A SUMMARY OF MULTIPHASE FLOW METHODS

This technology summary presents the multiphase flow methods to calculate phenomena relevant to design of emergency relief systems for runaway reactions. The document will help users acquire, assimilate and implement the vast amount of DIERS information by serving as both a reference and a training tool.

Pub# B-2 Spiralbound (200 pp) $210

BENCH-SCALE APPARATUS DESIGN & TEST RESULTS

Methods to measure runaway reaction data under adiabatic conditions in a vessel with a very low thermal inertia are presented. Measurement of vessel liquid disengagement regimes and viscous vs. turbulent pipe flow behavior are discussed. Methods are also provided for sizing emergency relief devices without a comprehensive computer program.

Pub# B-4 Spiralbound (5 reports, 286 pp) $90

SMALL/LARGE SCALE EXPERIMENTAL DATA & ANALYSIS

Ten reports present test data useful for the better understanding of vessel and vent line multiphase flow behavior applicable to emergency relief of chemical systems. Time/temperature/pressure/void fraction history and analysis of each test are given. Complete apparatus design details to facilitate independent analysis are also provided.

Pub# B-3 Spiralbound (10 reports, 1218 pp) $250

SAFETY VALVE STABILITY & CAPACITY TEST RESULTS

This study addresses problems arising when a safety valve adjusted for vapor flow is used to vent low-quality steam. The report also covers the effect of valve exit to orifice areas on the flow capacity and stability of the valve and the prediction of saturated liquid mass flow rates through valves.

Pub# B-5 Spiralbound (77 pp) $100

Send Orders to: AIChE Publication Sales, 345 East 47 Street, New York, NY 10017. Prepayment in U.S. funds required (check, international money order or bank draft drawn on a New York bank). VISA or MasterCard orders: call (212) 705-7657 for details. U.S. bookrate shipments prepaid. Foreign Extra: $6 per book. *(Europe, Middle East & Africa: Contact Clark Associates-Europe Ltd, Unit 2, Pool Road Trading Estate, W. Molesey, Surrey KT8 OHE England.)*

AMERICAN INSTITUTE OF CHEMICAL ENGINEERS

Adsorptive Capacities of Activated Carbon for Organic Constituents of Wastewaters

Wei-chi Ying, Edward A. Dietz, and George C. Woehr
Occidental Chemical Corporation Grand Island Technology Center, Grand Island, NY 14072

The adsorptive capacities of activated carbon for major organic constituents (target compounds) of a wide variety of wastewater were measured in pure water and in actual wastewater samples. Competitive adsorption due to the presence of other organic components of total organic carbon of the wastewater (background TOC) reduced carbon capacities for all target compounds in the wastewaters from the respective pure water isotherms. The capacity reduction for a target compound was found to depend on the relative adsorptivity of the target compound versus competing compounds (poorly adsorbed TOC components produced a small reduction in capacity for a more strongly adsorbed target compound), and the fraction of the background TOC attributable to the target compound. Those findings were validated by carbon column adsorption breakthrough data.

INTRODUCTION

Activated carbon adsorbers are widely employed in water and wastewater treatment processes for removing organic contaminants. The most important cost consideration in applying this technology is the capacities of carbon for regulated compounds and/or parameters. Adsorptive capacity (isotherm) data are utilized for estimating the carbon exhaustion rate and, thus, the expected service period between carbon bed changes and the size of carbon regeneration system, if on-site regeneration is desirable [*1*].

The carbon adsorption isotherm for a compound is defined under a given set of testing conditions: type of carbon, pH, temperature, initial concentration, range of equilibrium concentration, ionic strength, and composition of the test solution [*2, 3*]. The effects of competitive adsorption and biological activities further complicate predictions of adsorber treatment performance [*4*]. Therefore, isotherm data reported for a compound in pure water or reference isotherms [*5*] are not very useful when a mixture of organic contaminants are to be removed, such as in carbon adsorption treatment of landfill leachates, contaminated groundwaters, and POTW primary effluents [*6, 7*].

The adsorptive capacities of activated carbon for organic constituents of several types of industrial wastewater:process water from a petrochemical plant, raw and biotreated phenolic wastes, raw and pretreated (pH-adjusted, filtered, solvent-extracted, and biotreated) chemical waste landfill leachates, organic contaminated groundwaters, and publicly owned treatment works (POTW) primary effluents were measured in pure water and in the wastewater samples. Compounds investigated were: ethylene dichloride, phenol, color agents, benzoic acid, o-chlorobenzoic acid, Aroclor 1254, benzene, monochlorobenzene, p-dichlorobenzene, chloroform, trichloroethylene, toluene, and o-chlorotoluene. These organic compounds/parameters were selected for study because they represent several important classes of organic contaminants found in many industrial wastewaters and because actual carbon adsorber treatment performance data were available for comparison with measured isotherm capacities. Each compound was present in the wastewater samples either as one of the major organic constituents or a trace-level contaminant. Carbon adsorption isotherms for two gross organic concentration parameters of the wastewaters—total organic carbon (TOC) and total organic halide (TOX)—were also obtained to provide explanations for some of the experimental observations.

Carbon column breakthrough data were also obtained to illustrate the concept of capacity utilization in adsorption treatment as well as to validate some of the conclusions deduced from the isotherm data.

Correspondence concerning this paper should be addressed to Wei-chi Ying.

EXPERIMENTAL

Analytical Methods

Extensive efforts were made for identification and quantification of a large number of organic constituents of

TABLE 1. COMPOSITION OF PHENOLIC WASTEWATERS.[a]

Concentration parameter	Distillate	Raffinate
pH	9.0	3.2
TOC	29,500	5,100
COD	95,000	15,000
TSS	10	8
TDS	39,000	7,000
Phenol	34,000	5,800
Others	[b]	[c]

[a] All concentration parameters, except for pH, are given in mg/L.
[b] 6000 mg/L total diols (1,6-hexanediol, butanediol, ethylene glycol, propylene glycol, diethylene glycol).
[c] Formaldehyde, methanol, and isopropyl ether, concentrations not determined.

a variety of raw- and partially treated industrial wastewaters. Parameters commonly used for characterization of wastewater were measured in accordance with the American Health Association's standard methods [8]. These parameters included: pH (Section 423), TOC (505), chemical oxygen demand (COD, 508A), total dissolved solids (TDS, 209C), and suspended solids (SS, 209D). TOX was analyzed by a Dohrmann DX-20 analyzer using EPA Method 450.1.

Ethylene dichloride (EDC) concentration was measured by solvent (hexane) extraction followed by GC/ECD assay. Concentrations for phenol, benzoic acid, o-, m-, and p-chlorobenzoic acids (CBAs) in leachate were estimated using a high-performance liquid chromatography method, with a Perkin-Elmer Model 3B, adapted for analysis of the wastewater samples [9]; in the pure water, these compounds were measured by UV spectroscopy. GC purge and trap methods [6] were utilized for determining volatile organic compounds—chloroform, trichloroethylene, toluene, o-chlorotoluene (OCT), benzene, monochlorobenzene (MCB), o-, and p-dichlorobenzenes (DCBs). The intensity of the yellow color found in biotreated phenolic waste was measured by light absorbance in a 1 cm cuvette at 375 nm, using a spectrophotometer. A liquid scintillation counting technique was employed for measuring ^{14}C-labeled polychlorobiphenyls Aroclor 1254 (PCBs A-1254). The labeled material was purchased from Amershan Corporation, Arlington Heights, IL

Wastewater Samples

Carbon adsorption isotherm experiments were performed on five types of industrial wastewater—EDC plant process water, phenolic resin manufacturing wastewater, chemical waste landfill leachate, contaminated groundwater, and POTW primary treatment effluent. The EDC plant process water was an effluent sample from a steam stripper employed for recovery of EDC and other volatile organic compounds. The steam stripper effluent was typically basic (pH = 10.9), with an EDC concentration of 110 μg/L. It contained large amounts of inorganic impurities (TDS = 6300 mg/L), such as sodium sulfite/sulfate/carbonate, while its TOC was 138 mg/L, due mostly to ethylene glycol and chloroethanol resulting from hydrolysis of EDC.

The distillate waste sample from phenolic resin manufacture had a very high concentration of phenol (34000 mg/L, see Table 1). The phenol in such distillate can be substantially recovered by solvent extraction using isopropyl ether. Raffinate waste (solvent-extracted distillate) is presently disposed of by either incineration or biodegradation. Carbon adsorption of biotreated raffinate and/or distillate will be considered for treatment of the phenolic wastes.

The raw landfill leachate contained a variety of organic and inorganic contaminants. The organic constituents consisted of both straight-chain and aromatic compounds, including many halogenated compounds that were readily adsorbed on activated carbon. The leachate was mixed with other chemical manufacturing plant wastewaters prior to treatment by granular activated carbon adsorption. Solvent extraction, biological treatment, and chemical oxidation were evaluated as pretreatment methods for reducing the organic loading to the carbon adsorbers. Concentration of organic constituents in raw leachate fluctuated widely depending on the season; TOC had a range from 1,000 to 8,100 mg/L, as shown in Tables 2–4.

Two contaminated groundwater samples were obtained. Groundwater A was a low-TOC sample containing only a few volatile organic compounds. Groundwater B sample, which was obtained from a different site, contained, in addition to several volatile organics, high concentrations of inorganic compounds (TDS = 11,430 mg/L). Adsorption by activated carbon was found, in laboratory isotherm and column breakthrough studies, to be effective in removing the organic contaminants (see Table 5) from both groundwaters. Carbon adsorption has been considered as an attractive groundwater treatment technology.

Two primary treatment effluent samples were taken on different dates from a POTW that received more than half of its incoming wastewaters from local industries. The industrial discharges contributed most of the organic com-

TABLE 2. ADSORPTIVE CAPACITIES OF CALGON SERVICE CARBON FOR LEACHATE CONSTITUENTS.

	Concentration (mg/L)			Adsorptive capacity (mg adsorbed/g carbon)		
Concentration parameter[a]	raw leachate	combined[b] waste feed	absorber[c] effluent	carbon[d] loading	leachate[e] isotherm	pure[f] water isotherm
pH	5.3	5.5–6.4	5.5–6.4	5.5–6.4	4.9–5.5	5.0–6.0
Phenol	981	780	$ND_{0.1}$[g]	41.0	74.9	166
Benzoic acid	830	910	0.8	48.0	74.1	171
o-chlorobenzoic acid	562	372	7.4	19.6	22.9	109
m-chlorobenzoic acid	61	120	$ND_{0.5}$	6.4	23.0	160
p-chlorobenzoic acid	40	80	$ND_{0.1}$	4.2	15.7	171
TOC	3,080	2,618	318	137	143	

[a] Analytical methods discussed in text.
[b] Average concentrations for the adsorber feed during an adsorption service cycle.
[c] Concentrations were measured at the end of an adsorption cycle.
[d] Total removal of the compound at the end of an adsorption cycle.
[e] Capacities were estimated at the feed concentration from the raw leachate isotherms.
[f] Capacities were estimated at the feed concentration from the pure compound isotherms.
[g] ND_x = not detected at a detection limit of x mg/L.

TABLE 3. COMPOSITION OF RAW, SOLVENT-EXTRACTED, AND BIOTREATED LEACHATES.

Leachate sample	TOC (mg/L)	TOX (mg/L)	Phenol (mg/L)	Benzoic acid (mg/L)	o-CBA (mg/L)	m-CBA (mg/L)	p-CBA (mg/L)
Raw leachate	1400	110	375	469	211	33	35
Solvent-extracted[a] (octanol, 2 times)	1200	85	82	374	212	13	11
Solvent-extracted (octanol, 4 times)	1170	86	19	368	219	11	10
Solvent-extracted (octanol, 7 times)	1140	85	5	358	206	10	8
Feed leachate	1800	205	436	708	227	62	74
Biotreated leachate[b]	155	100	1.1	11.2	<0.5	<2	16

[a] Using a solvent: leachate ratio of 1/30 at room temperature.
[b] Biotreatment in a SBR operated a hydraulic retention of 2.5 days [9].

TABLE 4. ABSORPTIVE CAPACITIES OF CARBON FOR TOC AND TOX IN RAW AND BIOTREATED LEACHATES.[a]

Activated carbon type	Raw leachate[b] TOC	Raw leachate[b] TOX	Biotreated leachate[c] TOC	Biotreated leachate[c] TOX
	(mg adsorbed/g carbon)			
Calgon F-300	133	11.7	152	127
Calgon Service carbon	97.9	8.8	113	75.9
Ceca GAC 30	173	19.6	268	172
ICI Hydrodarco 3000	103	11.5	87.8	83.8
Laboratory reactivated spent Calgon Service carbon	148	18.3	115	91.6

[a] Adsorptive capacities were estimated from the Freundlich adsorption isotherms.
[b] Raw leachate: TOC = 3080 mg/L, TOX = 264 mg/L, pH = 5.3. The TOC capacities were estimated at TOC = 1500 mg/L, and the TOX capacities were estimated at TOX = 125 mg/L.
[c] Biotreated leachate: TOC = 400 mg/L, TOX = 334 mg/L, pH = 6.8. (The raw leachate had a TOC of 8100 mg/L and a TOX of 780 mg/L.) The TOC capacities were estimated at TOC = 300 mg/L. The TOX capacities were estimated at TOX = 125 mg/L.

TABLE 5. COMPOSIONS OF CONTAMINATED GROUNDWATERS.[a]

Concentration parameter	Groundwater A	Groundwater B
pH	6.6	5.9
TOC	25	337
COD	60	840
TSS	10	1150
TDS	700	11430
Trichloroethylene	0.03	4.8
Phenol	1.6	14.9
Toluene	0.04	15.0
o-chlorotoluene	0.7	2.0[b]
Benzene	4.8	1.0
Monochlorobenzene	3.9	9.6
o-dichlorobenzene	0.5	1.4[b]
p-dichlorobenzene	1.0	

[a] All concentration parameters, except for pH, are given in mg/L.
[b] Sum of o-, m-, and p-isomers.

pounds listed in Table 6. Granular activated carbon adsorbers are employed at the POTW to remove these and other organic compounds remaining after primary treatment by chemical coagulation, flocculation, and sedimentation.

Adsorption Isotherms

The conventional EPA carbon adsorption isotherm method [5] was modified, including a much smaller liquid sample volume (43 ml versus 1,000 ml) more efficient mixing (shaking or head-to-bottom rotation), and a longer time (up to 18 hours) for solid-liquid contact. The experimental isotherm data of carbon dosages (g or mg) and residual (equilibrium) concentrations (mg or μg/L) were utilized for calculating the adsorptive capacities of carbon (mg adsorbed/g carbon) for the compound studied (target compound):

$$X/M = (C_o - C_f) \times V/\text{carbon dose}$$

where C_o is the initial concentration (mg or μg/L), C_f is the residual concentration, and V is the volume (L) of the isotherm sample.

To facilitate the estimation of adsorptive capacity and the carbon exhaustion rate, at a given feed concentration, the calculated concentration-capacity data were then correlated by the Freundlich adsorption isotherm model [5]:

$$X/M = k \times C_f^{1/n}$$

TABLE 6. RESULTS OF CARBON ADSORPTION ISOTHERM EXPERIMENTS FOR POTW PRIMARY EFFLUENTS.

Concentration parameter	Effluent A Concentration[a]	Effluent A Ratio of G_c[b]	Effluent B Concentration	Effluent B Ratio of G_c
pH	7.0		7.0	
TOC	14,000		22,000	
COD	38,000		60,000	
Phenol			70	
Chlorform	26 (239)[c]	2.48	35 (239)[c]	2.88
Trichloroethylene	33 (217)	3.91	50 (184	5.45
Benzene	25		6 (180)	7.01
Toluene	14		43 (212)	6.26
o-chlorotoluene	35		230 (299)	7.09

[a] All concentration parameters, except for pH, are given in μg/L. Blank spaces indicate that those parameters were not measured for the effluent sample.
[b] Ratio of granular activated carbon exhaustion rate for removing 100 μg/L of the compound from the POTW primary effluent to that from pure water.
[c] Initial concentration for the isotherm run.

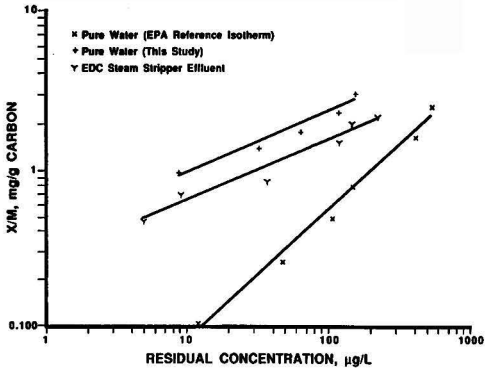

Figure 1. Adsorption isotherms for ethylene dichloride in pure water and EDC steam stripper effluent.

where k and $1/n$ are the Freundlich parameters for the isotherm data.

Figures 1 through 12 present both the experimental isotherm data and their Freundlich model representations. The data points shown are those that had a residual concentration less than 85% of the initial concentration [2]. Carbon exhaustion rate, G_c (g carbon/L), for granular carbon adsorption treatment of wastewater was calculated [5]:

$$G_c = C_{in}/(X/M)$$

where X/M is estimated from the isotherm for a compound in the wastewater sample or in pure water at the feed concentration, C_{in} (mg/L), to obtain the amount of carbon required for removing the target compound from the wastewater relative to that from pure water (Table 6).

Carbon Adsorber Performance

Effluent concentration profiles (effluent-influent concentration versus time or volume treated) were obtained for bench-, pilot-, and full-scale carbon adsorbers to define the practical loading levels of target compounds in adsorption treatment and to verify isotherm capacities.

Bench-scale adsorption breakthrough experiments were conducted for removing the yellow color of the biotreated phenolic waste. The results for four small carbon columns—two 10g and two 15g, empty-bed residence time (EBRT) of 50 and 75 minutes, respectively, at a flowrate of 0.43 ml/minute—are shown in Figure 13. The

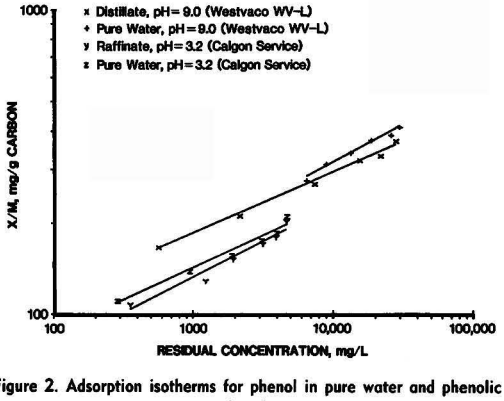

Figure 2. Adsorption isotherms for phenol in pure water and phenolic wastewaters.

percent utilization of the isotherm capacity found at the end of the experiment or when the color intensity of the effluent reached 20% of the feed in each of the four columns are shown in Table 7 [10].

The loading of major leachate constituents found at the end of adsorber service cycle was calculated in a similar manner using effluent data for the existing full-scale carbon adsorption system (two 20,000 lb carbon adsorbers operated in series) in treating the chemical landfill leachate. The results are presented in Table 2.

Data on apparent organic loadings found in two pilot-scale carbon columns (each 12.6 cm in diameter contained 14 kg of Calgon Service carbon and was fed with 1.14 L/min of POTW primary effluent) were analyzed and compared with the isotherm capacities. The pilot study was designed to simulate the performance of full scale carbon adsorbers (17 ft × 42 ft × 8 ft). Table 8 summarizes the apparent loadings found in the pilot carbon columns compared to the adsorption isotherm data obtained in this study and the POTW isotherm data for COD and total phenols [11]. Table 9 presents pertinent physical properties for the compounds monitored in the pilot study.

The time to exhaustion and fraction removed for each compound/parameter were calculated from the pilot study carbon column breakthrough curves [11]. The apparent loading (mg/g carbon) on the pilot carbon columns was calculated as:

$$X/M = Q \times t \times C_{ave} \times f \times 0.001/W$$

where Q is the daily flowrate (L/d), t is the time (d) to exhaustion, f is the estimated fraction of cumulative removal of the compound at carbon bed exhaustion, C_{ave} is the average feed concentration (µg/L) during the pilot study, and W is the amount (g) of carbon in the pilot carbon column.

RESULTS AND DISCUSSION

Adsorption Isotherm

EDC Process Water: Figure 1 presents the EPA reference isotherm for EDC [5] and experimental isotherms used for this investigation. The adsorptive capacities of Calgon F-300, a popular commercial granular activated carbon, shown in the EPA isotherms were significantly lower than the observed capacities of Calgon Service carbon, which is reactivated Calgon F-300 commonly employed in Calgon Adsorption Service adsorbers, over the entire EDC concentration range. The low EPA capacities probably resulted from the excessive carbon doses (up to 9,615 mg/L), the short test time (two hours), and insufficient solid-liquid contact (by magnetic stirring) in the one liter test sample employed in the EPA method. In this study, a smaller volume (43 ml) of sample was contacted for 18 hours with up to 250 mg/L (actual doses 1 to 10 mg) of pulverized carbon in a tightly sealed vial that contained a glass bead to enhance mixing, under continuous head-to-bottom rotation. The comparative results clearly demonstrate the need to experimentally confirm literature isotherm data, even for pure water systems.

The measured capacities for EDC in the steam stripper effluent sample were lower than those found in the pure water system. Given that EDC (319 µg/L, including the spiked amount) accounted for only 0.06% of the wastewater TOC (138 mg/L), the reductions in capacity were rather small. The experimental data show that when major TOC constituents (ethylene glycol and chloroethanol) are much less adsorbable than the target compound (EDC), the carbon capacity for the target compound is only reduced slightly, even though it is a minor component of the wastewater TOC.

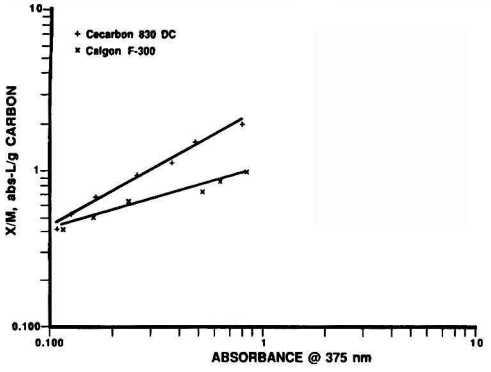

Figure 3. Adsorption isotherms for color in biotreated phenolic wastewater.

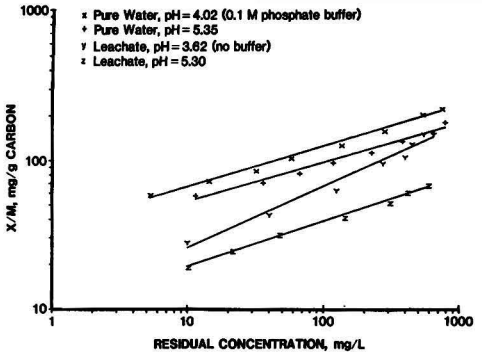

Figure 5. Adsorption isotherms for benzoic acid in pure water and leachate at two pH levels.

Phenolic Wastewaters: Figure 2 shows that the carbon adsorption isotherms for phenol in distillate and raffinate wastes were only slightly lower than the corresponding isotherms of phenol in pure water. The small capacity reductions were due to phenol being the predominant organic constituent of the phenolic wastes, accounting for about 88% and 87%, respectively, of waste TOC in the distillate and raffinate samples (Table 1).

Biological treatment of diluted distillate (phenol concentration = 6,200 mg/L) was performed in two sequencing batch bioreactors (SBRs), which were operated at a hydraulic retention time of 10 days and a mixed liquor suspended solids concentration of 5,000 mg/L. Granular carbon treatment was employed to remove the light yellow color of the effluent, which had a phenol concentration of less than 50 mg/L and a TOC about 350 mg/L. Carbon adsorption isotherm experiments were first performed on the effluent, using Calgon F-300 and Cecarbon 830 DC, a carbon found to be effective in removing color agents and large molecule organic contaminants [*10*]. The results (Figure 3) show that both carbons were effective in removing the light yellow color of the effluent, in addition to removing phenol and TOC. Cecarbon 830 DC had a higher capacity for color removal than Calgon F-300.

Chemical Waste Landfill Leachate: Carbon adsorption isotherms for five major organic leachate constituents (phenol, benzoic acid, o-, m-, and p-CBAs) were obtained in pure water and again in actual leachate samples. Carbon adsorptive capacities for TOC and TOX were measured in raw and pretreated (solvent extraction and biodegradation) leachate samples. Five granular activated carbons (four commercial types and one laboratory reactivated) were used for isotherm runs conducted at two pH levels.

Figure 4 shows that the adsorptive capacity of Calgon Service carbon (the carbon used in the adsorbers) for phenol in a raw leachate sample (composition given in Table 2) was reduced significantly from that measured in pure water. This reduction in the capacity for phenol, resulting from competitive adsorption due to the presence of other leachate constituents, was far more than the differences among isotherms of the three carbons (Calgon Service, Calgon F-300, and Ceca GAC 30).

Figures 5 and 6 show that the capacities of Calgon Service carbon for benzoic acid and o-CBA in leachate were similarly reduced from their pure water isotherms. For wastewater constituents of comparable adsorptivity, a close relationship between capacity reduction due to competitive adsorption and the fraction of background TOC (%TOC) attributable to the target compound can be seen by the greater capacity reduction for o-CBA (%TOC = 9.8) than that for benzoic acid (%TOC = 19) or phenol (%TOC = 24). Figure 7 shows that for PCBs A-1254, a trace constituent (%TOC = 0.0003), the capacity reduction was much more than observed for the major organic constituents of the leachate.

Because of the overall negative charge on the carbon surface, adsorptive capacity for an organic acid is generally higher for the undissociated acid species (molecules)

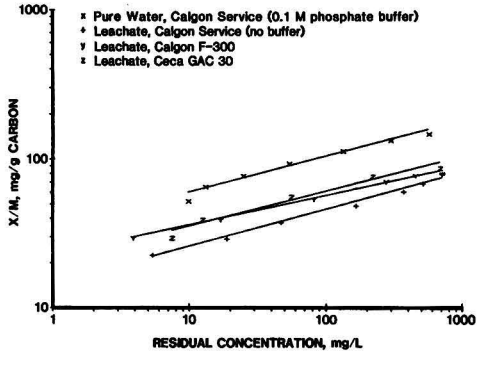

Figure 4. Adsorption isotherms for phenol in pure water and leachate.

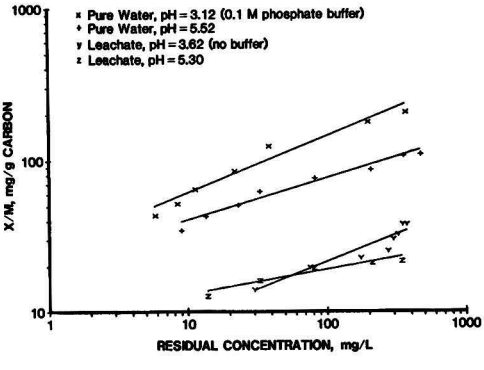

Figure 6. Adsorption isotherms for o-chlorobenzoic acid in pure water and leachate at two pH levels.

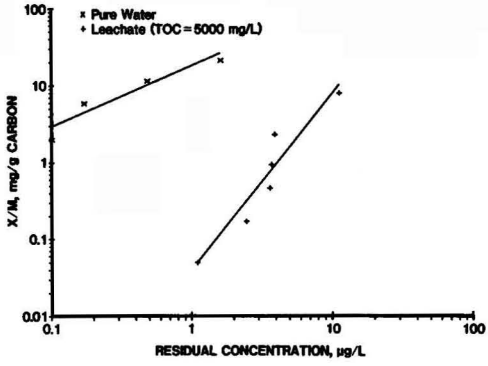

Figure 7. Adsorption isotherms for ^{14}C-labelled PCBs A-1254 in pure water and leachate.

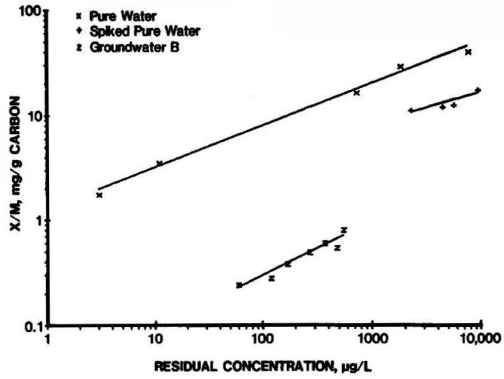

Figure 9. Adsorption isotherms for benzene in pure water and contaminated groundwater.

than for the anions. Since acid molecules predominate when the pH is less than the acid pk_a [15], capacity enhancement for benzoic acid ($pk_a = 4.20$) was more than that for o-CBA ($pk_a = 2.94$) when the leachate pH was lowered from 5.30 to 3.62. The smaller enhancements found in the lower pH isotherms, as shown in the low-concentration portion of these isotherms for high carbon-dosed samples, were due to increase pH's resulting from removal of hydrogen ions by adsorption [16]. A 0.1*M* phosphate buffer solution was used in the pure water isotherm experiments to minimize the pH rise as a result of the carbon addition. The pH effect on the pure water isotherms have similarly been demonstrated for the two compounds.

Table 2 presents the compositions of raw leachate, combined feed to the two-bed carbon adsorbers, and the final adsorber effluent. Raw leachate typically accounted for about 60% of the feed volume, but more than 80% of the TOC loading to the existing carbon adsorption system. Table 2 summarizes the estimated adsorptive capacities of Calgon Service carbon for phenol, benzoic acid, CBAs, and TOC, based on the leachate and pure water isotherms relative to the carbon loadings found in the full-size activated carbon adsorbers during an adsorption service cycle. The capacities for the five major organic constituents were found to be significantly reduced from the their pure water isotherms. The capacity reductions were inversely related to the respective percent TOC attributable to these compounds. At the time of bed exhaustion, the loadings for o-CBA and TOC found in the leading adsorber were nearly the same as the leachate isotherm capacities and the loadings for phenol, benzoic acid, m-, and p-CBAs were all well below the corresponding capacities, which established the validity of the leachate isotherms.

Using solvent extraction, chemical oxidation, and biodegradation as leachate pretreatment methods were investigated for reducing the organic loading of the existing carbon adsorbers. Octanol was evaluated as a candidate solvent because of its high solubility for phenol and relatively low cost. Biotreatment was accomplished in a pilot-scale SBR operated at a hydraulic retention time of 2.5 days [9]. Results from the extraction studies are presented in Table 3. Composition data are given for the raw and three octanol-extracted (twice, four, and seven times, each at a solvent to waste volume ratio of 1/30) leachate samples. Adsorption isotherms for TOC and TOX in the raw and the seven-time octanol-extracted leachate samples (Figure 8), show that the carbon exhaustion rate of the existing adsorbers will not be much reduced by such a pretreatment.

Table 3 also provides composition data for feed and biotreated leachate samples. Biotreatment was confirmed as an effective pretreatment method for reducing the leachate TOC. Octanol extraction was ineffective because it removed only phenol among the major organic leachate constituents. Table 4 shows that the capacities of five granular carbons for TOC in biotreated leachate were about the same as in the raw leachate and that the capacity for TOX was much greater after biotreatment. This demonstrated that biodegradation pretreatment in a SBR would reduce the carbon exhaustion rate by at least

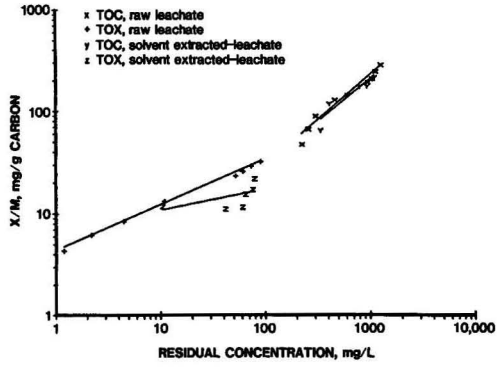

Figure 8. Adsorption isotherms for TOC and TOX in raw and solvent-extracted leachated.

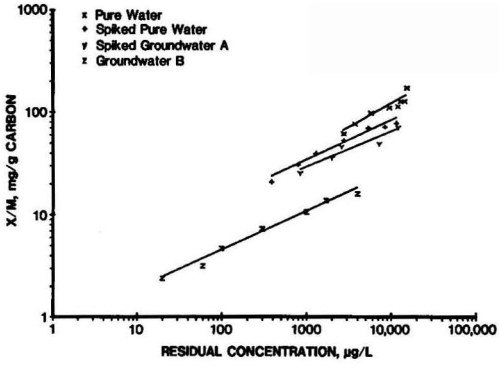

Figure 10. Adsorption isotherms for monochlorobenzene in pure water and contaminated groundwaters.

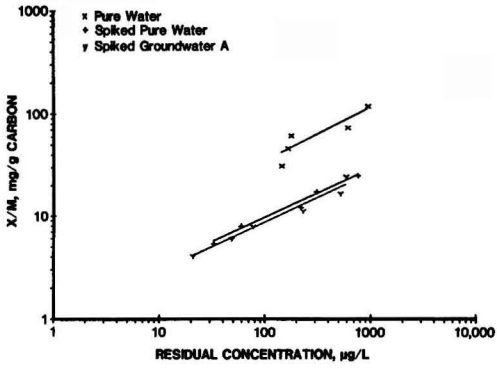

Figure 11. Adsorption isotherms for p-dichlorobenzene in pure water and contaminated groundwater.

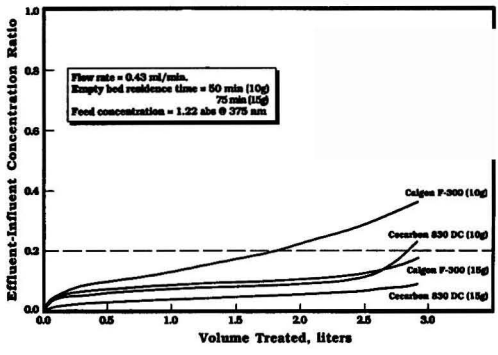

Figure 13. Carbon column breakthrough curves for removing color from biotreated phenolic wastewater.

90%—the TOC reduction due to biotreatment [9]. An SBR biotreatment system is being installed for treating the chemical waste landfill leachate waste before carbon adsorption.

Contaminated Groundwaters: As shown in Table 5, groundwater A was a low-TOC sample containing a few volatile aromatic compounds, while groundwater B had larger amounts of dissolved organic and inorganic contaminants (TOC = 337 mg/L, TDS = 11,430 mg/L). A mixture of organic compounds was spiked to pure water or groundwater to increase its concentration for benzene by 10 mg/L, MCB by 15 mg/L, OCT, o-, and p-DCBs by 2 mg/L each.

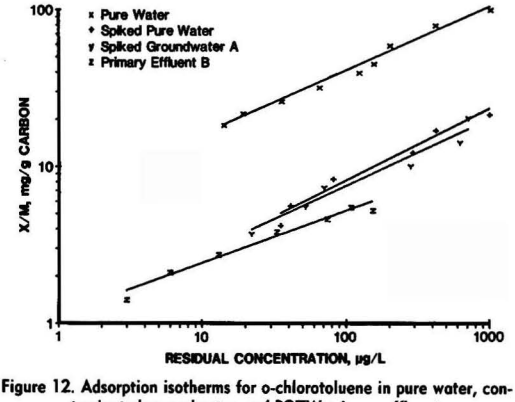

Figure 12. Adsorption isotherms for o-chlorotoluene in pure water, contaminated groundwater, and POTW primary effluent.

Figure 9 shows that the reduction in adsorptive capacity of Calgon Service carbon for benzene, relative to the pure water isotherm, was much less in the spiked pure water (%TOC = 43) than in groundwater B (%TOC = 0.27). The reductions in the capacity for MCB, in the spiked pure water, the spiked groundwater A, and groundwater B test systems, as shown in Figure 10, were inversely related to the percent TOC attributable to MCB-41, 26, and 1.8, respectively. Figure 11 shows that, as expected, the reduction in the capacity of carbon for p-DCB in the spiked pure water (%TOC = 4.6) was only slightly less than that in the spiked groundwater A (%TOC = 3.2).

POTW Primary Treatment Effluent: Two samples of POTW primary effluent were taken from the same source at different times. Effluent A had lower (relative to effluent B) concentrations of TOC, COD, and most of the organic constituents of concern, except for benzene (Table 6). Adsorption isotherm experiments were conducted for TOC, COD, chloroform, trichloroethylene, benzene, toluene, and OCT using Calgon Service carbon, which was the carbon employed in the pilot column study performed by Malcolm Pirnie, Inc. [11].

Figure 12 shows that the reductions in the adsorptive capacity for OCT were inversely related to its share of the TOC for the spiked pure water (%TOC = 6.2), the spiked groundwater A (%TOC = 3.9), and POTW primary effluent B (%TOC = 0.86), as demonstrated for other target compounds in several industrial wastewaters. The ex-

TABLE 7. ABSORBER CAPACITY UTILIZATION FOR REMOVING COLOR FROM BIOTREATED PHENOLIC WASTEWATER.

Feed—Composite effluent from SBR 1 and 2;
Average feed rate = 0.43 ml/min;
Average feed concentration—color = VIS abs 1.22 at 375 nm,
Total run time = 110 hours, total volume treated = 2.84 liters

Carbon Column	EBRT[a] (min)	Loading[b] (abs-L or mg/g)	Capacity[c] (abs-L or mg-g)	% Utilization[d]
Calgon F-300 (10 g)	50	0.191	1.10	17.4
Calgon F-300 (15 g)	75	0.216	1.10	19.6
Cecarbon 830DC (10 g)	50	0.320	2.90	11.1
Cecarbon 830DC (15 g)	75	0.220	2.90	7.7

[a] Empty bed residence time, assuming apparent density = 0.47 g/cc.
[b] Cumulative loading calculated from the breakthrough curves shown in Figure 13 at the end of the runs or when the color intensity of the effluent reached 20% of the feed. Loading = Feed concentration × total volume treated × % removed.
[c] Carbon isotherm capacity (Figure 3) estimated at abs 1.22.
[d] %utilization = loading/capacity.

TABLE 8. ABSORPTIVE CAPACITIES OF CALGON SERVICE CARBON FOR TRACE ORGANIC CONTAMINANTS IN POTW PRIMARY TREATMENT EFFLUENT.

Pilot carbon column[a]: diameter—12.6 cm, charged with 14 kg of Calgon Service carbon, flowrate—1.14 L/min

Parameter/compound	Ave. feed conc. & range (μg/L)	Time to[b] exhaustion (d)	Fraction[b] removed	Adsorptive capacity[c] column efflu. pure water loading isotherm (mg/g)		
COD	85,000 43–195,000	120	0.46	545	260[d]	
Total phenols	310 20–441	157	0.71	4.02	2.65[e]	8.25[f]
Chloroform	73 41–120	96	0.61	0.50	0.26	0.69
Trichloroethylene	73 47–134	238[g]	0.68[g]	1.37	0.82	4.00
Benzene	48 20-122	160	0.78	0.70	0.61	4.30
Toluene	213 9–2,400	250[g]	0.70[g]	4.33	2.25	14.7
Monochlorotoluene[h]	860 17–14,000	263[g]	0.77[g]	20.2	10.5	71.2

[a] Pilot column study conducted by Malcolm and Pirnie, Inc. [11].
[b] Estimated or calculated from the pilot carbon column breakthrough profiles.
[c] Adsorptive capacities given are all estimated at the average feed concentration.
[d] Average of 6/19 and 10/15/1980 POTW COD isotherms [11].
[e] 9/6/1980 POTW total phenols isotherm [11].
[f] Estimated from the EPA data for phenol using virgin Calgon F-300 [5].
[g] Estimated from the incomplete breakthrough curves.
[h] The column loadings are for the sum of three isomers; the isotherm data are for o-chlorotoluene only.

pected increase in carbon exhaustion rates, due to competitive adsorption, can be estimated from the ratios of G_c's (Table 6) for removing the trace organic contaminants from POTW primary effluent to those from pure water. Many times more carbon would be required to remove any of these compounds from effluent A than from pure water. Even more carbon would be required for treating the higher TOC effluent B. The capacity for trichloroethylene was reduced to a greater extent than chloroform in both effluent samples, indicating that the order of capacity reduction for target compounds might be preserved in samples having similar composition yet at different TOC levels.

Carbon Adsorber Performance

Removal of Color from Biotreated Phenolic Waste: The adsorption breakthrough curves depicted in Figure 13 confirm the higher isotherm capacity of Cecarbon 830 DC for color agents. The results also demonstrate premature breakthrough of color in single-bed adsorption treatment [10]. Capacity utilization, ratio of cumulative loading of color agents in the adsorber to the isotherm capacity, for the 10 g Calgon adsorber, which had the earliest color breakthrough, was about 17.4% (Table 7). At a carbon exhaustion rate of 6.4 g/L, a conventional 20,000 lb carbon adsorber has been proposed to provide for more than one year of polishing treatment for 1,000 gal/day of biotreated phenolic wastewater [17]. Actual carbon consumption rate may be much less, since bacterial growth on carbon, which we observed, will significantly enhance the overall treatment capability of the adsorption system in removing color agents and other organic constituents of the feed [18, 19].

Pilot Carbon Treatment of POTW Primary Effluent: The time to exhaustion for the pilot carbon column, i.e., the operating time when concentration of a target compound in the effluent had reached or exceeded that in the feed, was estimated from the pilot column breakthrough curves for COD and its six organic components' [6]. The results (Table 8) were consistent with the G_c's calculated from the adsorption isotherms for these target compounds obtained in the POTW effluent samples.

The pilot column apparent loadings observed for the six target compounds validated the reduced isotherm capacities found in POTW effluent samples. The values given for total phenols included all phenol-like compounds. Both the apparent loading and the POTW iso-

TABLE 9. PROPERTIES OF TRACE ORGANIC CONTAMINANTS IN POTW PRIMARY TREATMENT EFFLUENT.[a]

Compound	Molecular weight	Boiling point (°C)	Vapor pressure (torr)/(°C)	Solubility in water (mg/L)/(°C)	Henry's Law constant (atm-m^3/mole)	Biodegradability[b]
Phenol	94.1	182	0.53/20	67000/25	1.3×10^{-6}	fast/complete
Chloroform	119.4	61.7	150/20	9600/20	3.4×10^{-3}	slow/complete
Trichloroethylene	131.4	87	57.9/20	1100/20	11.7×10^{-3}	slow/partial
Benzene	78.1	80.1	95.2/25	1790/25	5.6×10^{-3}	slow/complete
Toluene	92.1	111	28.7/25	535/25	5.9×10^{-3}	fast/complete
o-chlorotoluene	126.6	159	3.5/24[d]	110/24[c]	5.3×10^{-3} [e]	slow/partial[c]

[a] From Ref. [12], except as noted.
[b] Biodegradation by acclimated bacterial cultures in static culture flask, excepted as noted, see Ref. [13].
[c] Unpublished data.
[d] Ref. [14].
[e] Calculated by vapor pressure/solubility in water.

therm capacity would have been lower if only phenol had been reported. The higher apparent loadings observed for these compounds in the pilot carbon columns relative to the their effluent isotherm capacities were results of biodegradation of phenol and stripping of the other five volatile compounds, see Table 9.

Daily backwashing, sometimes with air scour, was practiced during the six-month pilot study to prevent excessive pressure-drop across the carbon column. Such conditions promoted biodegradation of phenol [*18, 19*] and stripping of these adsorbed volatile compounds [*20, 21*], which accounts for the higher apparent loadings found in the pilot carbon columns. The pilot study results for monochlorotoluene are given for the sum of three isomers, while the isotherm data is for o-chlorotoluene alone. This fact also contributed to the higher apparent column loadings shown in Table 8.

CONCLUSIONS

Because of competitive adsorption, the capacities of carbon for the organic constituents of industrial wastewater samples were all reduced for their respective single compound isotherms. Reduction in capacity for a compound would be small when it is the predominant wastewater constituent, or when other organic wastewater constituents are much less adsorbable compared to the target compound. The capacity reduction for most wastewater constituents could be correlated with the %TOC attributable to the target compound—the smaller %TOC, the larger the capacity reduction.

The carbon exhaustion rate may be significantly lowered if a pretreatment step designed to reduce organic loading of the carbon adsorber is practiced. Biodegradation was found to be effective in reducing a leachate TOC and thus, extended the service period of the carbon adsorbers. Solvent extraction, however, was not an effective pretreatment for a high-TOC chemical landfill leachate since only a small portion of its organic constituents was removed. For a wastewater with a relatively constant composition, the order of capacity reductions for its organic constituents, due to competitive adsorption, would be likely to be preserved for samples having different background TOCs.

Independent treatment data for full-size carbon adsorber and column breakthrough curves for pilot-scale adsorbers have confirmed the lower adsorptive capacities of carbon for all compounds studied. These experimental findings are further validated by literature reports of similar observations [*22–27*]. The useful adsorber capacities (loading) for target compounds may also be signficantly reduced because of mass transport limitations, especially for removal of large size organic contaminants, such as color agents, in small single-bed adsorption system [*10, 28*].

Actual wastewater samples should be employed in adsorption isotherm and column breakthrough testings to define realistic adsorptive capacity and the maximum loading achievable under simulated operating conditions. Otherwise, premature breakthrough of many contaminants would result from overestimation of treatment capacity of the carbon adsorption system.

ACKNOWLEDGMENTS

Parts of the carbon isotherm data were presented at the 17th Mid-Atlantic Industrial Waste Conference at Lehigh University (Bethlehem, PA), June 23–25, 1985 and the 18th Mid-Atlantic Industrial Waste Conference at Virginia Polytechnic Institute and State University (Blackburg, VA), June 29–July 1, 1986. The paper was presented at the AIChE Spring National Meeting in Houston, Texas, April 2–6, 1989.

LITERATURE CITED

1. Swindell-Dressler Co., *Process Design Manual for Carbon Adsorption*, EPA Agency Technology Transfer Series, Chapter 4, October 1973.
2. Ying, W., Ph.D. Dissertation, Chapter IV, The University of Michigan, Ann Arbor, MI, 1978.
3. Weber, Jr., W. J., *Physiochemical Processes for Water Quality Control*, Wiley-Interscience: New York, NY, 210, 1972.
4. Weber, Jr., W. J. and W. Ying, "Integrated Biological and Physico-chemical Treatment for Reclamation of Wastewater", in *Proc. International Conference on Advanced Treatment and Reclamation of Wastewater*, IAWPR, Johannesburg, S. Africa, S. 131, June 1977.
5. Dobbs, R. A. and J. M. Cohen, "Carbon Adsorption Isotherms for Toxic Organics," EPA Report 600/8-80-023, 1980.
6. Ying, W., E. A. Dietz, and V. J. Hoffman, in *Toxic and Hazardous Wastes*, I. J. Kugelman, Technomic Publishing Co.: Lancaster, PA, pp. 166–185, 1985.
7. Ying, W., E. A. Dietz, and S. A. Sojka, in *Toxic and Hazardous Wastes*, G. D. Boardman, Ed., Technomic Publishing Co., Lancaster, PA, pp. 569–582, 1986.
8. *Standard Methods for the Examination of Water and Wastewater, 15th Ed.*, American Public Health Association, Washington, DC 1980.
9. Ying, W., R. R. Bonk, V. J. Lloyd, and S. A. Sojka, *Environ. Prog.* 5 (1), 41–50, 1986.
10. Ying, W. and M. E. Tucker, "Carbon Adsorption Treatment for Color Removal," presented at AIChE Summer National Meeting, Denver, CO, August 1988.
11. Malcolm Pirnie, Inc. "City of Niagara Falls Industrial Pretreatment Program, Phase 2 Report," Revised Draft, January 1984.
12. U.S. Environmental Protection Agency, *Treatability Manual, Vol. 1—Treatability Data*, EPA Report 600/8-80-042a, 1980.
13. Tabak, H. H., S. A. Quave, C. I. Mashni, and E. F. Barth, *J. Water Pollut. Control Fed.*, **53**, 1503–1518, 1981.
14. Shuzo, O., *Computer Aided Data Book of Vapor Pressure*, Data Book Publishing Co.: Tokyo, Japan, 984, 1976.
15. Snoeyink, V. L., D. Jenkins, *Water Chemistry*, John Wiley & Sons: New York, NY, 134, 1980.
16. Mattson, J. S. and H. B. Mark, Jr., *Activated Carbon—Surface Chemistry and Adsorption from Solution*, Marcel Dekker, Inc.: New York, NY, 129, 1971.
17. Ying, W., J. D. Duffy, and M. T. Jacobs, "Biological Treatment of Phenolic Wastewaters," Paper presented at 197th Am. Chem. Soc. Ann. Mtg., Dallas, TX, April 1989.
18. Ying, W. and W. J. Weber, Jr., *J. Water Pollut. Control Fed.*, **51**, 2661–2677, 1979.
19. Chudyk, W. A. and V. L. Snoeyink, *Environ. Sci. Tech.*, **18**, 1–5, 1984.
20. Ball, W. P., M. D. Jones, M. C. Kavanaugh, *J. Water Pollut. Control Fed.*, **56**, 127–136, 1984.
21. Lurker, P. A., C. S. Clark, and V. J. Elia, P. S. Gartside, and R. N. Kinman, *Am. Ind. Hyd. Assoc. J.*, **44** (2), 109–112, 1983.
22. Frick, B., R. Bartz, H. Sontheimer, and F. A. DiGiano, *Activated Carbon Adsorption of Organics from the Aqueous Phase*, Vol. 1, pp. 229–242, M. J. McGuire, and I. H. Suffit, Eds., Ann Arbor Science: Ann Arbor, MI, 1980.
23. Huang, J., C. T. Steffens, Competitive Adsorption of Organic Materials by Activated Carbon, Paper presented at 31st Purdue Industrial Waste Conference, May 1976.
24. Smith, E. H. and W. J. Weber, Jr., *Environ. Sci. Technol.*, **22**, 313-321, 1988.
25. Crittenden, J. C., P. Luft, D. W. Hand, J. L. Oravitz, S. W. Loper, and M. Arl, *Environ. Sci. Tech.*, **19**, 1037–1043, 1985.
26. Bilello, L. J., in *Application of Adsorption to Wastewater Treatment*, W. W. Eckenfelder, Jr., Ed., Enviro Press: Nashville, TN, pp. 151-174, 1981.
27. Chudyk, W. A., V. L. Snoeyink, D. Beckmann, and T. Temperly, *J. J. Am. Water Works Assoc.*, **71**, 529–538, 1979.
28. Ying, W., J. Duffy, and M. Tucker, *Environ. Prog.*, **7** (4), 262–269, 1988.

Fugitive Emissions From The Ethylene Oxide Production Industry

Ronald L. Berglund
Union Carbide Chemicals and Plastics Company Incorporated, South Charleston, WV
Robert R. Romano
Ethylene Oxide Industry Council, Chemical Manufacturers Association, Washington, D.C.
John L. Randall
Radian Corp., Austin, TX

As new programs are initiated by industry and federal or state regulatory agencies to reduce releases of hazardous air pollutants and reactive volatile organic compounds into the atmosphere, there are increasing questions over the loss of organic compounds from fugitive sources, the best method to estimate these losses, and the factors that influence these losses. The presently established method is to use generalized emission factors for each specific piece of equipment comprising a process unit. The accuracy of the estimates obtained using the available emission factors depends upon two features. These are first, the precision and accuracy of the actual emission factors or correlations themselves, and second, the resemblance of the systems from which the correlations were developed to those for which they will be applied.

INTRODUCTION

Significant fugitive emissions can occur due to design factors and inadequate monitoring or maintenance. To develop the existing industry–wide fugitive emission factors, the U.S. Environmental Protection Agency (EPA) sponsored an extensive sampling program and analyzed a large amount of data collected from various types of operating units. Based upon this analysis they determined that although much of the equipment in a process unit leaks to some degree, a small percentage with significant leaks contribute most of the equipment mass emissions from a typical unit. Following extensive public review and comment, the EPA evaluated the cost effectiveness of alternative control techniques for minimizing fugitive emissions, and defined a cost effective cutoff which would determine when a leak is of sufficient magnitude to warrant repair [*1*].

This cutoff, based upon a hydrocarbon screening measurement at the potential leak interface, was set at a concentration level of 10,000 ppm. In the absence of any data to the contrary, the present regulatory policy to apply these factors is to assume that leaking equipment of a specific type (i.e., gas valves, liquid valves, flanges, pumps, etc.) within a process unit tends to emit similar quantities of VOC as leaking equipment of the same type in another process unit [2]. Once a component is defined as leaking (i.e., above the 10,000 ppm cutoff), it is assumed to have VOC emissions at a certain average mass rate. Similarly, if the equipment of a specific type is defined as 'nonleaking' (i.e., below the 10,000 ppm cutoff), it is assumed to have emissions at a certain lower average mass rate. The average leak rate for specific types of equipment in a process unit was determined using a composite of the leaking and non-leaking equipment [*3*]. These fugitive emission factors for leaking, non-leaking and average equipment were known as the SOCMI (Synthetic Organic Chemical Manufacturing Industry) Fugitive Emission Factors. Up to the present time, state and federal regulatory staff have been limited to using these factors to estimate fugitive emissions of organic compounds from typical process units in developing emission inventories or specific emission standards and regulations.

Because these SOCMI factors were based upon measurements in only a few of the thousands of chemical processes represented in the chemical industry, and the estimates were not consistent with historical data obtained by ethylene oxide producers, it was believed by these producers that the SOCMI factors would not adequately characterize fugitive emissions from units handling chemicals which are toxic, explosive or otherwise hazardous.

In particular, it was believed that, independent of any regulatory guidance, most process units implement programs of visual, audible, olfactory or area monitoring, and inspection of operating equipment while others specifically design equipment to limit VOC losses for safety or economic reasons. If the equipment design or monitoring programs within an operating unit differs from that for which the EPA emission factors were developed, the percentage of equipment 'leaking' and the magnitude of the non-leaking emission rate may not be adequately represented by the EPA SOCMI factors [*4*].

TABLE 1. LOCATIONS AND CAPACITIES OF ETHYLENE OXIDE PRODUCTION FACILITIES

Producer	Location	Ethylene Oxide Nameplate Production Capacity Metric Tons/Year	Notes
1. BASF	Geismar, LA	218	a
2. Hoechst-Celanese	Clear Lake, TX	227	c
3. DOW Chemical	Plaquemine, LA	204	c
4. CAIN Chemical	Bayport, TX	204	a
5. Quantum	Morris, IL	100	c
6. Olin Chemical	Brandenburg, KY	57	d
7. PD Glycol (CAIN)	Beaumont, TX	68	a
8. Shell Chemical	Geismar, LA	363	a, b
9. SUN R&M	Claymont, DE	55	c
10. Texaco Chemical	Port Neches, TX	251	a
11. Texas Eastman	Longview, TX	97	a
12. Union Carbide	Seadrift, TX	286	a
13. Union Carbide	Taft, LA	572	a
		2,700	

a [9]
b One of two production units out of service at the time of this study.
c Data obtained directly from producing plant personnel.
d Out of service at time of study.

BACKGROUND

When the review of ethylene oxide as a possible hazardous air pollutant was initiated, the Ethylene Oxide Industry Council (EOIC) recognized that because of the highly reactive and explosive nature of the compound, and because of the low OSHA standard for ethylene oxide (1 ppm), the ethylene oxide production units were designed and operated to minimize fugitive emissions of ethylene oxide [*4, 5*]. In addition, a few limited studies had been conducted by some of the producers [*4, 5*] which also indicated that fugitive emissions from these sources would be low. However, the amount of data collected in these studies was limited and could not support the view that fugitive emissions of ethylene oxide from these production facilities were low throughout the industry. Furthermore, there was not an adequate sampling and data analysis procedure available which could be used to demonstrate that ethylene oxide fugitive emissions would be low. This limitation was eliminated, when, in late 1987, the EPA developed a new set of 'Protocols for Generating Unit-Specific Emission Estimates for Equipment Leaks of VOC and HAPS' [*6*]. At that time, a draft of these protocols was sent out for peer and public review, and they were finalized in November of 1988. In the interim, however, the Agency encouraged companies and industry groups to use these protocols to develop specific fugitive emission factors for their processes.

This paper summarizes the results of an industry–wide program to assess the magnitude of losses resulting from fugitive emissions at ethylene oxide production facilities, and presents a statistical analysis of the data collected. These results were collected from most ethylene oxide producers within the United States as part of a cooperative agreement between the Ethylene Oxide Industry Council (EOIC), a trade association of ethylene oxide producers and users within the Chemical Manufacturers Association, and the US Environmental Protection Agency. The data was collected during the second and third quarters of 1988, following the development of a special EOIC-EPA emissions estimation protocol, and the completion of an Ethylene Oxide Fugitive Emissions Workshop and Workbook [*7*] by Radian Corporation. An acceptable, standardized sampling protocol was essential in order to provide consistent and reliable results by all of the participants in the study.

OBJECTIVES OF STUDY

Three were four main reasons that encouraged the EOIC to initiate this study with the EPA. It was anticipated that the results of this EO industry-wide study could be used

1) to more accurately measure fugitive emissions of ethylene oxide for reporting under SARA 313;
2) to assist in developing priorities in internal company-wide air emission reduction programs;
3) to dispell potential public misconceptions regarding air emissions from these facilities which could occur from the use of existing SOCMI emission factors for EO units; and
4) to more accurately assess community exposure as the EPA evaluates the need for a specific air regulation for ethylene oxide.

ETHYLENE OXIDE PRODUCTION UNITS

Ethylene oxide has a molecular weight of 44, a vapor pressure of 1305 torr at 25°C, and is completely soluble in water [*8*]. Ethylene oxide is produced by the direct vapor phase oxidation of ethylene over a silver catalyst at 10 to 30 atmospheres pressure and 200°C to 300°C. The source of oxygen is either air or high purity oxygen. Nine of the present producers use the oxygen based process, while four use the air based process [*9*]. The main reaction is as follows:

$$H_2C = CH_2 + 1/2\,O_2 \rightarrow H_2C\text{—}CH_2 \quad (O)$$

Eleven companies at thirteen locations produce ethylene oxide in the United States. 2.6 million metric tons were produced in 1987. The majority of the ethylene oxide is used at the production site to produce ethylene glycol, glycol ethers and ethanolamines with capture feed levels being approximately 90 percent of actual EO production rates. The breakdown of ethylene oxide production is shown in Table 1 (taken from [*9*]), the location of these facilities is shown in Figure 1.

All of the current ethylene oxide producers listed in Table 1 participated in this study.

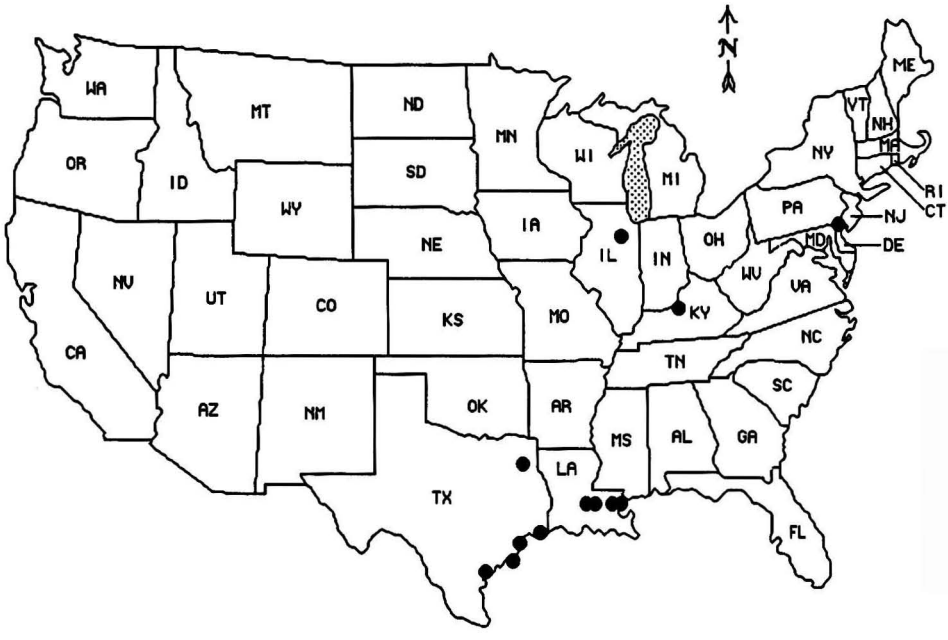

Figure 1. Locations of ethylene oxide production facilities.

SAMPLE COLLECTION

Equipment Included In Study

This study included all components on lines containing more than 1 percent ethylene oxide by weight that are accessible by platform, ladder or manlift device up to 40 feet above grade according to the following:

1. All valves, pumps, and compressors were included in the sampling program.
2. A statistical sample of connectors (including flanges and screwed fittings) were included in the study. Depending upon the number of components in the unit, a minimum of between 77 and 150 components in this category were to be sampled.
3. All safety valves not discharged to a header system, all sample points except those with a closed loop system, plugged or vented to a control device, and all open–ended lines except those plugged or blind flanged, were also included in the study.

A breakdown of the number of components included in the sampling program, by ethylene oxide concentration is shown in Table 2. Overall, 18,277 components in ethylene oxide service were included in this study. Four percent of these were inaccessable and were not actually sampled. Roughly 45 percent of all components were liquid valves, 18 percent were gas valves, 26 percent were flanges and connectors, 1 percent were pumps or compressors, 1 percent were safety valves, and 5 percent were sample points or open–ended lines. The number of flanges and connectors actually sampled represents about twenty-five percent of the total population of flanges and connectors in a typical ethylene oxide production facility.

Roughly 55 percent of the components sampled were on streams containing greater than 95 percent ethylene oxide. About twenty percent of the components were on lines containing less than 10 percent ethylene oxide.

Sampling Methodology

The approach used in the EOIC study would use EPA Method 21 to screen the components in the production units. This method describes the acceptable procedure for identifying and screening volatile organic compound leaks for valves, connectors/flanges, pumps, safety valves, process drains, open-ended lines as well as other sources. To use the method, several performance specifications are prescribed. These specifications require that the ana-

TABLE 2. ETHYLENE OXIDE PRODUCTION FACILITIES DISTRIBUTION OF COMPONENTS BY EO PERCENTAGE

	Number of Components In EO% Range						
Component Type	1%-2%	2%-5%	5%-10%	10%-50%	50%-95%	≥95%	Total
Valve (liquid)	294	415	245	912	1042	5418	8326
Valve (gas)	772	741	38	421	333	1001	3306
Flange	581	343	95	530	617	2576	4742
Sealed flange	1	0	1	2	13	8	105
Open-ended line	20	148	15	152	51	368	754
Pump	7	8	8	28	39	100	190
Safety valve	39	2	3	10	11	40	105
Sample point	0	4	3	4	2	17	30
Compressor	1	1	0	0	3	0	5
Total number:	1715	1662	408	2059	2111	9608	17563

lyzer used to monitor the equipment have a response factor of 10 or less for the compound of interest, a response time of less than 30 seconds, and must be intrinsically safe. In addition, it must be calibrated with a certified (±2%) standard gases. An Organic Vapor Analyzer (Foxboro OVA 108 or 128) was used to collect all the data included in this study. At most of the sites, a standard gas of ethylene oxide was used to check the response of the instrument to ethylene oxide on a regular basis. Atmospheric background measurements were also obtained every twenty sample points. The results were used to correct the equipment screening data for background hydrocarbons.

In addition to the measurements obtained from the analyzers on the actual equipment, specific ethylene oxide measurements were also obtained using Draeger Tubes or any other measurement device specific to ethylene oxide. These measurements were collected on a statistical portion of components containing mixtures of chemicals with ethylene oxide, very low or nondetectable screening measurements, or from the background air. At several of the sites a number of components were bagged (enclosed with tedlar), and actual emission rates from the component were measured. Some of the data obtained from these enclosed components was used to develop a default value for valves and flanges which had screening readings equal to background air.

Because of the potential hazard associated with ethylene oxide production facilities, and the complex nature of fugitive emissions screening, specific guidelines were provided to each participant. These included the need to stand upwind of sources being monitored, to calibrate instruments outdoors or in a hood, to undergo a safety review before initiating studies, and to cover the metal tip of the screening instrument with teflon tubing to prevent possible sparking from contact with rotating metal in the unit.

A typical fugitive emission screening program at one of the production units required between one and two weeks to complete, using a three-person crew.

DATA COLLECTION AND PROCESSING

A standardized ethylene oxide screening survey reporting form was prepared for all the participants in the study. This form was designed to provide the minimum data needed to meet the objectives of both the EOIC and the EPA as participants in the study. All participants in the program were encouraged to modify the forms as would best fit their own data collection needs. Information that would be needed in the study included:

- Plant ID = producers name and location
- Instrument ID = make, model number and serial number of the primary screening instrument
- Analyst name = identification of the persons doing the screening
- Date
- Background reading time
- Background value = instrument reading on the background air
- Average RF = average response factor from the most recent multipoint calibration of instrument using EO standard gases
- Location P&ID = specific ID number assigned by the producer
- Component Type: valves (VLV), flanges (FLN), pumps (PMP), safety valves (SV), compressors (COM), etc.
- Component Category: Valve type (globe, ball, gate, etc.), pump/compressor type (sealed, solvent flush etc.)
- Phase-type of material flowing through the component, gas (G) or liquid (L)
- EO% = amount of EO in the process stream (1 to 100%)
- Solvent Name = names of other materials in the stream
- Solvent % = percentages of other materials in the stream

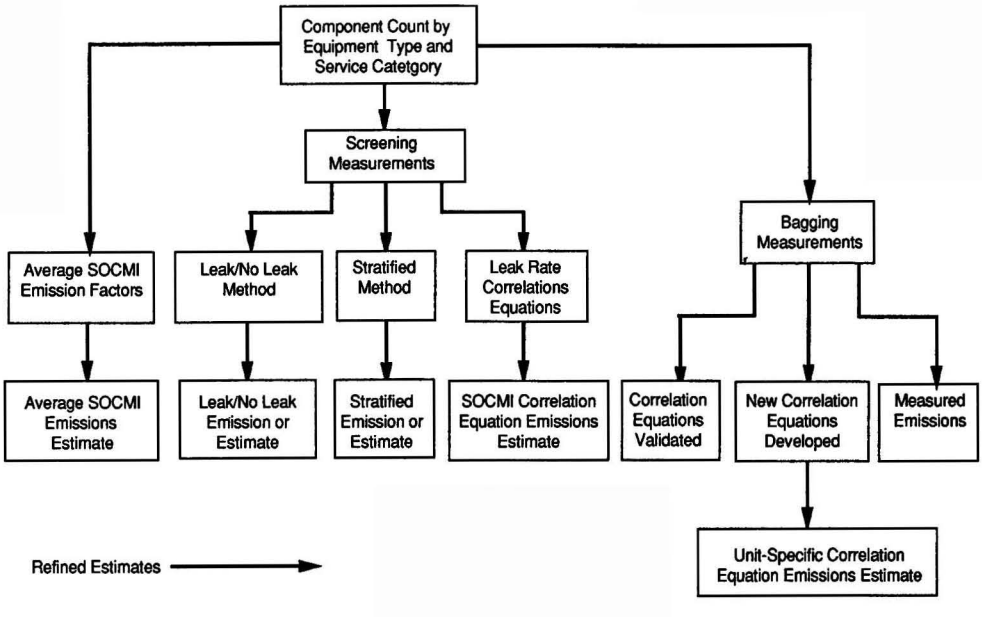

Figure 2. Overview of fugitive emissions estimation options.

TABLE 3. EPA SOCMI FUGITIVE EMISSIONS CORRELATION EQUATIONS[a,b]

Component Type	Service	Correlation Equation[c]	Number of Data Pairs	Correlation Coefficient	"Default Zero" Emission Rate (lb/hr)
Valve	Gas	$1.680 \times 10^{-5} \times (\text{SCRNVALU})^{0.693}$	99	0.66	0.000072
Valve	Liquid	$3.740 \times 10^{-4} \times (\text{SCRNVALU})^{0.470}$	129	0.47	0.001004
Flange	All	$3.731 \times 10^{-5} \times (\text{SCRNVALU})^{0.820}$	52	0.77	0.000209
Other	All	$1.335 \times 10^{-5} \times (\text{SCRNVALU})^{0.898}$	52	0.81	0.000088

[a] Emission estimates are calculated in lbs/hr.
[b] Taken from Table D-1 in Protocol for Generating Unit-Specific Emission Estimates for Equipment Leaks of VOC and VHAP, EPA Report, November, 1988 [6].
[c] SCRNVALU = Maximum OVA screening value in ppm.

DATA REDUCTION AND ANALYSIS

There are a number of steps that need to be taken to generate an industry wide fugitive emissions estimate for these ethylene oxide production facilities. The overall process is schematically represented in Figure 2 (adapted from [6]). As noted earlier, fugitive emissions in the chemical industry are considered to be those volatile organic compound (VOC) emissions that result when process fluid (either gaseous or liquid) leaks from plant equipment such as valves, pumps, pump seals, compressors, safety relief valves, and flanges. The first step in estimating fugitive emissions is to determined the population of sources, and the appropriate service category (gas or liquid), by counting or otherwise estimating, the number of process fittings in each source type/service category combination.

The next step after determining the source counts is to determine the appropriate method by which the emission factors are to be developed. With some overlap, and combination, there are presently five possible approaches using emissions factors that can be used to estimate fugitive emissions from a production unit. These are:

1) Use Average SOCMI Factors
2) Use SOCMI Leak/No-Leak Emission Factors
3) Use SOCMI Stratafied Emission Factors
4) Use SOCMI Leak Rate Correlations
5) Develop and use new Leak Rate Correlation

Average SOCMI Emission Factors

The first alternative does not require any additional monitoring. Under this option, the Average SOCMI Factors developed from the EPA's studies in the Synthetic Organic Chemical Manufacturing Industry would be applied to each of the components in the industry. However, the application of the average factors to existing ethylene oxide units is questionable in light of the special design and maintenance practices used in the units compared to those used to develop the average SOCMI factors.

All other emission estimation methods require that a screening survey be made of the components in the process area to be monitored.

SOCMI Leak/No-Leak Emission Factors

In Option 2, the EPA Leak and no-leak emission factors are used. In applying these factors, the screening data are first divided by component type, and then by screening value into leaker (greater than 10,000 ppm) or non-leaker (less than 10,000 ppm) categories. The number of components in either category are multiplied by the appropriate emission factor.

SOCMI Stratified Factors

Recognizing that the vast majority of components do not leak, or have very low emissions, the EPA redefined the Leak/no-leak strategy and developed a three tiered approach. Ranges of screening values were established at 0-1000 ppm, 1000 to 10,000 ppm, and over 10,000 ppm. The application of these factors follows the pattern of the leak/no-leak method (option 2). The components with screening values in each range are counted, then multiplied by the appropriate emission factor, and totalled.

SOCMI Leak Rate Correlation Curves

The emissions data collected by the EPA included both component screening measurements and actual fugitive emission leak rates from enclosed components. Statistical evaluation of this data led to development of correlation equations to relate screening values to leak rates for gas valves, liquid valves, flanges, and pumps (and all other components). Using this approach (option 4), the emission rate of each component is calculated from the appropriate correlation equation using the screening value. The total emissions would be a summation of all individual emission rates.

In using Option 5, screening of each component would be completed, but also a statistically significant number

TABLE 4. DISTRIBUTION OF SCREENING MEASUREMENTS FROM COMPONENTS AT EO PRODUCTION FACILITIES

Component	No. Components	<1 ppm	1-10 ppm	10-100 ppm	100-1000 ppm	1000-10000 ppm	>10,000 ppm (%)	*SOCMI >10000
Compressors	5	0	3	1	1	0	0 (0)	9.1
Flanges	4742	1372	2647	606	64	24	29 (0.6)	2.1
Open end lines	754	34	541	108	48	14	9 (1.2)	3.9
Pumps	190	27	87	32	30	6	8 (4.2)	8.8
Safety valves	105	0	98	6	1	0	0 (0)	3.6
Valves (gas)	3306	481	2345	227	70	43	40 (1.2)	11
Valves (liq)	8326	1600	5908	717	67	22	12 (0.1)	6.5
Total	17563	3514	11744	1811	281	111	102 (0.6)	

* SOCMI = % Expected to be greater than 10000 from SOCMI data base.

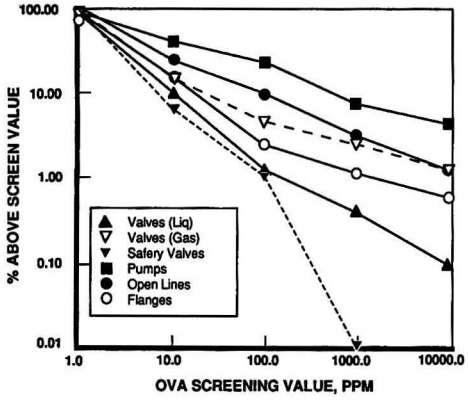

Figure 3. Distribution of screening measurements for major components in ethylene oxide production facilities.

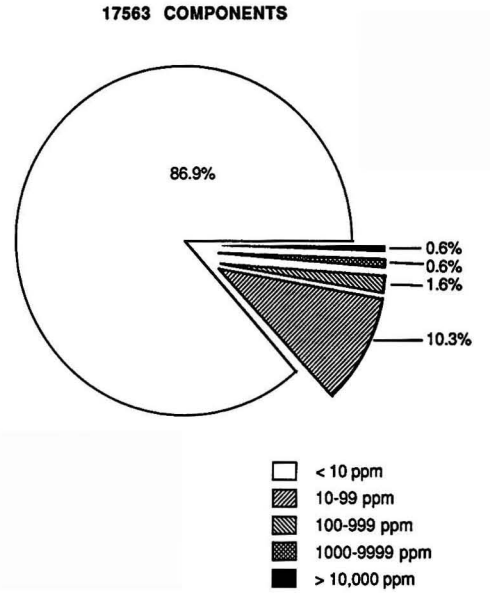

Figure 4. Ethylene oxide production facilities distribution of components by screening values.

of components would be bagged in order to develop a new leak rate correlation curve.

Data were collected in this study which would allow the use of any of the first four options. But, the fourth, more refined alternative was selected for use in this analysis. Under this alternative, screening measurements would be obtained for each of the components in the process, and the EPA Leak Rate Correlation (summarized in Table 3) for that source category would be used to estimate the actual emission rate. While this option had some significant limitations—most importantly that it uses a correlation curve comparing leak rate to screening value developed from data obtained for process units that were not representative of ethylene oxide production facilities—it was still believed that it would provide the best means of pinpointing potential problem areas as well as determining whether emissions from these units are significantly less than SOCMI values without requiring a costly complex bagging program.

DISCUSSION OF RESULTS

Because emissions resulting from leaks in the equipment present in a typical production unit are random stochastic occurrences, they cannot individually be predicted, but can best be handled statistically. A statistical breakdown of the screening measurements observed in this study are shown in Table 4. Also shown in this table is the percentage of 'Leakers' (components with screening measurements above 10,000 ppm) observed in the EPA/SOCMI analysis. Clearly, from this table, it can be observed that the data obtained from the ethylene oxide production units has a significantly lower amount of Leakers than was observed in the previous SOCMI studies. The most significant difference was for gas valves, where only 0.14 percent of the gas valves would be classified as 'Leakers', compared to 6.5 percent expected from the EPA/SOCMI analysis. The number of leaking pumps in this analysis (4.2 percent) was much closer to that expected from the SOCMI data analysis.

A further representation of the data in Table 4 is presented in Figure 3. This figure presents a probability distribution of the screening measurements obtained in this study for the major component types. The majority of the components monitored in this study for all component types had very low screening numbers (comparable to background air, or the lowest measurable level of the instrument). But, the distribution of screening measurements for the pumps and open-ended lines, were generally higher than those obtained from any of the remaining components, whereas the screening measurements for the safety valves were the lowest in the study. Over ninety percent of the safety valves had no measurable screening values, and no leakers or high emitters (components with screening values above 1,000 ppm) were observed.

TABLE 5. EMISSION FACTORS FOR EO PRODUCTION FACILITIES COMPARED TO AVERAGE SOCMI FACTORS
G/Hr/Component

Component Type	Number Components	Average SOCMI Factor	Average SOCMI Corr. Curve Factor	Average EO Factor
Liquid valves	8326	7.10	0.63	0.250
Gas valves	3306	5.60	0.22	0.200
Safety valves	105	104.00	0.07	0.070
Pumps	190	49.50	19.40	19.400
Flanges	4742	0.83	0.32	0.250
Open-ended lines	754	1.70	0.49	0.490
Compressors	5	228.00	0.35	0.350
Net Emissions*		100%		10%

* Net Emissions were calculated using the actual distribution of components screened in this study and assuming that only 25 percent of the actual flanges and connectors were actually sampled (this corresponds to a flange-to-valve ratio of 1.6).

TABLE 6. EOIC/EPA FUGITIVE EMISSIONS STUDY EMISSIONS IN EIGHT COMPONENT TYPES ATTRIBUTED TO "LEAKERS" AND "HIGH EMITTERS"

Component Type	"Leakers" % of Category	"Leakers" % of Total Emissions for Category	"High Emitters" % of Category	"High Emitters" % of Total Emissions for Category	Total % of Category	Total % of Total Emissions for Category
Gas valves	1.2	88	1.3	8	2.5	96
Liquid valves	0.14	49	0.26	9	0.4	58
Safety valves	0.0	0	0.0	0	0.0	0
Compressors	0.0	0	0.0	0	0.0	0
Pumps	4.2	95	3.2	3	7.4	98
Flanges	0.6	57	0.5	24	1.1	81
Open-ended lines	1.2	29	1.9	49	3.1	78
Sample points	0.0	0	0.0	0	0.0	0
Total	0.6	73	0.6	11	1.2	84

In summary, the screening data obtained in this study indicate that fugitive emission leakage from the ethylene oxide production units is lower than would have been expected from the previous SOCMI data. Figure 4 presents a summary of all the screening measurements from this study. Overall, 86.9 percent of the components were non-emitters (less than 10 ppm), 10.3 percent were very low emitters (100 to 1,000 ppm), 0.6 percent were high emitters and 0.6 percent were leakers. Based on estimates from the SOCMI data it would have been expected that between six and seven percent of all of the components would have been leakers.

EO Specific Emission Factors

Using the correlation between component screening value and emission rate developed from the previous EPA studies, an emission rate was calculated for each of the components monitored in this study, and an overall leak-rate for each source category developed. These are summarized in Table 5. Also shown in this table are the Average EPA SOCMI factors. Two separate emission factors for the ethylene oxide production units are included in this table. The first factor uses an EPA default value for any component which has a screening value below 8 ppm. The second feature was developed from the EPA Leak Rate Correlation curves—but using the bagging data for values and flanges—to calculate emissions from components with screening values less than 8 ppm.

As was seen in the screening estimates, the average emission factors developed for the ethylene oxide production units were significantly lower than the Average EPA SOCMI Factors. The average ethylene oxide emission factors varied from a factor of 2.5 times less than the average EPA value for pumps to a factor of over a thousand less for safety valves. Overall, emissions from the production facilities at the time of sampling would be equal to one tenth of the estimates from the Average EPA SOCMI emission factors.

The results in this study were also analyzed to determine the special influence or contribution of the high emitting sources, major component types, or ethylene oxide stream concentration to the overall emissions from the industry.

Table 6 shows the contribution of the equipment with screening measurements greater than 10,000 ppm (leakers), and greater than 1,000 ppm (high emitters) to the overall emissions for the different component types. The contribution of the "leakers" varied from 0 percent for compressors and safety valves where no leakers were detected, to 95 percent for pumps where only 4.2 percent of the components were leaking. Overall, the 0.6 percent of the components that were leaking accounted for 73 percent of the emissions estimated for these facilities. High emitters accounted for a much lower portion of the total emissions than leakers. High emitters also represented 0.6 percent of the components monitored in the study, but accounted for 11 percent of the total emissions. High emitters and leakers together accounted for 98 percent of the total emissions for pumps, and 96 percent of the total emissions for gas values. For all component types, high emitters and leakers represented 1.2 percent of the components monitored, but accounted for 84 percent of the total emissions.

Figure 5 summarizes the major source categories contributing to fugitive emissions in the ethylene oxide production industry. The single largest source of fugitive emissions was leaking pumps. Only eight leaking pumps were found in the study (out of 18,000 components screened), yet, they alone accounted for 30 percent of the total estimated EO emissions. The single largest component type contributing to the total emissions was flanges, which represents about 60 percent of the total number of components in a facility (only about one quarter of which were actually sampled), and would account for 40 percent of the total emissions. Overall, as noted above, leaking equipment accounted for over 70 percent of the total emissions measured in this study.

It is significant to note that the components in low ethylene oxide service (1 to 2 percent), which represented

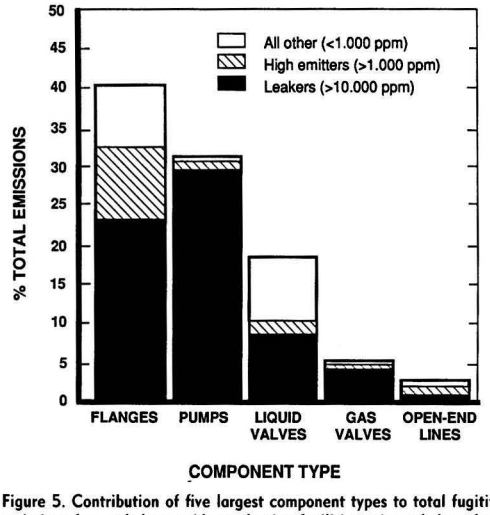

Figure 5. Contribution of five largest component types to total fugitive emissions from ethylene oxide production facilities using ethylene fugitive emission.

less than ten percent of the components sampled, accounted for over half (54 out of 102) of the leakers found in this study. Most of these were on gas valves and flanges. These emissions still only represented ten percent of the total estimated emissions for the industry.

WHY LOW FUGITIVE EMISSIONS IN ETHYLENE OXIDE PRODUCTION UNITS?

It was generally recognized that fugitive emissions of ethylene oxide would be low because of special programs in place in the units due to the hazardous and explosive nature of the chemical. After the results of this study were analyzed and low fugitive emissions verified, a special survey of ethylene oxide production facilities was initiated to determine why fugitive emissions from these sources are lower than has been observed in the previous SOCMI studies. In particular, the units were asked to summarize any monitoring, maintenance, or design programs in place that they believe limit fugitive emissions. In addition, a preliminary survey of special programs within the ethylene oxide production industry was conducted by the EPA several years ago [*11*] when the original emissions estimates for these units were prepared by the EPA. At that time a number of specific programs for ethylene oxide units were cited as influencing the low fugitive emissions. These included:

- Installation of ethylene oxide and flammable gas detectors in strategic plant locations, with sample analyses performed regularly
- Equipping ethylene oxide pumps with double mechanical seals having liquid buffer zones and alarms or automatic pump shutoffs in case of seal failure
- Using pressurized nitrogen in labyrinth shaft seals of centrifugal ethylene oxide compressors
- Use of all welded construction, where possible, to minimize the number of flange joints
- Using leak detectors for critical flanges in ethylene oxide piping
- Providing extra maintenance for ethylene oxide piping
- Analyses of rotating equipment for vibration characteristics to anticipate pending problems
- Collection, absorbing in water, and discharging to sewer any ethylene oxide leakage or drainage from sampling operations and pump vents
- Daily inspection for leaks by plant personnel
- Immediate leak repair

A few of the plants had been engaged in a formal state leak detection and repair program for a short time prior to this study (generally only one to two quarters). However, many of the components sampled as part of this study had not been included in the leak detection and repair programs. Thus, it would be expected that the average emission factors developed in this study would still be representative of fugitive emissions from the ethylene oxide production industry with no formal state or federal fugitive emissions control programs in place.

INDUSTRY RESPONSE TO STUDY

The companies involved in this study have been using data collected at their facilities and the industry-wide analysis to reevaluate their internal programs. All leaking components were repaired shortly after being detected. Thus, there was an immediate 75 percent reduction in estimated fugitive emissions from these facilities as a result of this program. In addition, some plants are modifying the special maintenance and monitoring programs discussed above to include components in low ethylene oxide service, and to give increased attention to pumps.

ACKNOWLEDGMENT

This study was completed as part of a cooperative agreement between the Ethylene Oxide Industry Council of the Chemical Manufacturers Association and the United States Environmental Protection Agency. However, the results have not been subjected to the Agency's peer and administrative review and therefore may not necessarily reflect the views of the Agency and no official endorsement should be inferred.

The authors of this paper and the Ethylene oxide Industry Council acknowledge the special efforts of the environmental and process unit staffs of the companies participating in this study, who needing to collect the data used in this analysis under very tight deadlines, completed the task admirably. We also appreciate the assistance provided by T. A. Kittleman and R. Henderson of Dupont, who, as representatives of the CMA Fugitive Emissions Workgroup, reviewed the protocol, and workbook developed for this study, and participated in the Ethylene Oxide Workshop, and to R. E. Rosensteel, and D. W. Markwordt of the USEPA who actively participated in this cooperative agreement, and to G. E. Harris of Radian.

LITERATURE CITED

1. Dimmick, W. Fred, and K. C. Hustvedt, "Equipment Leaks of VOC: Emissions and Their Control," Paper no. 84-62.1 presented at 77th Annual Meeting of the Air Pollution Control Association, San Francisco, California, June 24-29, 1984.
2. US Environmental Protection Agency, Control of Volatile Organic Compound Leaks For Synthetic Organic Chemical and Polymer Manufacturing Equipment, Research Triangle Park, NC. Publication No. EPA-450/3-83-006, 1983.
3. Radian Corporation, Emission Factors for Equipment Leaks of VOC and HAP, Research Triangle Park, NC. Publication No. EPA-450/3-86-002, January, 1986.
4. Berglund, R. L., and D. A. Wood, "Continuous Monitoring of Ethylene Oxide Fugitive Emissions," paper presented at the 80th Annual Meeting of the Air Pollution Control Association, New York, NY, June 23 to 26, 1987.
5. Nevell, M., Testimony on behalf of the Ethylene Oxide Industry Council before the National Air Pollution Control Techniques Advisory Committee (NAPCTAC), August, 1986.
6. United States Environmental Protection Agency, Protocols for Generating Unit-Specific Emission Estimates for Equipment Leaks of VOC and VHAP, EPA Report, November, 1988.
7. Ethylene Oxide Industry Council, Workbook for Estimating Ethylene Oxide Fugitive Emissions, March, 1988.
8. Conway, R. A., *et. al.*, "Environmental Fate and Effects of Ethylene Oxide," Environ. Sci. Technol., Vol. 17, No. 2, p. 107-112 (1983).
9. Markwordt, D. W., Sources of Ethylene Oxide Emissions, EPA-450/3-85-014, US Environmental Protection Agency, Office of Air Quality Planning and Standards, Research Triangle Park, NC, April, 1985.
10. United States Environmental Protection Agency, "Technical Report: Ethylene Oxide Production," July 30, 1986.
11. United States Environmental Protection Agency, Locating and Estimating Air Emissions From Sources of Ethylene Oxide, November, 1985 Draft.

Gas Reburning-Sorbent Injection for Controlling SO_x and NO_x in Utility Boilers

W. Bartok and B. A. Folsom
Energy and Environmental Research Corporation, 18 Mason, Irvine, CA 92718

M. Elbl
Illinois Department of Energy and Natural Resources, 325 West Adams Street, Springfield, IL 62706

F. R. Kurzynske
Gas Research Institute, 8600 West Bryn Mawr Avenue, Chicago, IL 60631

and

H. J. Ritz
U.S. Department of Energy, Pittsburgh Energy Technology Center, P.O. Box 10940, Pittsburgh, PA 15236

As part of DOE's Clean Coal Technology program, a field evaluation of Gas Reburning-Sorbent Injection (GR-SI) technology is being carried out by Energy and Environmental Research Corporation. The project is co-funded by the Gas Research Institute and the State of Illinois Department of Energy and Natural Resources. GR-SI technology is applicable to the control of emissions of acid rain precursor species, oxides of nitrogen and sulfur from coal fired utility boilers. Three units representative of pre-NSPS design practices, a 117 MW_e wall, a 71 MW_e tangentially, and a 33 MW_e cyclone fired boiler located in Illinois will be the host sites for this three-phase demonstration project.

Process specification studies have confirmed that GR-SI technology is capable of achieving the stated goals of the project, 60 percent reduction in NO_x and 50 percent reduction in SO_2 emissions. NO_x emissions will be reduced by staged fuel addition using natural gas as the reburn fuel, while SO_2 emissions will be reduced by capturing sulfur by dry, calcium based sorbent injection which will be augmented by the displacement of about 15-20 percent of the coal input by natural gas firing.

Phase 1, Design and Permitting, was completed earlier this year. In addition to process specifications which focused on injection system design criteria and precipitator enhancement approaches, detailed environmental information has been developed, including the assessment of waste disposal options and performing permitting work. In Phase 2 of the project, anticipated to be initiated in 1989, installation and check-out will be performed. The project will culminate in sustained 12-month demonstrations of the technology on each host unit. Results of Phase 1 and plans for subsequent work will be discussed.

INTRODUCTION

Sulfur dioxide (SO_2) and nitrogen oxides (NO_x) have been recognized as air pollutants for decades due to their effects on human and animal health, damage to vegetation, and the role of NO_x in producing smog. More recently, SO_2 and NO_x have been implicated as potential precursors of acid rain precipitation which has caused damage to lakes, streams, and vegetation in the northeastern portion of the United States, in Eastern Canada, and in Europe.

The inventory of SO_2 and NO_x emissions in the United States is produced by a wide range of sources, and coal combustion in utility boilers represents a significant fraction. Many coal fired utility boilers are already required to control SO_2 and NO_x emissions to some extent. Units erected after about 1971 are required to meet New Source Performance Standards (NSPS). In addition, in areas where ambient levels of SO_2 and/or NO_x exceed ambient air quality standards, some older units are also subject to controls. Concern over acid rain has prompted proposals

for "acid rain legislation" to provide further SO_2 and NO_x emission control. Since newer units are already controlled, the primary targets are older, pre-NSPS units.

Control of SO_2 and NO_x emissions has important consequences for the power generation industry. The most straightforward way of controlling SO_2 emissions is to switch to a lower sulfur coal. The emission control regulations now in effect have already resulted in significant coal switching causing severe economic hardship in areas where medium and high sulfur coals are mined. The primary SO_2 control alternative is a wet scrubber. Scrubbers are expensive both to install and to operate. They are particularly difficult to retrofit to older units where provisions for such emission control were not considered in the initial design. Also, the limited remaining lives of these older units makes capital intensive scrubber retrofits particularly costly.

NO_x emissions can be controlled to some extent by combustion modification techniques, such as low NO_x burners. However, the control effectiveness is very site-specific. Post combustion NO_x emission controls, such as selective and non-selective catalytic reduction, are effective but very costly.

There is a need for a new approach to SO_2 and NO_x emission control for coal fired utility boilers; an approach that will provide effective SO_2 and NO_x emission control on existing pre-NSPS units without coal switching or excessive costs. Several control technologies are now under development for this specific application. This paper discusses one of these technologies: gas reburning-sorbent injection (GR-SI). A field evaluation project is now in progress to bring this technology to commercial status by demonstrating its cost-effective emission control on three coal fired utility boilers with varying designs. The technology and its application to coal fired utility boilers is discussed. The field evaluation project and progress to date are also presented.

GAS REBURNING-SORBENT INJECTION

GR-SI is an integration of two developmental technologies: gas reburning for NO_x control and sorbent injection for SO_2 control. GR-SI can be retrofitted to existing coal-fired combustion equipment at low capital cost. SO_2 and NO_x emission control of 50 and 60%, respectively, should be achievable with virtually any type of combustion equipment.

Reburning

The concept of NO_x reduction by flames has been recognized for two decades. The flue gas incinerator was developed by the John Zink Company [*1*], and Sterneling, et al. [2] found that NO_x could be reduced in laboratory flames by injecting methane into the combustion products. Reburning for in-furnace NO_x control has been applied to boilers in Japan [*3, 4*]. Work is being supported in the United States by the U.S. Environmental Protection Agency, the Electric Power Research Institute, and the Gas Research Institute [5–7].

In the reburning process, most of the fuel is burned in conventional burners under fuel-lean conditions. A reburning fuel is injected downstream of the main combustion zone to reduce NO_x. The reburning process is illustrated in Figure 1. The overall process can be divided into three zones in series:

Main Combustion Zone. Approximately 80–85% of the heat is released in this zone under fuel-lean conditions producing NO, together with products of combustion that form the input to the reburning zone.

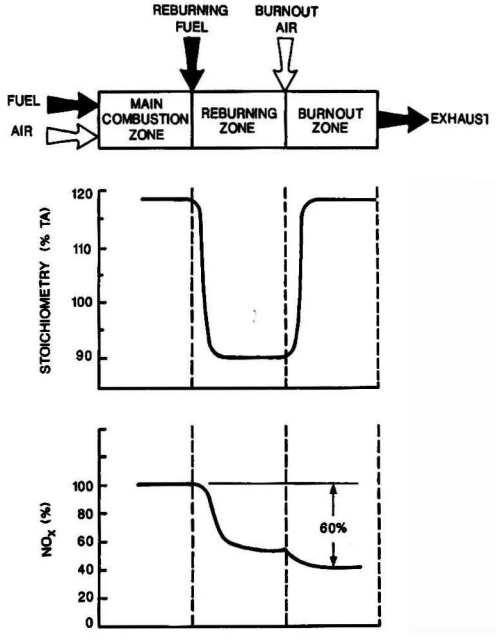

Figure 1. Reburning process.

Reburning Zone. The reburning fuel (normally 15 to 20% of the total heat input to the boiler) is injected downstream of the main combustion zone to create a fuel-rich, NO_x reduction zone. NO formed in the main heat release zone reacts with hydrocarbon free radicals during the oxidation of the reburning fuel to produce intermediate species such as HCN and NH_3, and the non-pollutant species, N_2. In the reburning zone, most of the NO produced in the main combustion zone is effectively reduced to N_2.

Burnout Zone. In the third and final zone, additional combustion air is added to oxidize any remaining fuel fragments and produce overall fuel-lean conditions. The remaining reduced nitrogen species (NH_3 and HCN) are either oxidized to NO or reduced to N_2.

Any fuel that produces hydrocarbon free radicals, including coal, oil, or natural gas, can be considered as a candidate for reburning fuel. Fuels that contain considerable amounts of bound nitrogen, such as coal and some oils, can increase the severity of the problem, since the bound nitrogen can be oxidized to form additional NO_x. Also, since residence time is limited in commercial systems, a fuel that is supplied in a gaseous state and does

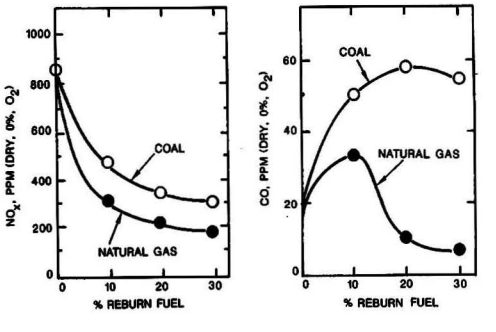

Figure 2. Comparison: coal and gas reburning in pilot scale tests.

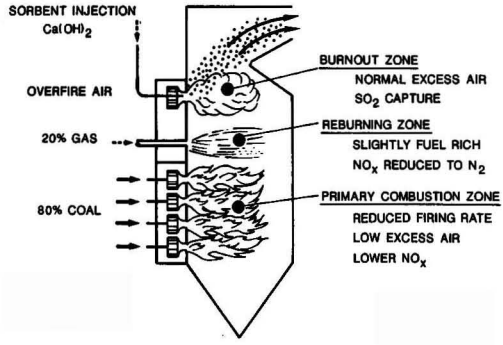

Figure 3. Gas reburning—sorbent injection.

not require vaporization or devolatilization and char or soot combustion (as oil and coal do) is desirable. Thus, natural gas offers distinct advantages as the reburning fuel of choice.

Extensive bench- and pilot-scale tests have been conducted to compare the performance of alternate reburning fuels and to evaluate NO_x control effectiveness and process design considerations [7]. Figure 2 shows the results of comparative tests with coal and gas reburning fuels in a pilot-scale combustion test facility. A high sulfur Illinois bituminous coal was fired in the primary zone. The reburning fuel (coal or gas) was injected downstream of the primary zone and burnout air was injected at 1622 K (2460°F). The NO_x and CO emissions were sampled from the exhaust. As shown in Figure 2, NO_x emissions decreased rapidly as the reburning fuel was increased from zero. Natural gas was more effective than coal, as expected.

CO emissions are an index of combustion efficiency. With gas as the reburning fuel, CO emissions increased slightly at low reburning fuel injection rates, probably due to incomplete mixing. However, as the reburning fuel injection rate was increased to the optimum level for NO_x emission control, 15–20%, CO emissions decreased to less than baseline levels. In contrast, with coal as the reburning fuel, CO emissions increased to about three times baseline levels. Measurements of carbon content of the fly ash confirmed that the reburning coal was not being burned effectively. The carbon content increased by about a factor of 10 with coal reburning. This highlights a significant problem in the application of coal reburning: limited residence time in the upper furnace of pre-NSPS coal fired units.

Sorbent Injection

Sorbent injection is an SO_2 control technology, whereby a calcium based sorbent is injected into the combustion products where it reacts with SO_2 to form a solid powder, either calcium sulfate, or calcium sulfite, which is collected in an electrostatic precipitator or bag filter. Ideally, the dust collection device will be the existing device used for fly ash control. Several sorbent injection processes are now in various stages of development. They differ primarily in the location of the sorbent injectors. Upper furnace sorbent injection has been studied most extensively and will be evaluated in this project [8]. The process involves injection of a calcium based sorbent which may be either a carbonate or a hydrate. The sorbent is calcined in the high temperature combustion products to produce reactive calcium oxide. The calcium oxide reacts with SO_2 and oxygen to produce solid calcium sulfate. Two major parameters control the utilization of the calcium in the sorbent and thus the cost effectiveness of the process. These are:

Calcium Oxide Reactivity. This depends strongly on the surface area of the calcine, which is a function of the sorbent type and the thermal history of the calcine. Reactivity tends to decrease as the sorbent particle temperature is increased.

Calcine Residence Time Available Under Sulfation Conditions. Significant sulfation cannot occur above approximately 1500 K (2250°F) and the rate of sulfation becomes negligible below approximately 1140 K (1600°F). Thus, the residence time of the calcine within this "temperature window" has a significant impact on sulfur capture potential.

The primary disadvantage of sorbent injection is that the sorbent is not utilized effectively. Under optimum conditions, only 20 to 30% of the sorbent is reacted with SO_2. The remainder exits the boiler as unreacted calcium oxide. Thus, high sorbent injection rates are required to achieve significant SO_2 emission reductions. This results in high sorbent cost and poses an extreme load on an existing ash collection system, such as an electrostatic precipitator. While the capital cost of sorbent injection is low, the cost of upgrading a precipitator is high. These factors limit the SO_2 control achievable by sorbent injection.

Technology Integration

Gas reburning and sorbent injection can be applied together to achieve combined SO_2 and control NO_x in an easily retrofitted low cost system. Figure 3 shows the application of gas reburning-sorbent injection (GR-SI) to a commercial wall-fired utility boiler. The main burners firing coal with excess air are turned down to about 80% of the full load heat input and are operated at the lowest practical excess air level, which reduces NO_x emissions slightly. The gas reburning fuel is injected above the burners, providing a slightly fuel-rich reburning zone. In this zone, the NO_x produced from the main combustion zone is reduced mostly to N_2. The optimum stoichiometry for NO_x reduction is in the range of 90% theoretical air. The remainder of the combustion air is injected through overfire air ports above the reburning zone to complete combustion. The sorbent is injected into the upper furnace, possible through the overfire air ports as shown, or through other ports into the right temperature window for optimum SO_2 control.

The gas reburning and sorbent injection processes are complimentary. They are physically compatible. Also, since their application does not depend on the characteristics of the primary combustion system, they should be applicable to virtually any coal fired boiler including stokers, cyclones, or pulverized coal fired equipment (wall- or tangentially fired). Of course, the GR-SI hardware must be designed within the specific constraints of the existing furnace and this requires a site-specific optimization. The gas reburning system alone achieves an incremental reduction in SO_2 emissions, since natural gas contains no sulfur. This reduces the amount of sorbent that must be injected to achieve a specific SO_2 emission goal, reducing sorbent cost and the need for dust collector upgrades.

GR-SI Cost Effectiveness

GR-SI has a low capital cost. The gas reburning system involves gas piping, some simple gas injectors, and overfire air ports. Sorbent injection requires sorbent storage and feeding equipment, sorbent injectors, some dust collector upgrades and ash disposal provisions. Neither

TABLE 1. HOST SITE CHARACTERISTICS

General			
Utility Company,	Illinois Power	CILCO	CWLP
Station, unit	Hennepin, 1	Edwards, 1	Lakeside, 7
Location: State	Illinois	Illinois	Illinois
Capacity (MW) net	71	117	33
Boiler			
Firing configuration	Tangential	Front wall	Cyclone
Capacity (10^3 lb/hr)	585	850	320
Manufacturer	CE	Riley	B&W
Precipitator			
Location	Cold side	Cold side	Cold side
Size (SCA)	223	137	333-1000
Manufacturer	Buell	American Standard	Smidth
Fuel			
Coal type	Illinois, bit	Blend Illinois, bit Kentucky, bit	Illinois, bit

technology requires re-routing of flue gas ducts, chemical processing equipment, major power consuming equipment, or significant changes to normal plant operation and maintenance. The total capital cost for GR-SI is in the range of 50 $/kW for small unites (under 150 MW) and somewhat less for larger units. GR-SI operating costs are primarily for sorbent. Thus, sorbent unit cost and sorbent utilization are the key factors influencing operational cost. Additional operational costs are for waste disposal, operation and maintenance labor, etc. Gas generally costs more than coal, but this cost element may abe mitigated by the ability to fire a higher sulfur coal in some cases. Depending on these factors, the operational costs for GR-SI are estimated to be in the range of approximately 6–9 mills/kWh.

GR-SI should have a definite market niche. Its very low capital cost and ease of retrofit make it very cost effective for older pre-NSPS units with limited life, especially if these units are operated with low capacity factors that minimize operating costs. It should be noted that GR-SI performance and costs are highly site dependent. Unit design and operational characteristics, unit location, the availability of sorbent, coal, and gas and their relative costs are key factors.

GR-SI FIELD EVALUATION PROJECT

Overview

Energy and Environmental Research Corporation (EER) is conducting a field evaluation project to demonstrate the technical feasibility and cost effectiveness of GR-SI [9, 10]. The project is funded jointly by the U.S. Department of Energy, the Gas Research Institute, and the State of Illinois Department of Energy and Natural Resources. The focus of this project is to demonstrate the application and performance of the combined technology that will allow cost-effective control of SO_2 and NO_x from pre-NSPS coal-fired utility boilers.

The project is being conducted in three phases:

- Phase 1—Design and Permitting
- Phase 2—Construction and Startup
- Phase 3—Operation, Data Collection, Reporting and Disposition

Phase 1 of the project was initiated in June 1987. The final third phase will be completed in 54 months from the starting date.

A major feature of this project is that GR-SI will be demonstrated on all three types of coal-fired boilers typical of pre-NSPS designs (i.e., wall-, tangential- and cyclone-fired units). Each host site is being considered separately, based on its unique design parameters, operating history, and performance requirements. These factors are being evaluated by reviewing historical operating and performance data and plant design specifications. At each site, field tests have been conducted to quantify performance and emissions over the normal duty cycle. Several alternative and complementary technologies will be considered: gas reburning for NO_x control, a range of approaches to sorbent injection for SO_2 control, and coal cleaning. A technology combination will be selected for each site that meets the emissions control and performance objectives at minimum total cost. This process definition includes specification of all major components and projection of performance for each host site.

Phase 1, has culminated in a complete plan for the remainder of the project. In Phase 2, the GR-SI system will be retrofitted to each utility unit in a staggered schedule commensurate with the utility's operating and outage plans. In Phase 3, each unit will be subjected to a comprehensive eighteen-month field evaluation. The first six months will include detailed tests to optimize performance for the best balance of SO_2 and NO_x emission control commensurate with normal utility operation, and tests with alternate coals and sorbents so as to provide a database for future GR-SI applications. The GR-SI operation will then be turned over to the plant operators who will operate each unit at normal dispatch for a one year period. Emissions and performance will be monitored by EER to confirm long-term performance.

Table 1 summarizes the characteristics of each host unit. The three sites selected are relatively small utility boilers now in commercial operation in the State of Illinois. All are pre-NSPS units and operate with relatively low capacity factors (less than 45%). This makes them attractive for cost-effective GR-SI installation if combined SO_2 and NO_x emission controls are required. All fire Midwest bituminous coals and are equipped with cold-side electrostatic precipitators for particulate emission control. These host units differ in several significant respects:

- Firing configuration and capacity
- Precipitator size
- Fuel characteristics
- Emission constraints

The tangential- and cyclone-fired units fire medium sulfur Illinois coals. The emission control goals for these units are reductions in NO_x and SO_2 emissions of 50 and 60%, respectively. While these reductions are not required to meet existing regulations, they could be used to meet acid rain control regulations, if and when they are promulgated.

The wall-fired unit has no NO_x emission limit at present, but blends medium sulfur Illinois coal with a low

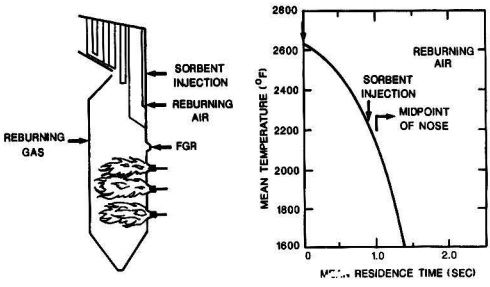

Figure 4. GR-SI for wall-fired host site.

sulfur Kentucky coal to meet an SO_2 emission limit of 1.8 lb/10^6 Btu. The SO_2 emission control goal for this unit is to increase the fraction of Illinois coal fired from 15 to over 50 percent, while maintaining SO_2 emissions in compliance. NO_x emissions will be reduced by 60 percent as in the other two cases.

Status

Phase 1 of this project was completed in 1989. An initial evaluation of each host site has confirmed that the project goals of 60% NO_x control and 50% SO_2 control at each site are achievable with gas reburning and upper furnace sorbent injection. Comprehensive process design studies have been completed. Physical models of each furnace (approximately one-tenth scale) have been constructed and isothermal flow visualization and measurement studies have been conducted. Field tests have been conducted to measure furnace velocities and temperatures. These data have been used to calibrate EER's three-dimensional furnace heat transfer model. Candidate locations for reburning fuel and burnout air have been selected. Mixing studies have been conducted in the physical model to define optimum injection nozzle configurations.

These process design studies provided the basis for the engineering design work. Details of the GR-SI process design studies related to NO_x and SO_2 emission control performance predictions, mixing studies for gas, reburn air and sorbent, injector nozzle specifications, thermal performance, and boiler impact predictions were made using the tangentially fired unit as an example [*11*]. For electrostatic precipitator performance enhancement, duct humidification that decreases the flue gas volumetric flow rate and decreases fly ash conductivity by cooling, injection of SO_3 for enhancing fly ash conductivity and precipitator plate area extension have been assessed on a site-specific basis.

The design approach for the wall-fired unit is illustrated in Figure 4. This unit has a relatively short distance between the upper row of burners and the furnace nose and requires careful placement of the reburning fuel and burnout air injectors so as to achieve adequate mixing in the limited residence time. During normal operation of this unit, all four rows of burners are in service. With GR-SI, the upper row of burners will be removed from service. Burner cooling will be provided by a bleed of recirculated flue gas. The reburning gas will be injected, along with some flue gas through a row of small injectors along the rear wall of the furnace opposite the upper burner row. Burnout air will be injected from the front wall between the waterwall platens. Sorbent will be injected at a higher furnace elevation opposite the nose where the gas temperature is optimum for SO_2 reaction.

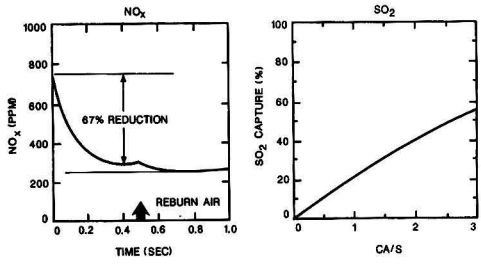

Figure 5. GR-SI performance predictions.

Predictions of NO_x reduction and sulfur capture are illustrated in Figure 5. This configuration provides a residence time of approximately 0.5 second in the reburning zone. NO_x decreases rapidly to about 300 ppm following gas introduction. Injection of the burnout air reduces NO_x emissions slightly further for a total predicted GR performance of 67 percent.

This wall-fired unit currently meets its 1.8 lb/10^6 Btu SO_2 emission limit by firing a blend of 85% low sulfur and 15% medium-to-high sulfur coal. GR-SI will allow this emission limit to be maintained while increasing the fraction of high sulfur coal fired to 57%. Figure 5 shows the SO_2 capture achievable with this blend. A Ca/S molar ratio of less than 2.0 will be adequate, because of the contribution of gas reburning to the overall reduction in SO_2 emissions.

Recent efforts have focused on translating these process designs into hardware designs, completing the baseline unit performance and emissions tests, and preparing environmental documents to demonstrate compliance with the National Environmental Policy Act [*12*]. As part of the environmental studies, permitting designs have been initiated. Waste management options have also been assessed on a site-specific basis. Dry disposal of the GR-SI into off-site landfills for the wall- and cyclone-fired units, and wet disposal into a new onsite ash pond for the tangentially fired unit are being considered. An industry panel has been organized for technology transfer and for ensuring the usefulness of the results to industry.

CONCLUSIONS

Phase 1 of a field evaluation project designed to demonstrate GR-SI technology for combined control of NO_x and SO_2 emissions from three pre-NSPS coal fired utility boilers in Illinois has been completed. The host units are wall-, tangential-, and cyclone-fired boilers, representative of pre-NSPS design practices. To achieve cost effective emission control with targets of 60% reduction in NO_x and 50% reduction in SO_2, process design studies have focused on mixing studies for specifying injector designs for reburn gas, overfire air and dry, calcium-based sorbent injection on a site-specific basis. Thermal performance and boiler impacts have also been predicted. ESP performance enhancement options and GR-SI waste disposal options have also been assessed.

Phase 1 will be followed by the preparation of detailed plans for equipment construction and startup in Phase 2, and the operating data collection, reporting, and disposal in Phase 3. The overall project will be completed by the end of 1992. For technology transfer to potential users, the Industry Panel will be briefed on the results of the study. It is expected that if acid rain regulations are promulgated for the control of NO_x and SO_2 emissions, the market niche for this low capital cost GR-SI technology will be for older, pre-NSPS units with limited life, operating at relatively low capacity factors.

ACKNOWLEDGMENTS

The information presented in this paper is related to work funded by the U.S. Department of Energy, Pittsburgh Energy Technology Center, through Cooperative Agreement No. DE-FC-22-87PC79796; the Gas Research Institute through Contract No. 5087-254-1494; and the State of Illinois, Department of Energy and Natural Resources through a Coal and Energy Development Agreement.

LITERATURE CITED

1. Reed, R. D., John Zink Company, U.S. Patent 1,274,637, 1969.
2. Sternling. C. V., et al., 14th Symp. (International) on Combustion, p. 897, The Combustion Institute, 1973.
3. Takahasi, Y., et al., "Development of Mitsubishi MACT In-Furnace NO_x Removal Process," Paper presented at U.S.-Japan NO_x Information Exchange, Tokyo, Japan, May 25–30, 1981.
4. Ogikami, N., et al., U.S. Patent 4,395,223, 1983.
5. Greene, S. B., et al., "Bench-Scale Process Evaluation of Reburning and Sorbent Injection for In-Furnace NO_x/SO_x Reduction," EPA-600/7-85-012, March, 1985.
6. Greene, S. B., et al., "Bench Scale Process Evaluation of Reburning and Sorbent Injection for In-Furnace NO_x Reduction," ASME Paper No. 84-JPGC-APC-9, 1984.
7. Seeker, W. R., et al., "Controlling Pollutant Emissions from Coal and Oil Combustors Through the Supplemental Use of Natural Gas," Final Report, GRI 5083-251-0905, 1985.
8. England, G. C., et al., "Field Evaluation Humidification for Precipitator Performance Enhancement," Paper presented at the 7th Symp. on the Transfer and Utilization of Particulate Control Tech., Nashville, TN, March 22–25, 1988.
9. Bartok, W. and B. A. Folsom, "Control of NO_x and SO_2 Emissions by Gas Reburning-Sorbent Injection," Paper presented AICE Ann. Mtg., New York, November, 1987.
10. Folsom, B. A., et al., "Field Evaluation of Gas Reburning-Sorbent Injection Technology for NO_x and SO_x Emission Control for Coal Fired Utility Boilers," Paper presented at the 15th Energy Technology Conf. and Expos., Washington, DC, February 17–19, 1988.
11. Payne, R., et al., "Demonstration of Gas Reburning/Sorbent Injection NO_x/SO_2 Control Technology on Three Utility Boilers," Paper presented at AIChE 1988 Summer National Meeting, Denver, August 21-24.
12. Nelson, L. P., et al., "Field Evaluation of Coal Fired Utility Boiler NO_x and SO_x Emissions Control by Gas Reburning-Sorbent Injection," Paper presented at APCA 81st Ann. Mtg. and Ex., Dallas, TX, June 22, 1988.

Air Stripping of Volatile Hydrophobic Compounds Using Packed Crisscross Flow Cascades

Dianne F. Wood, Larry L. Locicero, Kalliat T. Valsaraj Douglas P. Harrison and Louis J. Thibodeaux

Department of Chemical Engineering, Louisiana State University, Baton Rouge, LA 70803

The removal of four volatile organic compounds from aqueous solution by air stripping using a cascade crossflow device has been studied. This method of operation gave mass transfer coefficients and removal efficiencies quite similar to those achieved in conventional countercurrent operations. However, in terms of reduced pressure drops and greater range of stable operation, the advantages of the cascade crossflow device far outweigh those of the conventional countercurrent stripper.

INTRODUCTION

Groundwater contamination resulting from inadvertent spills at plant sites, leaking underground storage tanks, and improperly constructed surface impoundments and landfills is a major problem in several parts of the United States. Much of the contamination is due to volatile organic compounds (VOCs). A number of technologies exist for the removal and/or destruction of VOCs from groundwater such as: incineration, liquid phase adsorption, chemical oxidation, biological oxidation, steam stripping, and air stripping. All are capable of reducing VOC concentrations to acceptable levels, although additional treatment for the ultimate destruction of contaminants may be necessary since adsorption and stripping serve only to transfer and concentrate the VOCs. In situations where the VOC concentrations are a few ppm, such treatment methods as incineration and chemical or biological oxidation are prohibitively expensive. The feasibility of both liquid phase carbon adsorption and steam and air stripping have been demonstrated in large-scale tests.

Although all treatment processes are expensive, air stripping is generally less costly and is emerging as the preferred process for many groundwater decontamination applications, Bouwer, *et al.* [*1*] report that the cost for 99% organic removal by air stripping may range from \$0.15 to \$0.50/1000 gal. The cost for the same treatment using granular activated carbon is reported by the same source to range from \$0.30 to \$2.00/1000 gal. In a similar study, Clark, *et al.* [2] reported that trichloroethylene removal using granular activated carbon would be approximately five times more expensive than using air stripping. Additional cost reduction for air stripping, while maintaining high removal efficiency, would certainly accelerate the application of air stripping to groundwater treatment technology.

Correspondence concerning this paper should be addressed to D. P. Harrison.

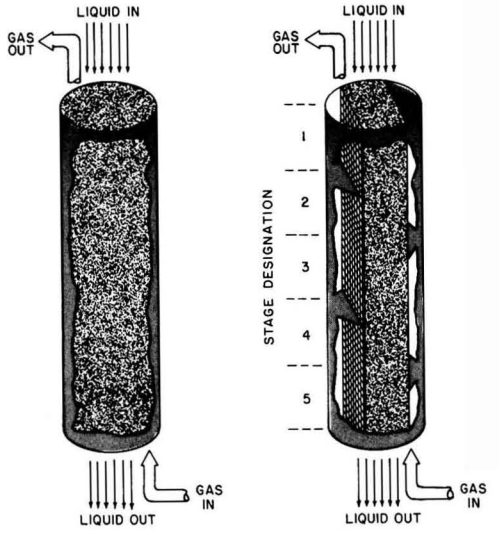

Figure 1. Schematic diagram of countercurrent and cascade crossflow contacting devices.

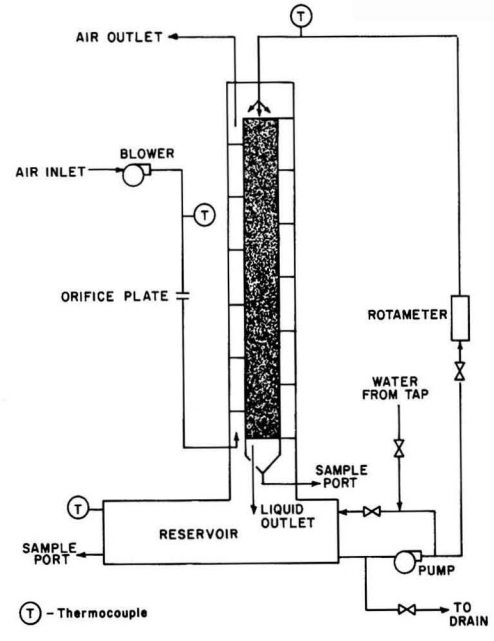

Figure 2. Schematic diagram of the semi-batch cascade crossflow air stripper.

Countercurrent packed columns are the most common air stripping devices used when high removal efficiencies are required [3]. The device is shown schematically in Figure 1a. For comparison purposes, the cascade crossflow unit that is the subject of this paper is shown in Figure 1b. In the conventional countercurrent operation, liquid flows from top to bottom by gravity while air is forced (by pressure) to flow from bottom to top. The general advantage of a countercurrent device is the large driving force for mass transfer, since incoming gas that contains no organics contacts the exiting liquid depleted of organics. Exiting gas, on the other hand, has a high organic concentration and is in contact with incoming liquid of high organic concentration. A relatively constant driving force exists throughout the column, giving rise to high mass transfer rates.

The uniqueness of cascade crossflow air stripping (Figure 1b) stems from disconnecting the areas through which the gas and liquid phases move within the packing. The overall operation is still countercurrent and the liquid flows vertically downward by gravity. However, the gas phase is deflected at regular intervals by partial baffles that cause the gas flow to cross the liquid flow several times at approximately 90 degrees before exiting the packing. Proper selection of baffle spacing can produce a marked reduction in gas velocity, and consequently, a lower gas phase pressure drop compared to normal countercurrent mode of operation. In systems that are liquid phase controlled, the reduction in gas velocity has little or no effect on the mass transfer coefficient and the overall removal efficiency. The principal cost factors in air stripping are the column amortization, pumping the liquid to the top of the column, and overcoming the pressure drop associated with the gas flow upward through the column. Therefore, reduction of gas-phase pressure drop can lead to considerable cost savings.

The crossflow concept was introduced by Baker and Shyrock [4] as an alternative to conventional countercurrent flow water cooling towers. The original devices were single cell units with limited mass transfer capability. Multistage crossflow units were subsequently created by interconnecting single cells to create a cascade. Thibodeaux [5] presented conceptual design procedures for single stage, crossflow devices for general-purpose chemical separations. Later, Thibodeaux, *et al.* [6] employed the "number of transfer units" (NTU) technique for the design and analysis of cascade crossflow towers. McCarty [7] used this procedure to analyze a single stage crossflow stripping tower for the removal of ammonia from reclaimed waste water. Hayashi, *et al.* [8] used a cascade crossflow device for cooling water with air and achieved efficiencies equivalent to the countercurrent arrangement.

Moncada and Thibodeaux [9] compared the overall mass transfer efficiency of a countercurrent packed tower with that of a crossflow packed tower for air stripping methanol from water. They observed that the raw efficiencies of countercurrent were slightly superior to that of crossflow, but when the comparisons were based on volume of packing and pressure drop the crossflow unit was more efficient than the countercurrent unit. Thibodeaux [10] reported the fluid dynamics and general gas-liquid contact patterns for cascade crossflow towers. Distillation experiments using cascade crossflow arrangements have also been conducted [11, 12]. Velaga, *et al.* [13] recently proposed that existing correlations for mass transfer in countercurrent packed columns can adequately predict the stage efficiencies of chemical separation in stripping and distillation in crossflow packed columns.

In this paper, we report preliminary laboratory-scale experiments on the air stripping of four VOCs from synthetic groundwater samples using a cascade crossflow packed system.

EXPERIMENTAL

The crossflow cascade system used for the experiments is shown in Figure 2. All experiments were conducted in a semi-batch mode, with contaminated water being pumped from the reservoir to the distributor where it

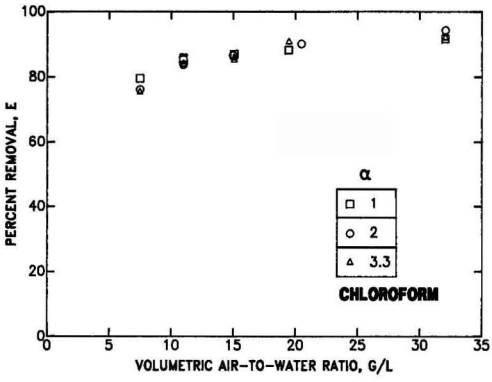

Figure 3. Chloroform stripping efficiency as a function of (G/L) and baffle spacing.

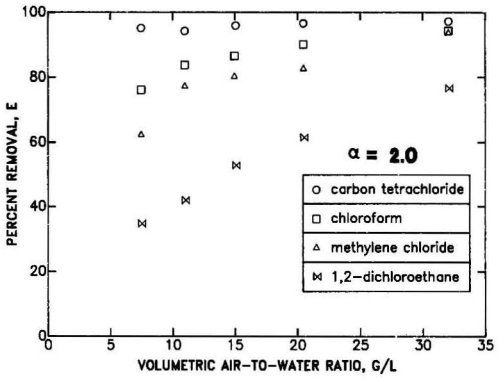

Figure 4. Stripping efficiency for four VOCs as a function of (G/L).

flowed down by gravity and back into the reservoir. Air was forced upward through the packing and discharged through a laboratory vent. The overall operation was batch with respect to the liquid, and once-through with respect to air. Organic concentration in the reservoir decreased with time as it was discharged from the system with the air. Simultaneous sampling of the liquid in the reservoir (equivalent to the liquid entering the packing) and the liquid leaving the packing (bottom sample port) allowed the stripping efficiency to be calculated directly from:

$$E = 1 - (C_B/C_T) \quad (1)$$

The column was constructed of plexiglass having an inside diameter of 0.152 m (6 inches). Five sections, each 1.22 m (4 ft.) high, allowed the unit to be operated with packed-heights ranging from 1.22 to 6.1 m (4 to 20 feet). The packed area was 65% of the total cross-sectional area. The packing material was polypropylene Pall rings (⅝ inch nominal diameter) that was held in place using stainless steel wire mesh frames. Baffles to control gas flow were bolted to the wire mesh. Each baffle contained a rubber insert that sealed against the column wall to prevent both liquid and gas bypassing. The design was such that the baffle spacing could be adjusted to permit gas velocity and volumetric flow rate to be controlled independently of liquid velocity and volumetric flow rate.

A March 7 centrifugal pump with a maximum capacity of 1.9×10^{-3} m^3/s (30 gpm) was used to deliver the liquid to the top of the column from the reservoir. It was also used to recycle liquid in the reservoir to ensure complete mixing. A rotameter (Omega Model 710B), with a maximum capacity of 6.3×10^{-4} m^3/s (10 gpm), was used to measure the liquid flow rate. A Powerbloc blower (model E 120751), with a Westinghouse Accutrol variable speed controller having a maximum capacity of 22.7 m^3/s (800 cfm), was used to deliver air to the column. Air flow was measured using an orifice with pressure taps connected to a U-tube manometer.

A saturated solution of organic and water was prepared for each compound studied. The reagents used were chloroform (MCB Reagents), methylene chloride (Mallinckrodt), 1,2-dichloroethane (Fisher Scientific), and carbon tetrachloride (Mallinckrodt). The reservoir was filled partially with water, and the saturated aqueous solutions were added to obtain nominal concentrations of 0.1 to 0.4 kg/m^3 (100 to 400 ppm) of each VOC. The spiked water was then mixed thoroughly by pumping liquid through the reservoir recycle loop. When the tank was thoroughly mixed, part of the liquid was diverted from the recycle loop through the rotameter and packed column. The blower was started, and the liquid and gas flow rates were adjusted. Samples were taken periodically from the sampler and the tank. The liquid flow rate, orifice pressure drop, and liquid and air temperatures were recorded at the start and end of each run.

Samples were collected in 5 ml Piece glass vials sealed with Teflon lined rubber septa and screw caps. The vials were filled to capacity to ensure no headspace, and were stored in a refrigerator until analysis.

Samples were analyzed on a Hewlett-Packard 5890 A gas chromatograph equipped with a Flame Ionization detector. The column used was of stainless steel (1.83 m long with 0.32 cm i.d.) packed with 80-120 Carbopack B coated with 3% SP-1500. The oven, detector, and injector temperatures were 383°, 493°, 493°K, respectively. Peaks were recorded and integrated using a Hewlett-Packard 3390A integrator.

RESULTS AND DISCUSSION

Experimental stripping efficiencies for chloroform at a liquid loading rate of 17.6 kg/m^{2}s (25.9 gpm/ft^2) as a function of air-to-water ratio (G/L) are shown in Figure 3. All experimental results were obtained using a packed height of 2.44 m (8 feet). The parameter α in the figure is defined as the ratio of the gas flow area to the liquid flow area. α is an independent parameter determined by the baffle spacing; large α's result in low gas velocity and (as will be seen) low gas phase pressure drop. α = 1 corresponds very approximately to the traditional countercurrent flow pattern in which the areas for liquid and gas flow are equal. Stripping efficiency is independent of α and almost independent of G/L above about 20, where stripping efficiencies equal to or greater than 90% were obtained.

Figure 4 compares the stripping efficiencies for four compounds using the same liquid loading rate at a constant value of α = 2. Differences in the stripping efficiency, which range from approximately 98% for carbon tetrachloride at high G/L to about 35% for 1,2-dichloroethane at low G/L, reflect differences in the Henry's Law constant for the compounds. At the experimental temperature (295°K), the dimensionless H varies from approximately 1.08 for carbon tetrachloride to 0.060 for 1,2-dichloroethane [*14*].

Overall volumetric mass transfer coefficients were calculated directly from experimental data using the following equation [*15*]:

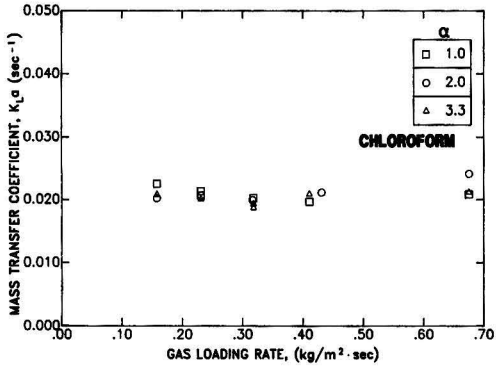

Figure 5. Overall mass transfer coefficients for chloroform as a function of gas loading rate and baffle spacing (constant liquid rate).

$$K_l a = \left(\frac{L}{AZ}\right)\frac{\ln\left[\frac{1}{1-E} - \frac{E}{1-E}\left(\frac{L}{GH}\right)\right]}{1-\left(\frac{L}{GH}\right)} \qquad (2)$$

Chloroform mass transfer coefficients as a function of G/L and α, calculated from the Figure 3 data, are shown in Figure 5. The values are approximately constant in the range of 0.020 to 0.023 sec^{-1}. These results again indicate that increasing α (decreasing gas velocity) has little, if any, adverse effect on the mass transfer characteristics of systems that are liquid phase controlled. The values of $K_l a$ compare quite favorably to a value of 0.023 sec^{-1}, recently reported [16] for air stripping of chloroform in a countercurrent system under similar conditions.

Figure 6 shows the mass transfer coefficients for the four organics as a function of G_m (constant L_m) at a value of α = 2. With the exception of 1,2-dichloroethane the mass transfer coefficients are essentially independent of G_m. The low Henry's constant associated with 1.2-dichloroethane suggests that gas-phase mass transfer resistance should be important, thereby justifying the apparent dependence of $K_l a$ upon G_m. In general, the overall mass transfer coefficients also reflect the differences in the Henry's Law constant.

Figure 7 shows that the volumetric mass transfer coefficient for chloroform at a constant gas rate is strongly dependent upon the liquid rate, but still effectively independent of baffle spacing. Values of $K_l a$ as high as 0.045 sec^{-1} were achieved at the highest liquid loading rate. These results are also consistent with the expected behavior of a liquid phase controlled system. Variation in the liquid velocity should have a direct effect on the mass transfer coefficient, while variation in the gas velocity (represented here by the variation in α) should have little effect.

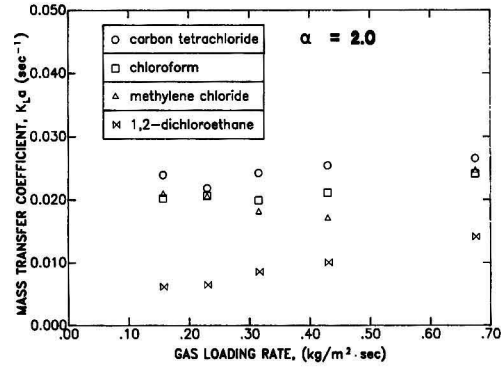

Figure 6. Overall mass transfer coefficients for four VOCs as a function of gas loading rate (constant liquid rate).

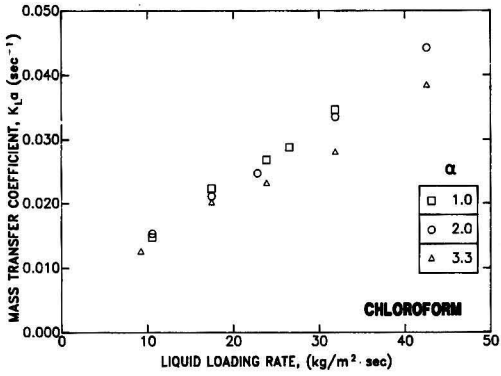

Figure 7. Overall mass transfer coefficients for chloroform as a function of liquid loading rate and baffle spacing (constant gas rate).

One of the most widely used correlations for predicting mass transfer coefficients for traditional countercurrent flow was developed by Onda [17]. This two resistance model was based upon studies on the absorption of hydrogen and carbon dioxide in water and various organic solvents. The individual film coefficients may be predicted from the following equations:

liquid film coefficient:

$$k_l\left(\frac{\rho_l}{g\mu_l}\right)^{1/3} = 0.0051\left(\frac{L_m}{\mu_l a_w}\right)^{2/3}\left(\frac{\mu_l}{\rho_l D_l}\right)^{-0.5}(a_t d_p)^{0.4} \qquad (3)$$

gas film coefficient:

$$\left(\frac{k_g}{a_t D_g}\right) = 5.23\left(\frac{G_m}{\mu_g a_t}\right)^{0.7}\left(\frac{\mu_g}{\rho_g D_g}\right)^{1/3}(a_t d_p)^{-2.0} \qquad (4)$$

wetted area:

$$\frac{a_w}{a_t} = 1 - \exp\left[-1.45\left(\frac{\sigma_c}{\sigma}\right)^{0.75}\mathrm{Re}^{0.1}\mathrm{Fr}^{-0.05}\mathrm{We}^{0.2}\right] \qquad (5)$$

The film coefficients can then be combined with Henry's constant to obtain the overall mass transfer coefficient:

$$\frac{1}{K_l} = \frac{1}{k_l} + \frac{1}{\mathrm{H}k_g} \qquad (6)$$

Equation (3) is claimed to be valid within ±25% for Raschig rings, Berl saddles, spheres, and rods with liquid loadings between 1 and 15 kg/m^{2}s. Equation (4) is said to be valid between ±30% for the same packings at gas loading rates of 0.02 to 1.7 kg/m^{2}s.

We modified the Onda equation for k_g, Equation (4), by basing G_m on the actual gas flow area, which is a function of α. The result is referred to as modified Onda. A parity plot of predicted $K_l a$ versus experimental $K_l a$ for chloroform is shown in Figure 8. All but one of the 49 experimental values lies between the ±20% deviation lines, and the results appear to be randomly distributed about the diagonal. Hence, we conclude that for systems that

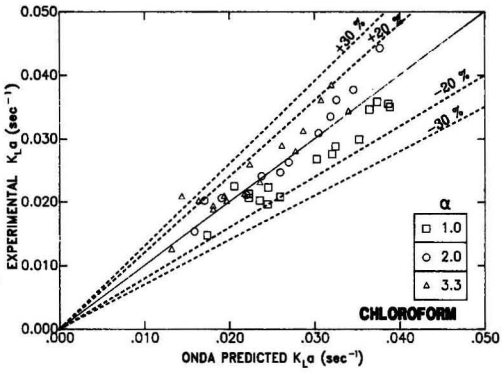

Figure 8. Parity plot for overall mass transfer coefficients for chloroform using the modified Onda correlation.

are liquid phase controlled, the modified Onda correlation describes cascade crossflow mass transfer coefficients to approximately the same level of accuracy as the original Onda correlation describes countercurrent mass transfer coefficients. Only the gas film coefficient k_g is altered by the modification and this term is unimportant in Equation (6), since chloroform stripping is liquid-phase controlled. The modification might not be satisfactory for gas-phase controlled systems. However, in most contaminated groundwater applications, the liquid phase resistance should be greater than the gas phase resistance.

Having established that the mass transfer characteristics of the cascade crossflow and countercurrent units are comparable, we turned our attention to the gas-phase pressure drop, where cascade crossflow operation has a distinct advantage. When the mass flow rates of water and air are constant, the mass velocity (kg/m^{2}s) of the air in contact with the liquid is directly related to the baffle spacing characterized by α. Increased α increases the area for gas flow, decreases the gas mass velocity, and as a consequence, should decrease the gas phase pressure drop. Such behavior has been found experimentally, as shown in Figure 9. The pressure drop per unit of packed height is plotted against the gas loading rate on a logarithmic plot. Experimental data for four values of α between 1.0 and 6.0 are compared to the expected pressure drop in a countercurrent column (at a slightly different liquid loading rate). The latter is based upon data supplied by the packing manufacturer. Note that the pressure drops for countercurrent and α = 1 are approximately equal and that the pressure drop in the cascade crossflow unit is a strong function of α. At a gas loading rate of 1 kg/m^{2}s, the pressure drop increases from approximately 18 N/m^2/m at α = 6 to 300 N/m^2/m for countercurrent flow, an increase of more than one order of magnitude. For those air stripping applications in which gas-phase pressure drop is a significant cost factor, such savings can be very important.

In addition to operating with lower pressure drop, the cascade crossflow column is capable of stable operation over a wider range of gas and liquid loadings. In countercurrent operation, as the gas rate is increased at a fixed liquid rate, conditions of loading and then flooding are encountered. Operation is impossible at gas rates above flooding. No comparable situation is encountered in cascade crossflow operation. Since the directions of gas and liquid flow are approximately normal, excessive gas velocity will impart a horizontal velocity component to the liquid and cause liquid build-up on the adjacent baffle. In the next stage, however, gas flow is in the opposite direction so that liquid overflowing from the baffle is forced back toward the center of the packed section. The alternating flow directions, therefore, produce a self-correcting system.

Figure 10 shows the experimental pressure drop data from the cascade crossflow system superimposed upon a standard Sherwood-Eckert diagram for countercurrent operation. Essentially all of the crossflow data lie above the loading curve and a few of the points are above the flooding line; however, the crossflow column exhibited stable operation throughout. This characteristic shows that cascade crossflow may be particularly useful in stripping components having small Henry's constants. High *G/L* ratios, which would be required by equilibrium constraints, but might cause flooding in countercurrent operation, would operate stably in crossflow.

CONCLUSIONS

Cascade crossflow air stripping for the removal of VOCs from contaminated water results in mass transfer characteristics equivalent to those expected from traditional countercurrent operation. Stripping efficiencies in excess of 90% have been obtained from a unit containing 2.44 m packed height, while measured mass transfer coefficients agree with predictions using the Onda correlation. The advantages of cascade crossflow are associated with re-

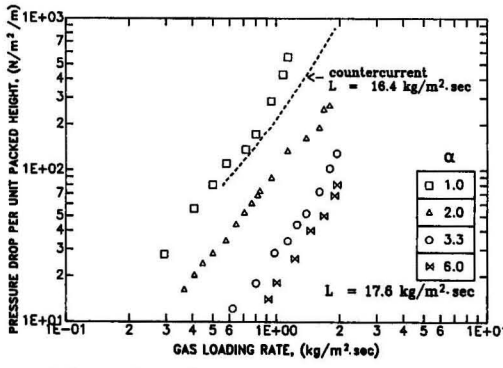

Figure 9. Pressure drop in the cascade crossflow column as a function of gas loading rate and baffle spacing (constant liquid rate).

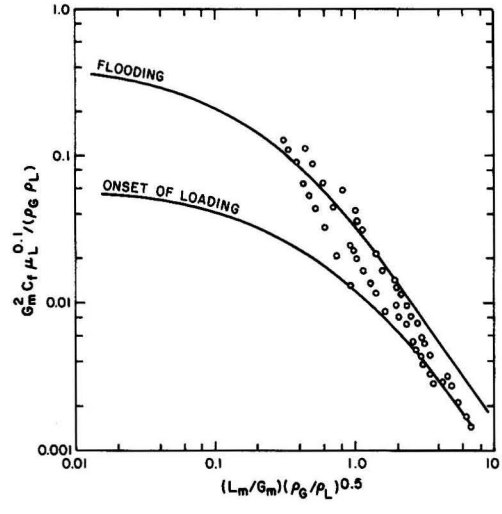

Figure 10. Sherwood-Eckert plot showing stable operation in the cascade crossflow system.

duced gas-phase pressure drop (more than one order of magnitude), and stable operation at gas and liquid rates that would not be possible in a countercurrent system. Column flooding, as experienced in countercurrent flow, does not occur since gas and liquid flow directions are approximately normal in crossflow. Instead of causing liquid backup in the column, the gas imparts a horizontal velocity component and causes liquid accumulation on an adjacent baffle. However, liquid overflowing from the baffle is contacted by gas flowing in the opposite direction, which tends to redistribute the liquid toward the center of the packing.

ACKNOWLEDGMENTS

This work was supported by the U.S. Air Force through the Air Force Engineering and Services Center, Tyndall Air Force Base, Florida (Contract NO: F08635-86-C-0159). We thank the project officers Capt. R. A. Ashworth and Lt. Michael C. Elliott for their input in this work.

NOMENCLATURE

- A cross-sectional area of packing, l^2
- a_t total interfacial area per unit bed volume, l^{-1}
- a_w wetted interfacial area per unit bed volume, l^{-1}
- C_B solute concentration in liquid exiting packing, m/l^3
- C_f packing factor, l^{-1}
- C_T solute concentration in liquid entering packing m/l^3
- D_g gas diffusion coefficient, l^2/t
- D_l liquid diffusion coefficient, l^2/t
- d_p nominal packing diameter, l
- E stripping efficiency, defined by Equation (1), dimensionless
- Fr Froude number, dimensionless
- G gas volumetric flow rate, l^3/t
- G_m gas mass velocity, m/l^2t
- g acceleration due to gravity, l/t^2
- H Henry's constant expressed as ratio of concentrations in gas phase to liquid phase, dimensionless
- K_la overall volumetric mass transfer coefficient, t^{-1}
- k_g gas phase mass transfer coefficient, l/t
- k_l liquid phase mass transfer coefficient, l/t
- L liquid volumetric flow rate, l^3/t
- L_m liquid mass velocity, m/l^2t
- Re Reynolds number, dimensionless
- We Weber number, dimensionless
- Z height of packing, l
- α ratio of gas to liquid flow areas, dimensionless
- μ_g gas viscosity, $m/l \cdot t$
- μ_l liquid viscosity, $m/l \cdot t$
- ρ_g gas density, m/l^3
- ρ_l liquid density, m/l^3
- σ surface tension of liquid, m/t^2
- σ_c critical surface tension with respect to packing material, m/t^2

LITERATURE CITED

1. Bouwer, E., J. Mercer, M. Kavanaugh, and F. Digiano, *J. Water Poll. Cont. Fed.*, **60**(8), 1415–1427 (1988).
2. Clark, R. M., C. A. Fronk, and B. W. Lykins, *Environ. Sci. Technol.*, **22** (10), 1126–1129 (1988).
3. Bilello, L. J., and J. E. Singley, *J. Amer. Wat. Wks. Assoc.*, **78** (2), 62–71 (1986).
4. Baker, D. R., and H. A. Shyrock, *J. Heat Transfer.*, Trans. AIME, 339 (1969).
5. Thibodeaux, L. J., *Chem. Eng.*, p. 165, June 2 (1969).
6. Thibodeaux, L. J., D. R. Daner, A. Kimura, J. D. Millican, and R. J. Parikh, *Ind. Eng. Chem. Proc. Des. Dev.*, **16**, 325–330 (1977).
7. McCarty, P. L., "Removal of Organic Substances from Water by Air Stripping," in, *Control of Organic Substances in Water and Wastewater*, B. B. Berger, Ed., EPA 600/8-83, p. 119 (1983).
8. Hayashi, Y., and E. Hirai, *Kagaku Kogaku*, **36**, 1249-1252 (1972).
9. Moncada, D. M., and L. J. Thibodeaux, "Performance Comparison of a Crossflow Cascade and a Conventional Countercurrent Operation in Packed Towers," Presented at the Symp. on Recent Advances in Separation Technol., Ann. AIChE Mtg., Chicago, IL, November 16–20 (1980).
10. Thibodeaux, L. J., *Ind. Eng. Chem. Proc. Des. Dev.*, **19**, 33–40 (1980).
11. Buchelli, A., M. S. Thesis, University of Arkansas, Fayetteville, AR (1986).
12. Velaga A., Ph.D. Thesis, University of Arkansas, Fayetteville, AR (1986).
13. Velaga, A., L. J. Thibodeaux, K. T. Valsaraj, R. B. Eldridge, D. M. Moncada, and J. S. Cho, *Ind. Eng. Chem. Res.*, **27**, 1481–1487 (1988).
14. Ashworth, R. A., G. B. Howe, M. E. Mullins, and T. N. Rogers, *J. Haz. Mat.*, **18**, 25–36 (1988).
15. Gross, R. L., and S. G. TerMaath, *Environ. Prog.*, **4**, 119–124 (1985).
16. Gosset, J. M., C. E. Cameron, B. P. Eckstrom, G. Goodman, and A. H. Lincoff., "Mass Transfer Coefficients and Henry's Constants for Packed Tower Air Stripping of Volatile Organics: Measurements and Correlation," U.S. Air Force Office of Scientific Research, Report NO: ESL-TR-85-18, 278 pages, June (1985).
17. Onda, K., H. Tadeuchi, and Y. Okumoto, *J. Chem. Eng. Japan*, **1**, 56–62 (1968).

Hazardous Waste Minimization and Management at an R&D Laboratory

M. J. Boortz
Chevron Research Company, Richmond, CA

Chevron Richmond Research Center (RRC), located in Richmond, California, conducts research and technical service in the fields of petroleum and petrochemical products, processes, and related matters. To assure proper disposal of all wastes generated, RRC has implemented a unique waste disposal system. The system entails the use of specific disposal procedures and color-coded waste receptacles for the different types of wastes. Communication with employees is vital for successful use of the waste disposal system. A written waste management plan documents the achieved and the projected reductions in waste generation. Most of the hazardous waste reductions realized prior to 1989 were from installation of equipment and offsite recycling. Much of the future reductions are expected to come from changes in laboratory procedures and practices. The ultimate goal is to increase employee environmental awareness so that waste minimization is a routine part of every job.

INTRODUCTION

The Richmond Research Center (RRC) is comprised of 48 buildings on 31 acres in Richmond, California. RRC is the headquarters of Chevron Research Company, a research company and analytical laboratory for Chevron Corporation. Approximately 2000 people work at the RRC. However, RRC is more than an R&D center and laboratory. Approximately half of the RRC employees work for other Chevron companies. Thus, the workforce includes chemists, engineers, technicians, pilot–plant operators, maintenance personnel, engine mechanics, various services personnel, and a large number of office workers (e.g., computer systems analysts) whose work may be unrelated to the laboratory or pilot–plant operations.

Sources of hazardous and nonhazardous wastes generated at RRC include:

- Analytical and research laboratories.
- Sample storage areas.
- Pilot–plants.
- Paint, carpenter, machine, welding, and glassblowing shops.
- Reprographic machines.
- Office copier machines.
- Test engine laboratories.
- Motor vehicle maintenance.
- Drum/can filling and blending operations.
- Facility maintenance and alterations.
- Office work.
- Food consumption.

The RRC waste disposal system, in its current form, was implemented in 1984. We designed the system to ensure that all types of wastes generated are properly and legally disposed. A basic premise of the system was that it be easy to use with plenty of help readily available. We felt that people would be more likely to follow the system if it were easy to use and put minimum burden on them.

Since 1984, we have clarified and revised the disposal procedures in response to various questions or problems that have arisen. The RRC waste disposal system is unique to match the unique qualities of the RRC Facility. We are not aware of any waste disposal system like it–within or outside of Chevron.

The RRC Waste Disposal System

In this waste disposal system, there is a specific color-coded waste receptacle to be used for each type of waste generated at RRC. Waste disposal stations, where several of the different receptacles are grouped together, are located in laboratory, pilot–plant, and maintenance operations areas. A disposal tag must be completed and affixed to those waste containers which will be further sorted by waste handling personnel. The different waste receptacles, waste disposal stations, and the disposal tag are described below.

Blue Drum (Return Oil)

"Return Oil" is oil which is suitable for return to a petroleum refinery where it is co-mingled with crude oil feed. Materials are suitable for recycling in the refinery if

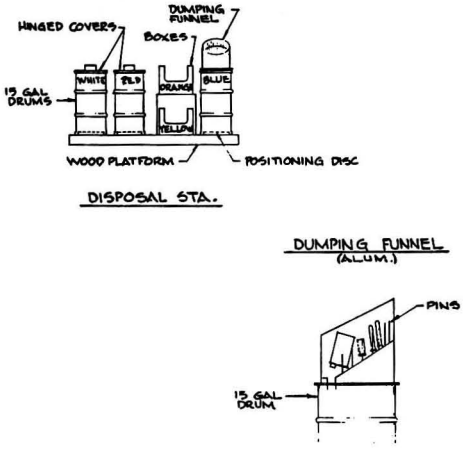

Figure 1. Typical waste disposal station.

they are not hazardous wastes and are petroleum fractions with no more than normal product levels of additives. Return oil in containers 4 oz and larger are drained into a return oil drum. Most of the return oil is oil samples which were tested or produced at RRC.

Red Drum, Box, or Dumpster (Oily, Trash)

Oily trash is emptied oil, solvent, and paint containers plus other oily articles (e.g., hardware and glassware). Only empty containers are to be disposed in oily trash receptacles.

Orange Box (Chemicals)

Full, part-full, and contaminated containers of chemicals, reagents, catalyst, additives, solvents, and nonreturn oil are to be disposed of in an orange box. The wastes must be in compatible, closed, and nonleaking containers. The container contents must be identified by a completed disposal tag affixed to the container.

Yellow Box, (Synfuels)

The yellow box is for full or part-full containers of synfuels. Procedures for use of the yellow box are the same as for the orange box.

White Drum, Can, or Dumpster (Clean Trash)

Clean trash is regular garbage. It includes such items as clean glassware, hardware, household-type items, wood, metal items heavier than a paper clip, food garbage, and paper towels.

Wastepaper Baskets (Black-, Gray-, and Beige-Colored Trash Receptacles)

Wastepaper baskets are primarily for work paper destined for shredding. Other acceptable items include staples, standard paper clips, and magazines.

Other Waste Receptacles

There are other types and colors of waste receptacles for some wastes that are only generated in a few areas.

Figure 2. Waste disposal station being serviced.

For example, the shops have beige-color drums labeled "scrap metal" for metal scrap. Some areas have light green-color cans for clean and dirty rags.

Waste Disposal Stations

Waste disposal stations are strategically located throughout the laboratory, pilot–plant, and maintenance operation areas at the RRC facility. Each disposal station consists of a number of color-coded containers designed to handle different types of wastes. Depending on the types of wastes generated in the particular area, not all colors may be present and container sizes may vary. A typical disposal station, shown in Figure 1, has: clean trash can, oily trash can, orange box, yellow box, and return oil drum. There are about 70 waste disposal stations. Each station is serviced (e.g., waste picked up and liners

DISPOSAL TAG

(Please Print Using Ball Point Pen)

Recyclable to Refinery Crude Feed?

Petro. frac. with no more than trace quan. of detergents, surfactants, emulsifiers, phenols, sulfides, sulfonates, naphthenates, lube oil additives, heavy metals, halogenated solvents.

☒ Yes Describe: Gasoline

☐ No ☐ See Label or Describe:

Special Precautions:

Call Ext. 4385 if identification assistance is needed.

Print Name A. Spencer Phone 9999 Date 11-1-84

CRR-5600(SM-3-84) Printed in U.S.A.

DISPOSAL TAG

(Please Print Using Ball Point Pen)

Recyclable to Refinery Crude Feed?

Petro. frac. with no more than trace quan. of detergents, surfactants, emulsifiers, phenols, sulfides, sulfonates, naphthenates, lube oil additives, heavy metals, halogenated solvents.

☐ Yes Describe:

☒ No ☐ See Label or Describe: Potassium Hydroxide

Special Precautions:

Call Ext. 4385 if identification assistance is needed.

Print Name K. Thompson Phone 8888 Date 11-1-84

CRR-5600(SM-3-84) Printed in U.S.A.

Figure 3. Disposal tag.

in drums replaced) about once per day. Figure 2 shows a waste disposal station being serviced.

The Disposal Tag

An example of a completed disposal tag is shown in Figure 3. The disposal tags are preprinted, bright orange-color adhesive labels. They are stocked in the stationery stockroom and at all waste disposal stations. All containers (except clean trash and oily trash) put into the waste disposal system must be identified by a completed disposal tag affixed to the container.

TOOLS OF THE WASTE DISPOSAL SYSTEM

Written Waste Disposal Procedures

How to use the waste disposal system is described in the RRC Waste Disposal Procedures. A list of help phone numbers is included. The procedures are available as a separate booklet and are also contained in the RRC Environmental Compliance Manual. The booklets are stocked in the three chemical stockrooms. In some work areas, the personnel have hung a booklet in their laboratory or at the waste disposal station so that it is readily accessible to them.

Division Waste Disposal Monitors

When we implemented the waste disposal system, waste disposal monitors were appointed by each department/division at RRC. The monitors worked in the department/division and were the designated contact person that employees could go to for help with waste disposal. The monitors were also focal points that the waste management personnel could go to when waste disposal problems were discovered in a particular department's/division's area.

The monitors are a vital part in the successful implementation of the waste disposal system. People can get waste disposal help from someone they know and work with and who are familiar with that area's operation.

In 1986, the waste disposal monitor function was expanded slightly and renamed "Environmental Monitor." In 1988, the name was changed again to "Environmental Coordinator," but the function remained the same. There are currently 28 division environmental coordinators. Most of the divisions/departments appoint new environmental coordinators annually.

Waste Disposal Assistance Phone Number

The telephone number for waste disposal assistance is assigned to an answering machine. People are instructed to call the number and leave a message in the following instances:

- Request assistance in the identification of an unknown waste.
- Get guidance on proper waste packaging or labeling.
- Request the pickup of high hazard wastes, such as water reactives or highly toxic materials.

The hazardous materials technician reviews the messages and responds to the callers' questions or requests. The Analytical Division of Chevron Research is responsible for assisting in identification of unknown wastes.

The RRC Waste Minimization Successes

RRC has had a written waste management and minimization plan since 1985. The plan is updated annually and contains the following elements:

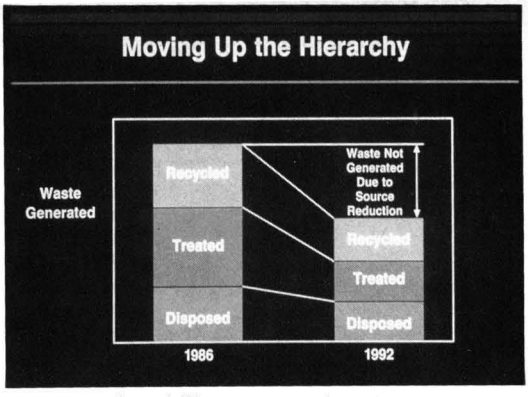

Figure 4. Waste management hierarchy.

- Inventory of wastes generated.
- Current practices and procedures which minimize waste generation and the degree of hazard.
- Recycle, reuse, treatment, and waste minimization opportunities which are being or will be investigated.
- Past and projected future waste generation quantities.
- Current list of treatment, disposal, and recycling facilities and transporters used.

Chevron Corporation has a corporatewide program for waste minimization called Save Money and Reduce Toxics (SMART). The RRC waste management plan is also the Chevron Research SMART Plan which is updated and submitted annually to the Corporation.

Two main objectives of SMART are: minimize generation of both hazardous and nonhazardous wastes, and move up the hazardous waste management hierarchy. "Moving up the waste management hierarchy" means managing waste by more environmentally protective methods. The least desirable and lowest management level is disposal by landfill. The most desirable and highest management level is source control (or source reduction) to avoid waste generation. The waste management hierarchy is depicted in Figure 4. Figure 5 shows the SMART objectives.

Some changes made at RRC to minimize hazardous waste generation and move up the waste management hierarchy are discussed below.

Substitution of Solvent

Personnel are encouraged to substitute solvents which can be disposed of in return oil for solvents which must

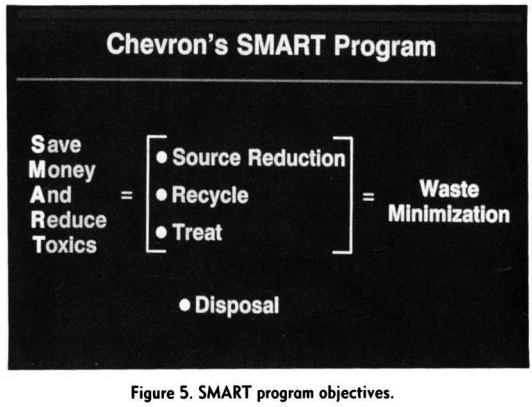

Figure 5. SMART program objectives.

WAIT!!!!! CAN YOU USE ANOTHER SOLVENT?????

USE OF THIS SOLVENT CREATES HAZARDOUS WASTE
DO NOT DISPOSE OF THE USED SOLVENT IN RETURN OIL

Disposal of this solvent costs 5$/gallon

NOTE: It is OK to dispose of moderate amounts of this solvent in laboratory sinks and oily drains when the solvent is used to hand-clean laboratory glassware and equipment.

Figure 6. Label on 1-gallon cans of dispensed solvents which must be disposed of as hazardous waste.

be disposed of as hazardous waste (e.g., substitute a heavier aromatic solvent for toluene). Cans containing dispensed solvents which, after use, must be disposed as hazardous waste are labeled. The label asks if another solvent could be substituted. A copy of the label, which is canary-yellow color, is shown in Figure 6. In addition, we replaced one dispensed solvent (a high toluene content solvent which had to be disposed as hazardous waste) with an equivalent solvent which could be recycled to a petroleum refinery. Solvent disposal procedures are included in the written RRC waste disposal procedures.

Recycling Pure Solvents

Drums of used, relatively pure solvents (single solvent or mixture of only a few solvents) are sent to an offsite solvent recycler. Users of large quantities of solvent are encouraged to segregate, not mix, solvents so that they can be recycled.

Triple-Rinse Clean

Many chemical and solvent jugs are triple-rinsed clean prior to disposal. The clean jugs are labeled with a triple-rinse clean sticker and disposed of with clean trash (regular garbage). Figure 7 is a copy of a triple-rinse clean procedure. The procedure is included in the RRC waste disposal procedures.

Follow the procedure below for disposal of empty 1-gallon glass jugs of the following solvents: xylenes, toluene, isopropyl alcohol, hexane, acetone, chloroform, methylene chloride, methanol, isooctane, acetonitrile, tetrahydrofuran, methyl ethyl ketone. Use the procedure on other empty chemical bottles only after first obtaining your supervisor's approval. If you have any questions, ask your supervisor or your division's Environmental Monitor.

CAUTION: Wear gloves while rinsing the bottles. Chloroform and acetonitrile bottles must be rinsed in sinks located under hoods.

1. If the material is not miscible with water, wash the bottle three times with small portions of acetone (or other suitable solvent which is miscible with both water and the material). Flush the rinse solutions with water into a laboratory sink.

2. Thoroughly rinse the bottle three times with water in a laboratory sink.

3. Put a green "triple-rinsed clean" sticker on the bottle.

4. Dispose of the bottle as clean trash. Put the bottle in a white, clean trash container or place it in the hall for pickup, as appropriate for your work location.

TRIPLE-RINSED CLEAN

Figure 7. Triple-rinse clean procedure.

Figure 8. Oily vial crusher.

Environmental Awareness

Hazardous waste quantity and cost data is publicized by holding meetings with and sending informational memos to the division environmental coordinators. Suggestions on ways to reduce waste generation are also publicized.

Oily Vial Crusher

Oily vials are small plastic and glass vials containing oil samples. A vial crusher was installed to consolidate the contents of oily vials into return oil. Oily vials were previously disposed of in lab pack drums as hazardous waste. The crusher breaks the vials and separates the vials and

Figure 9. Solvent mixing vessel.

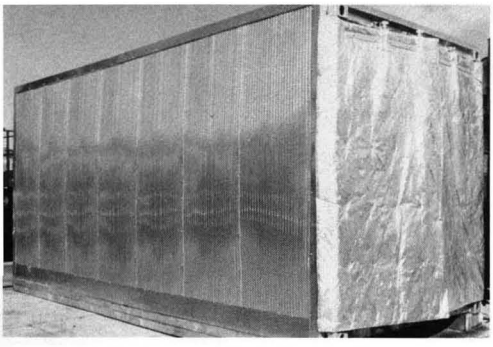

Figure 10. Hot box for solid and semi-solid hydrocarbons.

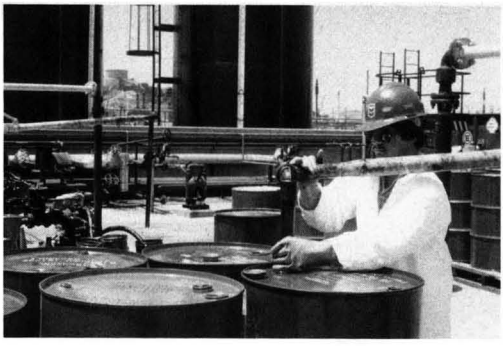

Figure 12. Pumping out a drum of return oil using a drum stabber.

Figure 11. Pouring small container of return oil into the return oil bin.

caps from the oil. The vial remnants are disposed of in oily trash. The recovered oil is put into return oil. Figure 8 is a picture of the crusher.

Bulking of Waste Solvents

A mixing vessel was installed to facilitate bulking of waste solvents. The solvents, mainly in 1-gallon jugs, were previously disposed of in lab packs. The bulking decreases waste disposal costs and increases the amount of waste solvent which can be recycled. A picture of the mixing vessel is shown in Figure 9.

Hot Box for Solid and Semisolid Hydrocarbons

Drums of meltable solid hydrocarbons which will not harm refinery processes, such as heavy crude oil and residuum, are melted in a designated hot box and pumped into return oil. This practice nearly eliminates the disposal of solid and semi-solid hydrocarbons as hazardous waste. The hot box is shown in Figure 10.

Return Oil

Return oil, which is petroleum oils and organics which will not harm petroleum refinery processes, is collected and sent to a petroleum refinery for processing with crude oil feed. Figure 11 shows small containers of return oil being poured into a collection bin. The bin is pumped out to an above-ground return oil tank. In Figure 12, a 55-gallon drum of return oil is being directly pumped out to a return oil tank.

FUTURE WASTE MINIMIZATION OPPORTUNITIES

To date, much of the waste minimization at RRC has resulted from changes in waste handling after the waste has been generated. We are currently evaluating more of these recycling and waste treatment opportunities. Much of the future waste minimization successes beyond that, however, will come from greater emphasis on front-end approaches like source control. Some source control opportunities we will be working on are discussed below.

Changes in Chemical Stockroom Practices

To help reduce generation of partially used waste chemicals, we will review the container sizes of stock chemicals. If container sizes more closely matched laboratory needs, the entire container contents would be consumed with no residual to be disposed.

Changes in Laboratory Practices

We will continue encouraging laboratory personnel to implement waste minimization practices in their laboratories. Suggested laboratory practices include: neutralize reactive and corrosive wastes as part of the laboratory procedure, make test materials in small batches, segregate waste materials, obtain only the quantities of chemicals needed, return surplus commercial plant samples to the plant, and modify or not use standard test methods which generate wastes which are difficult and costly to dispose.

The ultimate goal is to increase employee environmental awareness so that waste minimization is an automatic part of every job.

Chitosan in Crab Shell Wastes Purifies Electroplating Wastewater

Robert W. Coughlin
Department of Chemical Engineering, University of Connecticut, Storrs, CT

Michael R. Deshaies
Pratt & Whitney Div., of United Technologies Inc., East Hartford, CT

Edward M. Davis
SymBiotech Inc., Wallingford, CT

Chitosan, a polyglucosamine, can be formed by de-acetylating chitin, a major structural component of crustacean shells. Crab shell particles were treated and deacetylated to elaborate chitosan on their outer peripheries. Experimental data and an approximate preliminary economic analysis are presented to show the potential of using treated crab shell waste for purifying electroplating rinsewater. This approach is compared with currently used precipitation technology for removing metal ions.

INTRODUCTION

Waste from the shellfish industry has usually been disposed of by landfilling or ocean dumping. In some instances, waste crustacean shells are converted into a low value livestock feed or a fertilizer. Within the last decade, Muzzarelli [*1*] focused on one of the major components of crustacean shells, namely, chitin and its deacetylated derivative, chitosan, as a raw material for a large number of potentially useful products. In 1936–1937, Rigby [2] was granted U.S. patents for a method of making deacetylated chitin by a series of boilings and washings with acid, alkali, and detergent that required more than 14 hours. This suggests duPont (Rigby's employer) may have perceived potential value in chitin, the second most widely distributed natural polymer (after cellulose) about the time of the discovery of nylon.

In addition to its many other uses, the ion-complexing ability of deacetylated chitin (chitosan) has been measured and explored [3–6]. However, many of the methods reported for producing chitosan from crustacean shells are slow and consume significant amounts of reagents [2], [7] and [8].

This paper describes a rapid, less costly method of producing a metal ion-complexing material from the shells of crab and other crustaceans. The approach involves brief mild treatments of the shell waste (i.e., deacetylation times as short as only a few minutes) that apparently develop chitosan at the outer periphery of the shell particles without substantially converting the interior regions of the particles. We have used this ion-complexing material to remove copper, nickel, and other ions from the wastewaters produced by rinsing electroplated parts. Thus, waste from the seafood industry (estimated at between 5,000 and 8,000 tons/year by Hattis and Murray [*9*] and more recently at millions of tons/year, *Business Week* [*10*]) has been used successfully for treating wastewater from the electroplating industry as reported below.

EXPERIMENTAL

Crab shell waste was obtained from East Bay Crab Company of Peabody, MA. This consisted of shell particles and remnants of flesh not removed in the crab meat plant that processes the New England red edible crab.

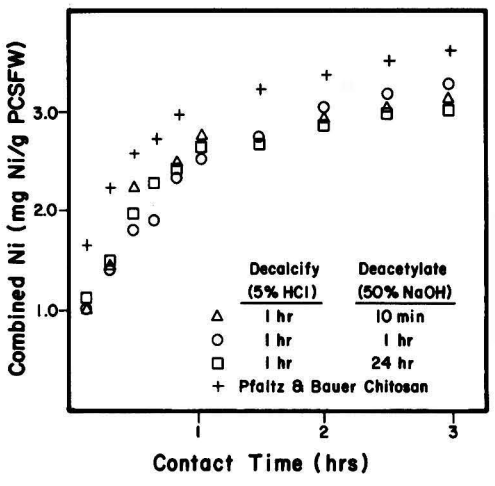

Figure 1. Time Course of Ni(II) Sorption from Prepared Solution. Solution (150 ml) initially containing 1,000 mg/L Ni prepared in laboratory from $NiSO_4$. Dosage: 3g PCSFW or of Pfaltz & Bauer chitosan per 150 ml of solution. Solution stirred at 25°C. Initial pH = 6.6; final pH = 7.2. One ml of solution removed periodically for assay by atomic absorption spectrophotometry (AAS).

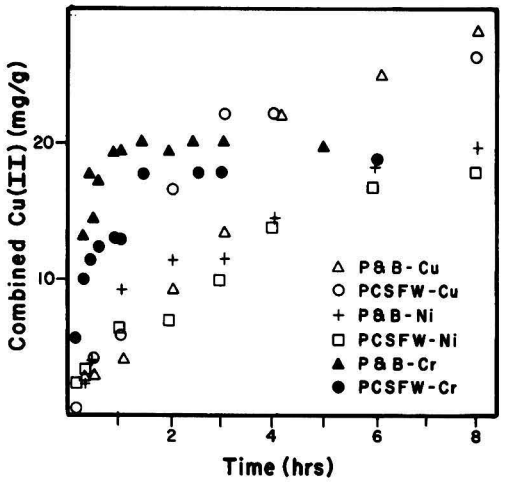

Figure 2. Time Course of Cu(II) and Ni(II) Sorption from Electroplating Rinsewater; Cr(III) from Prepared Solution. Solution (100 ml) initially containing 1,000 mg/L metal. Dosage: 1 g of PCSFW or Pfaltz & Bauer chitosan per 100 ml of solution. PCSFW was prepared by demineralizing (5% HCl) for 1 hour and deacetylating (50% NaOH) for 1 hour. Solution stirred at 25°C. Initial and final pH's: 2, 5.4 for Cu; 2.1, 5.6 for Ni; 2.7, 5.6 for Cr. One ml of solution removed periodically for assay by AAS.

Chitosan was obtained from Pfaltz and Bauer, Inc. of Waterbury, CT (product CO7640). Samples of plating solutions and rinsewaters from the electroplating operations were supplied by National Chromium Company, Putnam, CT. All chemicals employed were reagent grade, e.g., copper sulfate, nickel(II) sulfate, and chromium(III) nitrate from Brand Nu Labs, Meriden, CT.

Partially converted shellfish waste (PCSFW) was prepared from air-dried waste that had first been chopped in a Waring blender. A size range of about 1 mm to 10 mm was used; smaller particles were discarded. The shells were then soaked in a 5% HCl solution for one hour at room temperature to remove calcium salts (demineralization). After washing in water to remove HCl, the shells were stirred in 50% NaOH solution at 90°C for varying time periods to cause different extents of deacetylation. Protein was also removed by the foregoing NaOH treatment, after which the shells were again rinsed in water and dried in air. Although chemically similar, these treatments are shorter, milder, less extreme, and employ less chemical reagents than other methods reported for making pure chitosan from crab shells [2], [8], [7].

The aim of the less drastic treatment is to produce chitosan only at the surface rather than throughout the volumes of the particles. Allan, et al., [11] employed partially deacetylated chitin and shell particles to modify paper. However, it is likely their particles were uniformly deacetylated throughout their volumes because they had been previously ballmilled to very small size (44–100 micrometers). Grinding shells to very small sizes may be expected to rupture chemical bonds and produce sites active for adsorption as well as high specific surface areas. For example, Hung and Han [12] found considerable sorption capacity for metal ions by shells that had merely been ground to particles of 100/200 mesh size. Unfortunately, it is more difficult to use particles of such small size as a practical sorbent on a large scale; moreover, grinding to small sizes is costly.

Metal ion concentrations in solution were measured by atomic absorption (AA) flame spectrophotometry, and in some cases, by specific-ion electrodes. Removal of metal ion from solutions was studied at 25°C in a typical procedure by adding 1 g of PCSFW or purchased chitosan reagent to 100 mL of a solution and monitoring the concentration of metal ion versus time. Starting concentrations ranged from 10 to 1,000 mg/L. Elution of metal ions from PCSFW or chitosan was accomplished by contacting 1 g of the solid with 30 ml of N H_2SO_4 for 15 minutes at room temperature. This was followed by washing in tap water and contacting it with a N NaOH solution in the same proportions used for the H_2SO_4 and under the same conditions, to regenerate the PCSFW, much as ion-exchange resins are regenerated.

RESULTS AND DISCUSSION

The common feature of the results is the similar performance (regarding metal-ion removal) of the minimally treated PCSFW as compared to more exhaustively deacetylated material, including the material supplied by Pfaltz and Bauer as relatively pure chitosan. Figure 1 shows the specific amount of nickel removed from a prepared solution versus time. It is evident from the graph that the rates of removal are about the same for Pfaltz and Bauer (P & B) chitosan and all the PCSFW samples. P & B chitosan appears to offer a slight advantage regarding initial rate and specific amount of Ni(II) adsorbed after 2–3 hours of contact. For the PCSFW, it appears to make little difference whether the deacetylation/deproteination step is conducted for 24 hours, 1 hour, or 10 minutes. The extent of deacetylation were about 10% for 10 minutes and about 65% for 1 hour of this treatment. Thus, it appears that sorption of heavy metal ions during practical contacting times of up to several hours is limited to the outer portion of the particles, even when the particles are as extensively deacetylated as 65%. The similar behavior of all the samples may arise from similar kinetic limitations that might confine access of metal ions only to the periphery of the particles. The result being that all interior amino groups were probably not accessible to metal ions, even during sorption experiments as long as 12 hours. In the experiments described below, the PCSFW employed had been deacetylated for only 1 hour.

Figure 2 shows the time course of removal of Cu(II) and Ni(II) from electroplating rinsewaters obtained from

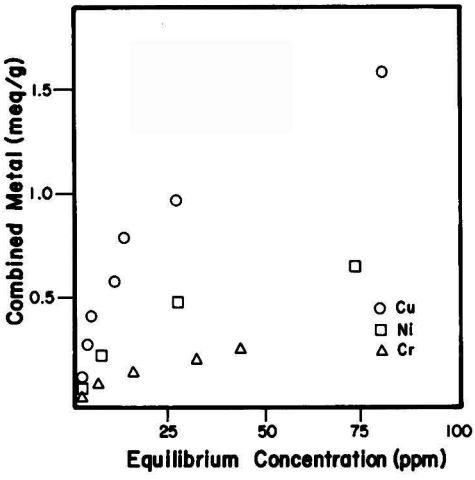

Figure 3. Sorption Isotherms of Ni(II), Cu(II) and Cr(III) from Prepared Solutions. Each data point was generated by adding 1 g of PCSFW to 100 ml of solution containing initial concentrations ranging from 10 mg/L to 1,000 mg/L of Ni(II), Cu(II), or Cr(III); solutions prepared in laboratory from $NiSO_4$; $CuSO_4$, or $Cr(NO_3)_3$. After 12 hours of contact, metal ion concentration in solution was determined by AAS.

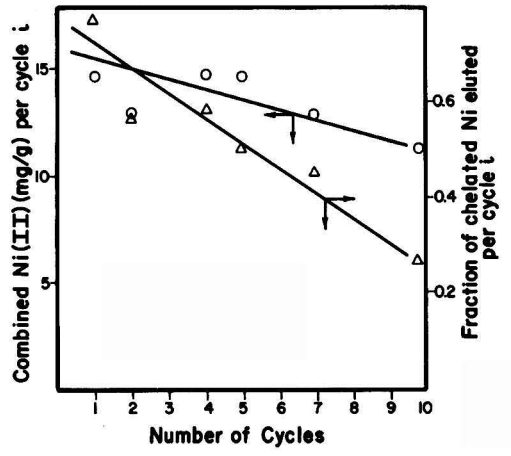

Figure 4. Elution of Ni from PCSFW. Each cycle comprises a sorption, an elution and a regeneration step. Sorption: 1 g of PCSFW contacted with 100 ml of electroplating rinse solution containing 500 mg/L Ni for 2 hours. Elution: 1 g PCSFW contacted with 30 ml of NH_2SO_4 for 15 min. Regeneration: 1 g PCSFW contacted with 30 ml of NNaOH for 15 min. Experiments conducted at 25°C with stirring.

a commercial operation, and of Cr(III) from a laboratory-prepared solution of $Cr(NO_3)_3$. Control experiments to measure Cu(II) sorption by untreated shells (particle sizes 3–5 mm) revealed capacities smaller by a factor of 5 than those indicated in Figure 2. It was visually apparent that copper sorbed preferentially at the fracture edges of the shell particles. Again, there is no significant difference between the general behavior of Pfaltz and Bauer chitosan and 1-hour-deacetylated PCSFW as ion-removal agents.

Figure 3 compares adsorption isotherms for Cu(II), Ni(II), and Cr(III) on PCSFW. Adsorption capacity (meq/g) is roughly in the order of 0.5 to 1.0. By way of comparison, the sorption capacity of PCSFW for copper evident in Figure 3 is about three times less than the values obtained for chitosan by Blair and Ho [*13*], who used equilibration times up to one week and extrapolated their results to infinite time. They used exhaustively deacetylated chitosan prepared by refluxing demineralized, decolorized, fine (<75 micrometers) shell particles in 50% NaOH solution for two hours. The isotherm of Figure 3 for Cr(III) is roughly equivalent quantitatively to comparable isotherms reported by Eiden, et al. [*14*] for sorption of Pb(II) and Cr(III) by chitosan. The same investigators reported sorption capacities of these metals on chitin that were smaller by about a factor of five. In further comparison, typical sorption capacities for commercial ion-exchange resins are in the range of about one milliequivalent per gram.

Initial pH does not have a strong influence on these isotherms, although adsorption capacity for Cu seemed to be increased slightly when initial pH was 2 as compared to 6.0. During the adsortion process pH increased, probably owing to some replacement of transition metal cations removed from solution by sodium cations leaving the PCSFW. Eiden, et al. [*14*] also observed increases in pH caused by sorption of Cr(III) by chitosan, but made no suggestion to explain the phenomenon.

Recovery of metal ions from PCSFW was studied by contacting it with N H_2SO_4 for 15 minutes in proportion of 30 ml of the acid solution to 1 g of original PCSFW. The metal-ion sorption capacity of the PCSFW was then partially restored by contacting it 15 minutes with N NaOH solution in the same proportion of mass of PCSFW to volume of solution. The results of performing these operations 10 times for sorption and elution of Ni are shown in Figure 4, where a cycle refers to the sequence described: metal-ion sorption followed by metal-ion elution with N H_2SO_4 and the restoration of sorption capacity with N NaOH. Similar behavior was observed with Cu and Cr, except that the elution of Cr(III) was considerably slower than Ni(II) and Cu(II). Figure 4 shows that both sorption capacity and amount of metal ion recovered by elution decrease gradually over the 10 cycles.

The decrease in sorption capacity and in recovery by repeated sorption and elution might be associated with phenomena such as:

- Gradual degradation and dissolution of pellicular chitosan by repeated elution and regeneration.
- Incomplete demineralization of the interior regions of the particles (see discussion of Figure 5 below), with protection and densification of the chitin matrix maintained by unremoved calcium carbonate.
- Transport of a portion of metal ions into the undemineralized and undeacetylated interior where the ions could be trapped, e.g., by precipitation as hydroxides or carbonates, or simply limited in mobility within a denser matrix of lower diffusivity. Eiden, et al. [*14*] reported good evidence that Pb and Cr formed nodular flakes on the surface of chitosan particles, perhaps as aggregates of $Cr(OH)_3$ and $Pb(OH)_2$.
- Partial immobilization of sorbed polyvalent ions by crosslinking, a phenomen observed and reported by Blair and Ho [*13*].

Several particles of PCSFW containing sorbed Ni(II) were investigated by energy dispersive x-ray analysis of their surfaces and interiors. Typical, representative results, shown in Figure 5, indicate high concentration of Ni at the surface and low concentration of Ni in the interior of a particle. This is in accord with the view of selective pellicular sorption of Ni(II) near the surface of the PCSFW particle, but not in the interior, probably owing to a corresponding distribution of deacetylation and kinetic limitation. Figure 5 also shows the converse distribution of Ca within the PCSFW particle. The low Ca concentration at the surface reflects the removal of surface Ca

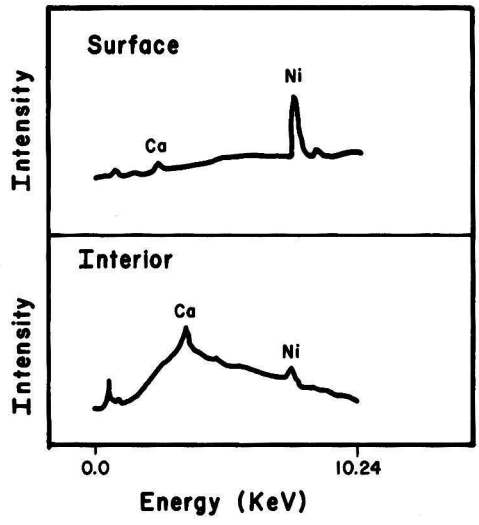

Figure 5. Energy Dispersive X-Ray Analysis of Particle of PCSFW. Upper spectrum-particle surface; lower spectrum-particle interior. Particle had first been equilibrated with a solution of Ni(II).

by the mild demineralization step with HCl for one hour. The high residual Ca concentration within the interior of the particle reflects the mild, partial conversion of the shell during which removal of Ca was not accomplished in the interior, but only near the surface of the particle. It seems likely that the non-uniform distribution of Ca (and therefore probably also of carbonate) within the PCSFW particles may also relfect non-uniform transport resistance from the surface to the interior of the particle.

POTENTIAL FOR TREATING ELECTROPLATING WASTEWATER

A common and traditional approach to treatment has been precipitation of the metals as the hydroxides from electroplating wastewaters, followed by filtering, and burying the solid precipitate in a landfill. In some cases, it is necessary to use bases other than lime or caustic for precipitation, e.g. $Mg(OH)_2$ is used to precipitate Ni hydroxide in order to obtain a precipitate that has good filtration properties. In the case of chromium-containing wastewater, it is necessary first to reduce hexavalent chromium ions using sodium bisulfite to form Cr(III) ions, which can then be precipitated as the hydroxide. Burying metal precipitates in a landfill is costly, and a practice that must eventually be replaced by better technology.

The ability of PCSFW to sorb and to release metal ions during elution offers another possible approach to treating electroplating wastewaters. Because metal ions can be eluted from PCSFW, which can then be re-used, this approach has promise as a possible method of reclaiming and recycling the metals, in contrast with past and present practices. Table 1, which shows a comparison of simple flow sheets for the two treatment processes, indicates major equipment items and costs for treatment of 11,350 L/mo of Ni(II) rinsewater (1000 mg/L, pH = 2) and 11,350 L/mo of Cr(VI) rinsewater (1000 mg/L, pH = 2). This is a typical treatment scenario for a small, electroplating job shop. For sorption by PCSFW, the Cr(VI) must be reduced to Cr(III), and also done for the precipitation process. A major cost contribution to the conventional precipitation approach arises from the rotary filter that is

TABLE 1. MAJOR EQUIPMENT ITEMS AND COSTS (1987 U.S.$).

Item	Precipitation Process Number	Precipitation Process Cost	PCSFW Sorption Process Number	PCSFW Sorption Process Cost
Waste collection tanks, 3,783 liters (1,000 gal)	3	4,500	3	4,500
Chem. storage tanks, 63 liters (250 gal)	4	1,800	4	1,800
Pumps	5	2,500	5	2,500
Elution tank, 63 L (250 gal)	—	—	1	500
Rotary filter	1	10,000	—	—
Total Cost		18,800		9,300

TABLE 2. TOTAL CAPITAL INVESTMENT (FACTORS FROM PETERS AND TIMMERHAUS [15].

		Precipitation	PCSFW Sorption
Direct Cost			
equipment	= cost	$18,800	$ 9,200
installation	= 0.47(cost)	8,800	4,300
piping	= 0.66(cost)	12,400	6,100
electrical	= 0.11(cost)	2,100	1,000
	subtotal	$42,100	$20,600
Indirect Cost			
engineering	= 0.15(cost)	$ 2,800	$ 1,400
supervision	= 0.15(cost)	2,800	1,400
fees	= 0.14(cost)	2,600	1,300
		$ 8,200	$ 4,100
Total Capital Cost		$50,300	$24,700

required, because the precipitates do not readily settle and dewater to form a concentrated mass that could be easily handled. Total capital investment for each process is summarized in Table 2. Note that the equipment for PCSFW sorption includes provision for storing reagents to convert crab-shells to PCSFW, to regenerate the PCSFW by acid elution, and to reduce Cr(VI) to Cr(III). Similarly, the equipment list for precipitation includes reagent storage for precipitation/neutralization and for reduction of Cr(VI) to Cr(III).

Table 3 provides an economic comparison of the two processes. The operating and maintenance costs for the PCSFW process are based on the assumption that the sorbent can be used for 10 cycles, and that the eluted Ni(II) and Cr(III) (after re-oxidation to Cr(VI)) are recycled to the electroplating process. The high cost of chemicals for the precipitation process reflects the use of magnesium hydroxide, which is required to produce a sludge that can be conveniently filtered and disposed of following current practice. Disposal costs (for burying sludge in a landfill) and capital and depreciation costs (expensive filter) are also high for precipitation. If precipitation using lime had been assumed, the cost of chemicals would be less. However, the cost of sludge disposal would be correspondingly greater, owing to the larger specific volume of the sludge precipitated by lime rather than $Mg(OH)_2$. The net effect on the economic comparison would be small.

The disposal costs shown are also somewhat large for the PCSFW sorption process and are based on the assumption that used PCSFW will be buried in a landfill after 10 cycles of sorption and regeneration. This assumption is conservative because it is likely that PCSFW can be used for more than 10 cycles before it must be disposed of. It is also likely it will be cheaper, more convenient, as well as environmentally more acceptable to

TABLE 3. TOTAL COST OF TREATMENT.[1]

Basis: 11,350 L/mo (3,000 gal/mo) Cr(VI) wastewater (1,000 mg/L)
11,350 L/mo (3,000 gal/mo) Ni(II) wastewater (1,000 mg/L)
Cr(VI) reduction by sodium bisulfite
Precipitation with magnesium hydroxide
assumed capacity of PCSFW = 50 mg Ni/g, 20 mg Cr/g

	Precipitation	PCSFW Sorption
Total capital investment	$50,300	$24,700
Monthly costs:		
capital cost	500	200
depreciation	400	200
operating & maintenance		
a. chemicals[2]	1,350	300
b. disposal[3]	850	400
c. maintenance[4]	200	100
d. labor[5]	360	400
credit for recovered Cr and Ni[6]	—	−100
Total monthly cost	3,660	1,500
Treatment cost per gallon	0.61	0.25
Treatment cost per liter	0.15	0.06

[1] Prices based in part on information supplied by National Chromium Company, Putnam, CT.

[2] Chemicals: $Mg(OH)_2$ $1.72/kg ($0.78/lb)
NaOH, 50% (w/w) $215/metric ton ($195/ton)
HCl, 36% (w/w) $71.65/metric ton ($65/ton)
H_2SO_4, 95% (w/w) $105.70/metric ton ($95.90/ton)
$NaHSO_3$ $0.66/kg ($0.30/lb)

[3] Disposal cost $460/m^3 ($13/cu ft).

[4] Annual maintenance taken as 5% of total capital investment.

[5] Labor estimated at $12/hr, 30 hr/mo.

[6] Recovered metal mean credit assumed to be about $4.50/kg; overall treatment cost is relatively insensitive to this item.

incinerate exhausted PCSFW than to bury it in a landfill. It should be noted that landfill toll costs are high in that they reflect severe technological requirements (e.g., the mandated use of lining membranes and monitoring) for disposal of such heavy metal sludge. Furthermore, such disposal methods are likely to be banned by statute in the future. The treatment of wastewater generated by the production of PCSFW would add a cost of more than one dollar for the basis of Table 3, therefore, this has been neglected as relatively inconsequential. Moreover, it would be possible to recover protein and sodium acetate, perhaps with favorable economics, from such a wastewater.

CONCLUSION

Partial conversion of crab shell waste to chitosan in the outer, pellicular regions of the particles produces a useful sorbent for transition metal ions that is nearly as effective as relatively pure chitosan. It is technically feasible to use this material (PCSFW) to sorb metal ions from electroplating wastewaters, to elute the metals therefrom, and recycle them to the electroplating process. An approximate economic comparison of the conventional precipitation process to a conceptual process based on sorption on PCSFW indicates that the latter is economically more favorable under reasonable assumptions.

ACKNOWLEDGMENTS

This work was supported by a grant from the U.S. Department of the Interior through the Institute of Water Resources of the University of Connecticut. Additional support from the Environmental Research Institute of the University and the U.S. National Science Foundation under Grant Number CBT-8717768 is also acknowledged. Important experimental assistance was given by Ann Carella and Amy Gaunya. Joseph Zoghbie contributed to the calculations for economic comparisons. We thank National Chromium Company, Putnam, CT for supplying samples of electroplating wastewater and providing information about treatment by precipitation. We also thank East Bay Crab Company, Peabody, MA for supplying samples of crab shell waste.

LITERATURE CITED

1. Muzzarelli, R. A. A., *Chitin*, Pergamon Press, NY (1977).
2. Rigby, G. W., "Substantially undegraded deacetylated chitin and process for producing the same," U.S. Patent 2,040,879 (May 19, 1936); "Chemical products and process of preparing the same," U.S. Patent 2,072,771 (Mar. 2, 1937).
3. Masri, M. S., and V. G. Randall, "Chitosan and Chitosan Derivatives for Removal of Toxic Metal Ions from Manufacturing Plant Waste," in *Proc. 1st Intl. Conf. Chitin and Chitosan*, p. 286, R. A. A. Muzzarelli and E. R. Pariser, Eds., MIT Sea Grant 78-7, Cambridge, MA (1978).
4. Schlick, S., *Macromolecules*, **19**, 192 (1986).
5. Yaku, F., and T. Koshijima, "Chitosan = Metal Complexes and Their Functions," in *Proc. 1st Intl. Conf. Chitin and Chitosan*, p. 386 (1968).
6. Muzzarelli, R. A. A., *Natural Chelating Polymers*, p. 188, Pergamon Press, NY (1973).
7. Peniston, Q. P., and E. L. Johnson, "Method for treating an aqueous medium with chitosan and derivatives of chitin to remove an impurity," U.S. Patents 3,533,940 (Oct. 13, 1970); 3,862,122 (Jan. 21, 1975); 4,195,175 (Mar. 25, 1980).
8. Broussignac, P., *Chimie et Industrie-Genie Chimique*, **99**, No. 9, 1241–7 (1968).
9. Hattis, and Murray, "Industrial Prospects for Chitin from Seafood Wastes," MIT Sea Grant Report No. 27, MIT, Cambridge, MA, Aug. 1976.
10. Anonymous, "Stop—Don't Throw Those Crab Shells Away," *Business Week*, p. 112 (March 23, 1987).
11. Allan, G. G., J. F. Friedhoff, M. Korpella, and J. C. Powell, *ACS Symposium Series*, **10**, 172 (1975).
12. Hung, T. C. and S. L. M. Han, *Acta Oceanograph*, Taiwan **7**, 56–63 (1977).
13. Blair H. S., and T.-C. Ho, *J. Chem. Technol. Biotechnol.*, **31**, 6 (1980).
14. Eiden, C. A., et al, *J. Appl. Poly Sci.*, **25**, 1587 (1980).
15. Peters, M. S., and K. P. Timmerhaus, *Plant Design and Economics for Chemical Engineers*, p. 180, McGraw Hill, NY (1980).

Prediction of Activated Carbon Adsorption Performance Under High Relative Humidity Conditions

Tim C. Keener and Derong Zhou

Civil and Environmental Engineering Department, University of Cincinnati, Cincinnati, OH 45221

Humidity effects on carbon adsorption were investigated using five volatile organic compounds (VOCs). Relative humidities ranged from 54% to 92%. Under these high relative humidity conditions, the Dubinin–Polanyi equation was used to analyze the results of activated carbon adsorption capacity. Based on the Dubinin–Polanyi equation and the concept of a mass transfer zone, an adsorption kinetic equation was derived to predict the carbon adsorption (MTZ) velocity and the adsorbate concentration profile in the bed.

INTRODUCTION

Carbon has been known throughout history as an adsorbent; its usage could date back centuries. Presently, activated carbon plays an important role in water, air pollution control (such as controlling emissions of Volatile Organic Compounds, VOCs) and material recovery.

Emissions of VOCs are of concern primarily because of their contribution to localized atmospheric pollution. In general, the formation of smog results from photochemical reactions between VOCs, nitrogen oxides, and ozone. These produce a variety of noxious compounds such as peroxyacetyl nitrate (PAN). The presence of these compounds form aerosol particles which cause eye irritation, and are possibly carcinogenic. These situations are prevalent in heavily industrialized urban areas. Primarily, VOC emissions are from industries such as the semiconductor, auto paint baking, aluminum siding paint baking, appliance paint baking industry and so on.

Although adsorption with activated carbon has been used commercially for many years, significant research on the fundamental behavior (such as adsorption mechanisms and adsorbent structures), and industrial applications (such as optimal adsorption system design and adsorbent regeneration as well as adsorbate recovery) are still being undertaken.

There are many theories concerning adsorption of vapor on activated carbon. Among them, the Dubinin–Polanyi (D–P) equation is a simple and practical equation used for design purposes. Once certain parameters in the D–P equation are obtained with a reference adsorbate, adsorption efficiencies of other similar adsorbates may be predicted without experiment [*1, 2*]. Further, these parameters may be introduced into a kinetic model for describing the entire adsorption process. However, currently available data for adsorption is limited to low relative humidities. VOC control applications are concerned with flow streams at any level of humidity. Since a decrease of adsorption efficiency occurs at relative humidities greater than approximately 50% to 70% [*3, 4, 5*] there is a need for design information at these conditions.

The goals of this research included using the Dubinin–Polanyi relationship to analyze activated carbon adsorption capacity under high humidity conditions, to quantify the effects of high relative humidity on adsorption and to predict adsorption breakthrough profiles and compare these with experimental results.

THEORY

Adsorption Capacity: Dubinin–Polanyi Equation

The Dubinin–Polanyi model is an extention of the potential theory for multilayer adsorption. This equation represents the theory of adsorbate adsorption potential and the filling of the adsorbent micropore volume. According to experimental data and theoretical considerations [6] the characteristic curve for microporous carbon adsorbents can be given in the explicit form as:

$$\ln(W/W_o) = -k\alpha^2 \tag{1}$$

where,

α = $RT\ln(P_s/P_o)$
W = the adsorption space occupied by the condensed adsorbate (ml/g)
W_o = limiting amount of adsorption space for each adsorbent (ml/g)
k = a parameter for each system of adsorbent and adsorbate, $(J/mol)^{-2}$
T = the absolute temperature of adsorption, °K
P_s = saturated vapor pressure at absolute temperature T (°K), atm
P_o = adsorbate equilibrium partial pressure under operating conditions, atm
R = gas constant (8.3143 J/K · gmol)

For a reference adsorbate, equation 1 can be written as follows:

$$\ln(W/W_o) = -k_s\alpha_s^2 \tag{2}$$

(where subscript s represents the reference adsorbate.)

Comparing Equation 1 with Equation 2 for any adsorbate on the same adsorbent, the adsorption equation is

$$\ln(W/W_o) = -(k_s/\beta^2)\alpha^2 \tag{3}$$

$$(k_s/k) = (\alpha/\alpha_s)^2 = \beta^2 \tag{4}$$

Reucroft and co-workers [7] found that the affinity coefficient, β, was best expressed by the ratio of the electronic polarization of the adsorbate to that of a reference adsorbate.

Consequently, Equations 1-4 may be solved to yield the following:

$$\ln(W) = \ln(W_o) - \frac{k_s}{\beta^2}\left[RT\ln\frac{P_s}{P_o}\right]^2 \tag{5}$$

Therefore, when experimental values for $\ln(W)$ are plotted against $(RT\ln(Ps/P_o))^2$, a straight line with an intercept equal to $\ln(W_o)$ and a slope of k_s/β^2 will be obtained.

The value of W_o is independent of both the operating temperature and the nature of the adsorbate vapor [3, 4]. Therefore, the value of W_o, once determined, can be used for other adsorbates and adsorption conditions. Having estimated the value of the affinity coefficient, β, the value of k_s can be calculated since the slope of the straight line is determined by k_s/β^2.

Dubinin [6] suggested that the values of the three parameters, W_o, β, and k_s remained constant over adsorption temperatures and conditions of adsorption. Therefore, if the parameters, W_o, β, k_s are obtained from experiment on adsorption capacity with a reference adsorbate, the theoretical adsorption capacity for another similar adsorbate can be predicted for various adsorption temperatures and pressures by use of Equation 5.

Adsorption Kinetics

An adsorption kinetic equation was developed based on the concept of a mass transfer zone (MTZ) [8], and the Dubinin–Polanyi equation. The assumptions used in this approach are as follows:

1. Adsorption conditions such as temperature and flow rate are constant.
2. There are no radial temperature, concentration, and flow rate gradients in the adsorbent bed.
3. Adsorption heat effects are negligible.
4. Physical adsorption predominates with negligible chemisorption.
5. The thickness of the adsorption zone is constant under the conditions of these assumptions.
6. The velocity of the adsorption zone is constant throughout the adsorption process and small in comparison to the gas superficial face velocity.
7. The adsorbate condenses (through capillary condensation) to a liquid.

The amount of adsorbate entering the adsorption zone essentially equals the amount transferred to the adsorbent. As a result, a mass balance of the adsorbate between the gas and solid phase in the adsorption zone is:

$$\frac{m_a C_o}{\rho_a} = \rho_{ad} A\, V_{ad}\, X_{sat} \tag{6}$$

where,

m_a = carrier gas, air mass flow rate, kg/min
C_o = adsorbate inlet concentration, kg/m^3
A = cross-sectional area of adsorber, m^2
ρ_{ad} = adsorbent packed density, kg/m^3
ρ_a = carrier gas density, kg/m^3
X_{sat} = equilibrium adsorption capacity, kg/kg
V_{ad} = adsorption zone velocity, m/min

The adsorption zone velocity or, MTZ velocity, may be obtained from Equation 6 as:

$$V_{ad} = \frac{m_a C_o}{\rho_a}\cdot\frac{1}{X_{sat}\rho_{ad}A} \tag{7}$$

Equation 5 may be rewritten as follows:

$$W = W_o\exp\left[-\frac{k_s}{\beta^2}[RT\ln Ps/Po]^2\right] \tag{8}$$

From the assumption of total liquid condensation of the adsorbed vapor we may write:

$$W_e = W\rho_{ab} = X_{sat} \tag{9}$$

where,

W_e = adsorption capacity, kg/kg or g/g
ρ_{ab} = adsorbate density, kg/m^3 or g/ml

Then, Equation 8 can be rewritten as follows:

$$W_e = X_{sat} = \rho_{ab} W_o \exp\left\{-\frac{k_s}{\beta^2}\left[RT\ln\frac{P_s}{P_o}\right]^2\right\} \tag{10}$$

Equation 10 and 7 may be combined, and assuming the adsorbate vapor behaves as an ideal gas, the adsorption velocity equation may be obtained as the following:

$$V_{ad} = \frac{M_a}{\rho_a\rho_{ab}\rho_{ad}AWo}\cdot\frac{P_oM_{ab}}{RT}\exp\left\{\frac{k_s}{\beta^2}\left[RT\ln\frac{P_s}{P_o}\right]^2\right\}$$

$$= B\frac{P_oM_{ab}}{RT}\exp\left\{\frac{k_s}{\beta^2}\left[RT\ln\frac{P_s}{P_o}\right]^2\right\} \tag{11}$$

Equation 11 indicates the relationship between the adsorption velocity, and the D-P equation.

The transfer of mass from the gas phase to the solid phase within the MTZ may be expressed by

$$dm_{ab} = -\frac{m_a}{\rho_a} dC \tag{12}$$

where,

m_{ab} = adsorbate mass flow rate, kg/min

The adsorbate mass flowrate from the gas phase to the solid phase within the MTZ is proportional to the concentration difference between that in the gas phase and the equilibrium concentration which could exist on the adsorbent. This condition may be expressed by the relationship

$$m_{ab} = KV\,(C - C_e) \tag{13}$$

where,

K = an overall mass transfer coefficient, s^{-1}
C = adsorbate concentration
C_e = adsorbate equilibrium concentration
V = volume of the bed

and the change of m_{ab} with respect to position within the MTZ is therefore

$$dm_{ab} = KA\,(C - Ce)dx \tag{14}$$

where,

x = position along the MTZ, m

The relationship expressing concentration change within the MTZ as a function of position may now be obtained by combining Equations 12, 14 and the Dubinin–Polanyi equation. The result is as follows:

$$dx = -\frac{m_a dP}{\rho_a KA\left\{P - P_s \exp\left[-\frac{\beta}{RT} k_s^{-1/2}\left[\ln\frac{P_o}{P} + F\right]^{1/2}\right]\right\}} \tag{15}$$

The boundary conditions for Equation 15 are as follows:

$$\text{at} \quad x = 0,\ P = P_o, \text{ and at } x = x,\ P = P$$

$$\text{Let } \eta = P/P_o,\ dP = P_o d(P/P_o) = P_o d\eta$$

Integration of Equation 15 from 0 to x yields an expression for the adsorption zone thickness δ.

$$\frac{\rho_a KA\delta}{m_a B'} = \int_{\eta}^{1} \frac{d\eta}{\eta\, B'\eta - exp\,(-G\,(F - \ln\eta)^{1/2})} \tag{16}$$

where

$$G = \left(\frac{\beta}{RT}\right) k_s^{-1/2},\ F = \frac{k_s}{\beta^2}\left[RT \ln\frac{P_s}{P_o}\right]^2,\ B' = P_o/P_s$$

Equation 16 may be integrated in order to obtain δ, the mass transfer zone thickness. A value of η, the ratio of outlet concentration to inlet bed concentration is normally set in order to estimate the bed breakthrough time. For instance, if a ratio of outlet concentration to inlet bed concentration of 0.1 is defined as the breakthrough point, then Equation 16 is integrated for values of η from 1 to 0.1 in order to obtain δ. The breakthrough time then is obtained from the following equation:

$$t_b = \frac{L - \delta}{V_{ad}} \tag{17}$$

where,

t_b = the breakthrough time, hours or minutes

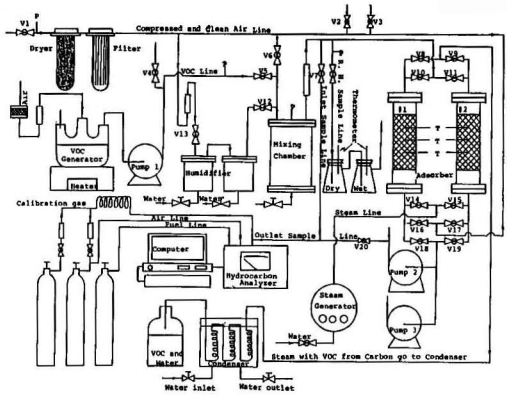

Figure 1. Flow diagram of adsorption system.

δ = thickness of adsorption zone, m
V_{ad} = adsorption velocity, m/min or m/sec

The breakthrough time, t_b, may be obtained from experimental data. The MTZ velocity, V_{ad}, may be calculated from Equation 11 for the adsorption conditions. The thickness of the adsorption zone may be calculated with Equation 17 for a given bed length. Finally, with the values of δ used in Equation 16, the mass transfer coefficient, K, may be obtained for the various adsorption conditions.

ADSORPTION SYSTEM OVERVIEW

The bench–scale adsorption system (as shown in Figure 1.) used in this research consisted of five sub-systems. They were:

1. Clean Air System, 2. VOC Vapor Generation System, 3. Humidity Generation System, 4. Adsorption and Regeneration System, 5. Calibration and Analysis System.

System 1, 2, and 3 provided a known VOC stream to the adsorbers. System 4 and 5 included the means of regeneration of the saturated carbon beds and VOC concentration analysis.

The VOC concentration analysis of the inlet and outlet of the adsorber were monitored by a Beckman Model 400 hydrocarbon analyzer. All the concentration values were logged by microcomputer.

Five different organic compounds were used in this study; toluene, carbon tetrachloride, ethylbenzene and methylene chloride. These were certified from Fisher Scientific. Ethyl alcohol was also used from Pharmaco Products Inc.

In order to test the adsorption model, a series of experiments were conducted in which the adsorption test parameters were varied as follows: relative humidity ranged from 54% to 92%; the carrier gas (air) flow rate ranged from 300 to 320 SCFH (8.5-9m^3/hr); the concentration of the adsorbates ranged from 300 ppm to 900 ppm.

The air as a VOC carrier gas was filtered and cleaned of oil, water vapor and particles. The carrier air passed through a dryer (Fauver Company, Inc. Model X03-02-000 1/4 descant dryer) which removed water vapor and oil. The air was filtered by a Gelman 12510 Housing and Gelman 12570 cartridge. Particles larger than 0.45 micron are removed in this type filter.

One-third to two-thirds of the conditioned air was directed to the humidity system, then to the mixing chamber. For the case of the dry adsorption tests, the cleaned and dryed air was totally directed to the mixing chamber except for a small part which was used for the analyzer.

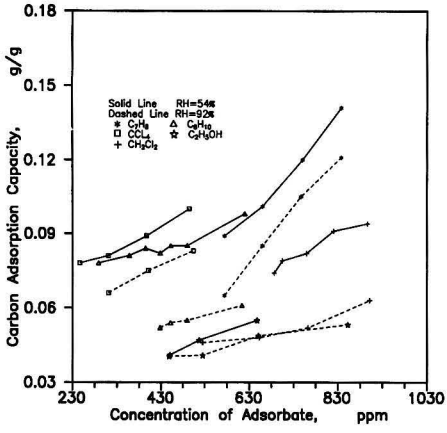

Figure 2. Carbon adsorption capacity versus adsorbate concentration.

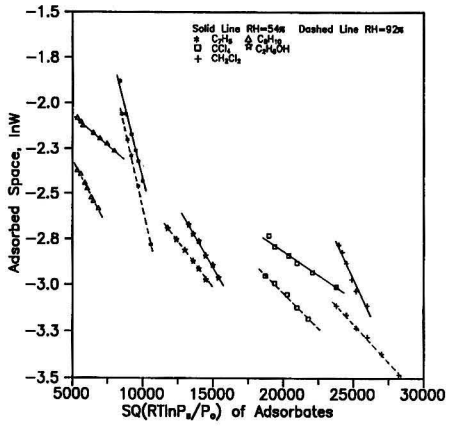

Figure 4. Test of the Dubinin–Polanyi isotherm form.

For the case of the high humidity adsorption tests (ranging from 60% to 90% relative humidity), the air stream was divided into two parts; one was directed to the humidity generator while the other was directed to the mixing chamber.

The humidity generation system was comprised of two stainless steel tanks both 4.2 inches inside diameter (10.7cm) and six inches in height (15.25cm). Both tanks were periodically filled with water. The water in the tanks was heated by an electric heat tape wrapped on the surface of the tank. The temperature was controlled by varying the voltage applied to the heating tape.

A three-neck flask was partially filled with the liquid organic compound being tested. The glass flask was heated by an electromantle. Air used to dilute the VOC vapor was directed through a rotameter into the flask. The mixture of air and absorbate vapor were exhausted by the vacuum pump 1. (See Figure 1). Adjustment of the vapor concentration was controlled either by adjusting the flow rate of the dilution air, or the temperature of the liquid absorbate.

A stainless steel cylinder, 12 inches inside diameter and height (30.48 cm), was used as the mixing chamber. Dry or humid air and the VOC stream individually entered into the mixing chamber and formed a uniform VOC/air mixture. The pressure of the mixing chamber was usually under 30 psig (207 k Pa). The pressurized air stream with VOC mixture was directed to the adsorbers.

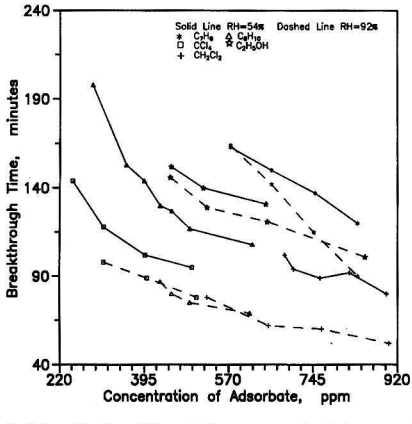

Figure 3. Adsorption breakthrough time versus adsorbate concentration.

The adsorbers consisted of two stainless steel tanks, both 4.20 inches inside diameter (10.7 cm) and 20 inches height (50.8 cm). Each adsorber was filled to a height of five inches (12.7 cm) with 469.5 grams of pelletized activated carbon (Witco Corp., type JxC).

The activated carbon was regenerated with steam to recover the activity of the carbon. The steam was produced by an electrical steam generator (Sussman Model MB-6L). The steam, with pressures from 20 to 30 psig (138-207 k Pa), was directed into the saturated adsorber at the rate of three pounds of steam per pound of carbon. The steam and VOC vapor mixture was condensed by a chiller where the VOC was decanted. Conditioned air was used to cool and dry the hot, wet carbon bed prior to the initiation of a new adsorption cycle.

Experiment Results and Discussions

The experimental adsorption capacities for two levels of relative humidity are given in Figure 2. The breakthrough times (10%) for these experiments are given in Figure 3. A test of Equation 5 for the Dubinin–Polanyi isotherm for the data is given in Figure 4. The experimental data fit the linear form as given by the Dubinin–Polanyi equation even though the adsorption experiments took place under high humidity conditions.

The adsorption capacity for the different adsorbates varied from 0.041 to 0.141 g adsorbate/g carbon. Ranking the adsorption capacity, from the highest to the lowest is toluene, ethylbenzene, carbon tetrachloride, methylene chloride and ethanol. Ranking the molecular weight, from the highest to the lowest is carbon tetrachloride, ethylbenzene, toluene, methylene chloride and ethanol. The experimental results shown in Figure 2, and set in the Dubinin–Polanyi form in Figure 4, indicate possible changes in either the values of k_s, β or W_o due to the configuration of the isotherms.

Unparallel adsorption lines as shown in Figure 4 for a given adsorbate indicate that the value of either β or k_s is not constant. The values of β represent an adsorbate property which measures the strength of adsorption interaction of a given adsorbate on a carbon relative to a reference adsorbate.

In order to determine if β stays constant under high humidity conditions, it is necessary to understand the adsorption mechanism of water molecules on activated carbon. Because water is a polar molecule, the adsorption capacity of water on activated carbon as a result of disper-

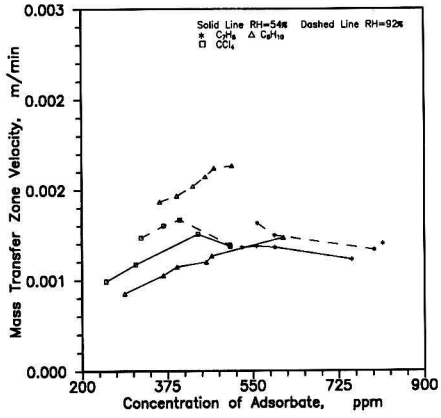

Figure 5. Mass transfer zone velocity versus adsorbate concentration.

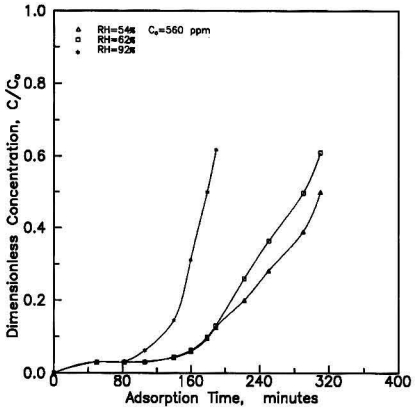

Figure 6. Comparison of the exit stream concentration of toluene.

sion forces alone should be very small. Activated carbon, because of contact with atmospheric air, will form "surface oxides" [6] as a result of the stable chemisorption of oxygen. These oxides are essentially oxygen containing radicals attached to the individual carbon atoms forming the wall of micropores. For examples, Adams, *et al.* [9] found the adsorption performance of hexane on "aged" charcoals to be inferior to that of the control charcoals. The "aged" charcoals were from the same stock as the control but contained more surface functional groups. Dubinin described these oxygen–containing radicals as primary adsorption centers localized in the adsorption space of the micropores. The molecular adsorption of water is chiefly due to the formation of hydrogen bonds between water molecules. The adsorption of other adsorbates is dependent largely on forces of dispersion between molecules, while adsorption of polar water molecules is controlled by electrostatic interactions with adsorption centers. Due to differences in adsorptive mechanisms, the water molecules only reduce the number of adsorption centers. The value of β should not be changed with the number of adsorption centers or presence of water molecules. In other words, the values of β should be a constant whose value only depends upon the reference adsorbate. As a result, the reason for the unparallel adsorption lines should be attributed to k_s.

The phenomenon of k_s varying with the adsorption conditions may be explained by noting that k_s is a function of the ratio of limiting adsorption space, W_o, and the volume of micropores, V_{mi}. As the ratio of W_o/V_{mi} increases, the value of k_s also increases. The values of V_{mi} vary with relative humidity. These experimental results found in this study are similar to those reported by Werner [3], who reported k_s values ranging from 4.70×10^{-9} to 13.2×10^{-9} over a relative humidity range of 4.7% to 80%. The values of k_s as found in this study are shown in Table 1 and are believed to account for the changes in the isotherm slopes.

A second phenomenon, adsorption lines with different intercepts, $\ln(W_o)$, should also be attributed to the decrease in carbon adsorption capacity due to humidity effects. An analysis of the intrusion pore volume (Micrometrics Model 9100 Mercury Intrusion Porosimeter) of our dry carbon versus carbon treated with gas containing water vapor at 92% relative humidity showed a reduction of 53%. Therefore, it is impossible for the intercept to be at the same value for different relative humidities because the number of adsorption centers varies with relative humidity. Of course, under the same concentration value, different humidities resulted in the different adsorption capacities. The quantitative relationship between relative humidity and adsorption capacity is probably more complicated. Based on data given in Figure 1, when relative humidity increased from 54% to 92%, carbon adsorption capacity decreased about 11% for C_7H_8, about 37.5% for C_8H_{10}, about 39% for CH_2Cl_2, about 19% for CCl_4 and about 6% for C_2H_5OH. Perhaps adsorption capacity is not significantly decreased in the 54% to 92% relative humidity range because both relative humidity levels are usually considered as high humidity. If we compare the adsorption capacity data at low humidity with the adsorption data at high humidity, a large decrement is seen. Taking toluene as an example, when the concentration is 575 ppmv, these results indicate an adsorption capacity equal to 0.089 g/g for 54% relative humidity, and an adsorption capacity equal to 0.079 g/g for 92% relative humidity. However, the adsorption capacity for this concentration is given as 0.28 g/g for an assumed low humidity condition (data from Witco Inc., no adsorption conditions and system were indicated) [*10*]. Comparing these results, the toluene adsorption capacity decreases by 68% at 54% relative humidity and by 71% at 92% relative humidity. Werner [3] reported that activated carbon adsorption capacity for trichloroethylene decreased by 70% when relative humidity increased from 5% to 85%. The above experimental data and analysis results clearly indicate that humidity effects should be considered in adsorption system equipment design and operation for vapor phase adsorption.

TABLE 1. k_S(J/MOL)$^{-2}$ VALUES AT RELATIVE HUMIDITY

		54%	92%
C_7H_8	(β = 1.182)	4.65×10^{-4}	4.65×10^{-4}
C_8H_{10}	(β = 1.385)	3.07×10^{-4}	1.59×10^{-4}
CCl_4	(β = 1.00)	5.00×10^{-5}	6.00×10^{-5}
C_2H_5OH	(β = 0.487)	1.42×10^{-5}	1.18×10^{-5}
CH_2Cl_2	(β = 0.619)	7.40×10^{-5}	3.44×10^{-5}

The calculated adsorption velocities are presented in Figure 5. When adsorption concentration increases, the adsorption velocity or MTZ velocity increases. Assuming one adsorption center only needs one adsorbate molecule, when the molecular number of an adsorbate increases, the limited adsorption centers in the MTZ are occupied quickly. Another point shown in Figure 5 is, that for the same conditions, the adsorption velocity at high humidity is greater than that at low humidity. Under the conditions of high humidity, part of the adsorption centers are occupied by water molecules. Finally, the entire MTZ velocity increases with humidity increment. This phenomenon can be observed in Figure 6. In this figure,

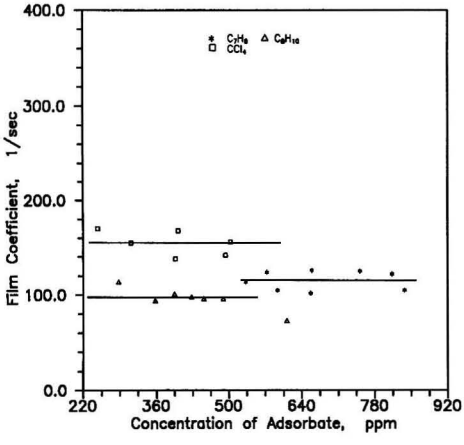

Figure 7. Adsorption film coefficient versus adsorbate concentration.

for the same concentration, the breakthrough time for high humidity is less than that of low humidity.

Average values of the mass transfer coefficient, K, were obtained for each adsorbate (the average values of K for three of the adsorbates are shown in Figure 7). By combining Equation 16 with the adsorption velocity values, the concentration profiles with adsorption time were obtained, and are shown in Figure 8 through Figure 10. An example of the impact of relative humidity on carbon adsorption using the results obtained above is given in Table 2. The value of k_s for 0% relative humidity was obtained from Equation 10 for a value of $W_e = 0.28$. Table 2 indicates that the bed depth required to maintain a breakthrough time of 120 minutes is increased by over 150% for high humidity conditions compared to low humidity conditions.

TABLE 2. EXAMPLE OF APPLICATION

Concentration of Toluene:	800 ppm
Flow Rate of Carrier Gas:	28.30 m^3/min:
Superficial Velocity:	30.48 m/min
Cross-Section Area of Adsorber:	0.928 m^2
Breakthrough Time:	120.0 min
Pore Volume of Carbon W_o:	0.60 ml/g

RH	V_{ad}	δ	L
%	m/min	m	m
0.00	0.00048	0.00105	0.0580
54.0	0.00108	0.00150	0.1311
62.0	0.00110	0.00165	0.1336
92.0	0.00120	0.00620	0.1502

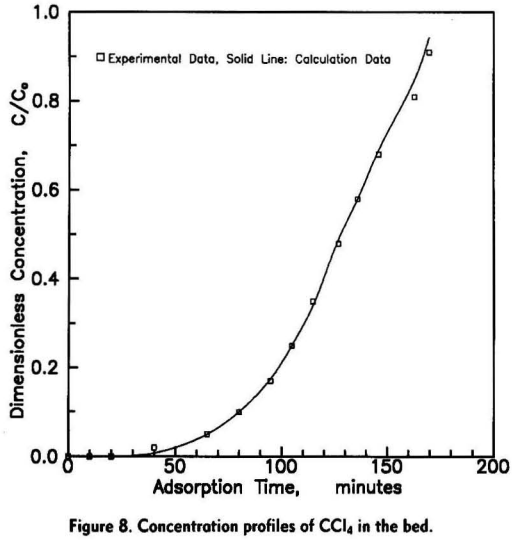

Figure 8. Concentration profiles of CCl_4 in the bed.

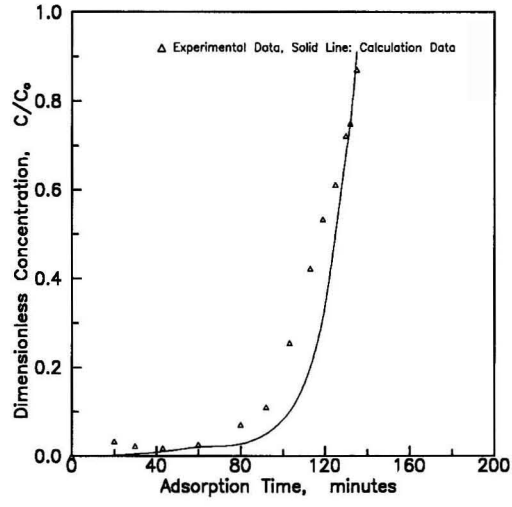

Figure 9. Concentration profiles of C_8H_{10} in the bed.

CONCLUSION

Summarizing all of the experimental data and analysis results, some useful conclusions are obtained. The presence of water vapor can make carbon adsorption capacity decrease by as much as 65% for some organic vapors for a humidity change from 50 to 92%. From low relative humidity values (e.g. 5%) to 92% relative humidity, the carbon adsorption capacity for toluene decreased 75%. The

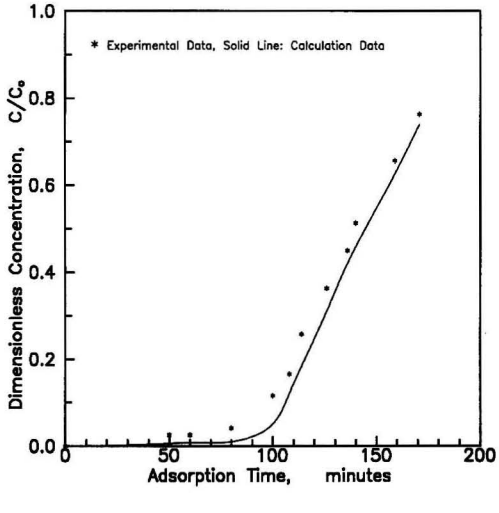

Figure 10. Concentration profiles of C_7H_8 in the bed.

Dubinin–Polanyi equation can be used to predict carbon adsorption capacity for different adsorbates and the MTZ equation derived from this isotherm model can be used to accurately predict adsorption kinetic behavior, such as the breakthrough time and the concentration profile in the bed for high humidity conditions.

ACKNOWLEDGMENT

The authors wish to thank the Ohio Board of Regents for financial support of this work.

LITERATURE CITED

1. Urano, K., S. Omori and E. Yamamoto, "Prediction Method for Adsorption Capacities of Commercial Activated Carbons in Removal of Organic Vapors," *Env. Sci. & Tech.*, Vol. 16, No. 1, pp. 10-13 (1982).
2. Jonas, L. A. and J. A. Rehrmann, "Prediction Equations in Gas Adsorption Kinetics," *Carbon*, Vol. 11, No. 1, pp. 59-64 (1973).
3. Werner, Martin D., "The Effects of Relative Humidity on Vapor Phase Adsorption of Trichloroethylene by Activated Carbon." *Am. Ind. Hyg. Assoc. J.*, **46**, (10) 585-590 (1985).
4. Werner, Martin D., "Predicting Carbon Adsorption of Organic Compound from Humid Air." Proceedings of the 1985 Env. Engrg. Specialty Conference, Env. Engrg. Division of ASCE, Boston, Mass., July 1-5 (1985).
5. Jonas, L. A., E. B. Sansone and T. S. Farris, "The Effect of Moisture on the Adsorption of Chloroform by Activated Carbon," *Am. Ind. Hyg. Assoc. J.*, Vol. 46, No. 1, pp. 20 (1985).
6. Dubinin, M. M., "Porous Structures and Adsorption Properties of Activated Carbon," *Structures and Properties of Activated Carbon*, Vol. 2, Marcel Dekker Inc., New York, pp. 51-121 (1966).
7. Reucroft, P. J., "Sorption Properties of Activated Carbon." *The J. of Phys. Chem.* Vol. 75, No. 23 (1971).
8. Crawford, Martin, *Air Pollution Control Theory*, McGraw-Hill, pp. 508-516 (1976).
9. Adams, L. B., C. R. Hall, R. J. Holmes and R. A. Newton, "An Examination of How Exposure to Humid Air Can Result in Changes in the Adsorption Properties of Activated Carbons," *Carbon*, Vol. 26, No. 4, pp. 451-459 (1988).
10. Witco Inorganic Specialties Division, 520 Madison Avenue, N.Y., N.Y., 10022.

Modeling and Simulation of Bioremediation of Contaminated Soil

J. C. Wu, L. T. Fan, and L. E. Erickson
Department of Chemical Engineering, Durland Hall, Kansas State University, Manhattan, Kansas 66506

A mathematical model has been developed for in situ biodegradation of contaminants in a soil bed. The model equations comprise three convection-dispersion partial differential equations and one ordinary differential equation. Dimensional analysis of the model equations has been performed, and solution of these equations has been conducted by the newly-developed three-point backward finite difference method. The effects of insufficient oxygen supply, growth of biomass and resistance to contaminant migration on the rate of biodegradation have been examined by numerically simulating the dynamic behavior of in situ biodegradation processes. The results of numerical simulation indicate that the rate of biodegradation of contaminants in soil may be constrained not only by insufficient oxygen supply, but also by resistance to contaminant migration within the pore network. The effect of recycling the unreacted contaminants from the bottom of the bed to the top has been examined through simulation, showing that biodegradation takes place mainly in the upper part of the bed.

INTRODUCTION

In situ bioremediation of contaminated soil is an innovative and cost-effective treatment technology. This technology exploits the capability of naturally occurring microorganisms to decompose toxic substances deposited in a soil bed; it can be applied to the cleanup of organic sludge, where organic compounds with high molecular weights are adsorbed on the soil particles. To aerobically operate the biodegradation process, water containing oxygen is allowed to flow through the soil bed. The flow behavior of water through the soil bed is very similar to that observed in bioremediation of contaminated groundwater.

Several mathematical models have been proposed for simulating *in situ* bioremediation of contaminated groundwater [*1-6*]. These models focus mainly on contaminant transport from the bulk liquid to microorganisms attached to particle surfaces [*7*]. Few models have been proposed for bioremediation of contaminated soil. In this process contaminants are initially adsorbed in soil particles. Consequently, the rate of biodegradation may be controlled by transport resistance to contaminant migration within the pore network [*8*]. In contrast, transport resistance to contaminant diffusion across a stagnant liquid layer adjacent to particle surfaces is negligible.

In the present work, a mathematical model has been developed for simulating bioremediation of contaminated soil. The effects of insufficient oxygen supply, growth of biomass and resistance to contaminant migration on the rate of contaminant degradation have been examined by numerically simulating the dynamic behavior of *in situ* biodegradation processes.

MODEL DEVELOPMENT

Organic contaminants are initially deposited in a soil bed. Water is allowed to flow through the bed continuously, thereby saturating the bed. The dissolved oxygen in the water affects aerobic biodegradation. By consuming substrate, including all contaminants, oxygen and other nutrients, naturally occurring microorganisms grow both in the solid phase as immobile microcolonies, which are clusters of microorganisms attached to the surface of soil particles, and in the liquid phase as suspended microorganisms.

Assumptions

The following major assumptions are made in deriving the model equations for bioremediation of contaminated soil.

a. Water in interstices or pores of the soil bed constitutes the liquid phase and the remaining part of the bed is considered as the solid phase. No gas phase exists because the bed is saturated with water.

b. Only three components, substrate, oxygen and biomass, are involved in biodegradation.

c. Macroscopically, one dimensional flow prevails through the liquid phase. The void fraction in any cross-section of the soil bed is constant, and thus, the pore velocity of water is constant.

d. No convective flow and dispersion occur in the solid phase.

e. The microcolonies in the solid phase are attached to the surface of soil particles, i.e., the interface between the solid and liquid phases.

f. The biodegradation by microcolonies takes place only at the interface between the liquid and solid phases; in other words, no reaction proceeds in the bulk of the solid phase.

g. The concentration gradients across the stagnant liquid layer, adjacent to the interface between the liquid and solid phases, are negligible, and thus, the concentrations of substrate and oxygen experienced by the microcolonies are equal to those in the bulk of the liquid. The stagnant layer is extremely thin due to the small average diameter of the macropores in soil which is generally less than 0.5 mm [9].

Derivation of General Model

The schematic diagram of the transport and biodegradation in a controlled volume is given in Figure 1. The mass balance of component i in the liquid phase gives rise to

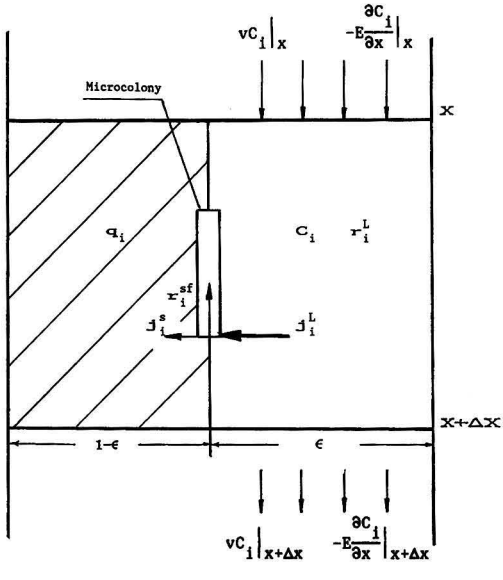

Figure 1. Schematic diagram of transport and biodegradation in a controlled volume.

$$\epsilon A(\Delta x)\frac{\partial C_i}{\partial t} = \epsilon A\left(-E\frac{\partial C_i}{\partial x} + vC_i\right)\Big|_x - \epsilon A\left(-E\frac{\partial C_i}{\partial x} + vC_i\right)\Big|_{x+\Delta x} + \epsilon A(\Delta x)\, r_i^L - A(\Delta x)\, aj_i^L \quad (1)$$

where subscript i is s, o, or b, standing for substrate, oxygen, or biomass, respectively; A is the cross-sectional area; a is the interfacial area per unit volume of the bed; and ϵ is the void fraction of the bed or the volume fraction of the bulk of the liquid phase. Dividing both sides of equation (1) by $A\Delta x$ and letting Δx approach to zero give

$$\epsilon\frac{\partial C_i}{\partial t} = \epsilon E\frac{\partial^2 C_i}{\partial x^2} - \epsilon v\frac{\partial C_i}{\partial x} + \epsilon r_i^L - aj_i^L \quad (2)$$

The corresponding mass balance in the solid phase yields

$$\rho A(\Delta x)\frac{\partial q_i}{\partial t} = A(\Delta x)\, aj_i^s \quad (3)$$

where ρ is the bulk density of the bed. This equation can be simplified to

$$\rho\frac{\partial q_i}{\partial t} = aj_i^s \quad (4)$$

The rate of mass transfer of component i from the liquid phase to the interface must be equal to the sum of the rate of its transfer from the interface to the bulk of the solid phase and the rate of its consumption at the interface, i.e.,

$$aj_i^L = aj_i^s + \rho(-r_i^{sf}) \quad (5)$$

Substituting this equation into equation (2) leads to

$$\epsilon\frac{\partial C_i}{\partial t} = \epsilon E\frac{\partial^2 C_i}{\partial x^2} - \epsilon v\frac{\partial C_i}{\partial x} + \epsilon r_i^L + \rho r_i^{sf} - aj_i^s \quad (6)$$

Equations (4) and (6) are the general transport equations for component i in the solid and liquid phases, respectively. This set of equations gives rise to two classes of transport models, equilibrium and nonequilibrium.

If the rates of adsorption and desorption of all components are sufficiently fast so that the concentrations in the liquid phase, C_i's, are in equilibrium with those in the solid phase, q_i's, the resultant model will be an equilibrium model. For component i in such a model, equations (4) and (6) merge naturally into a single equation through an equilibrium relation (see Appendix I). The equilibrium model is widely used in simulating *in situ* bioremediation of contaminated groundwater (see, e.g., Valocchi [*10*]). In contrast, if the rates of adsorption and desorption of any one of the components are controlled by transport within the pore network in the solid phase so that its concentration in the liquid phase is not in equilibrium with that in the solid phase, the resultant model will be a nonequilibrium model. Separate equations, equations (4) and (6), are required for this component.

In bioremediation of contaminated soil, the substrate, i.e., contaminants, is initially deposited in soil particles and the rate of substrate desorption from the soil particles to the liquid phase is generally controlled by transport within their pore network; thus, the concentration of substrate in the liquid phase is not in equilibrium with that in the solid phase. Consequently, the nonequilibrium model is more appropriate than the equilibrium model for bioremediation of contaminated soil.

Derivation of the Nonequilibrium Model

As stated earlier, both equations (4) and (6) are required for substrate. In terms of the film model, the mass flux of the substrate, j_s^s, in these equations can be expressed as

$$(-j_s^s) = k'_s (q_s - q^*_s) \tag{7}$$

where q^*_s is the concentration of substrate in the solid phase which would be in equilibrium with that in the liquid phase, i.e.,

$$q^*_s = K_{ds} C_s \tag{8}$$

Substituting this expression into equation (7) yields

$$(-j_s^s) = k_s \left(\frac{q_s}{K_{ds}} - C_s \right) \tag{9}$$

where

$$k_s = k'_s K_{ds} \tag{10}$$

Substitution of equation (9) into equations (6) and (4) results, respectively, in

$$\epsilon \frac{\partial C_s}{\partial t} = \epsilon E \frac{\partial^2 C_s}{\partial x^2} - \epsilon v \frac{\partial C_s}{\partial x} + \epsilon r_s^L + \rho r_s^{sf} + a k_s \left(\frac{q_s}{K_{ds}} - C_s \right) \tag{11}$$

$$\rho \frac{\partial q_s}{\partial t} = -a k_s \left(\frac{q_s}{K_{ds}} - C_s \right) \tag{12}$$

The flux of oxygen, j_o^s, is negligible because the solid phase hardly adsorbs oxygen; thus,

$$\frac{\partial q_o}{\partial t} = 0 \tag{13}$$

$$\epsilon \frac{\partial C_o}{\partial t} = \epsilon E \frac{\partial^2 C_o}{\partial x^2} - \epsilon v \frac{\partial C_o}{\partial x} + \epsilon r_o^L + \rho r_o^{sf} \tag{14}$$

The rates of exchange between biomass in the form of immobile microcolonies and that in the form of suspended microorganisms are not controlled by transport within the pore network of the solid phase because the microcolonies are mainly at the interface between the liquid and solid phases. Thus, a local adsorption-desorption equilibrium exists, which can be expressed as

$$q_b = K_{db} C_b \tag{15}$$

where K_{db} is the partition coefficient of biomass. Substituting equation (15) into equation (4) and combining the resultant expression with equation (6) lead to a single expression, i.e., (see Appendix I)

$$\epsilon R_b \frac{\partial C_b}{\partial t} = \epsilon E \frac{\partial^2 C_b}{\partial x^2} - \epsilon v \frac{\partial C_b}{\partial x} + \epsilon r_b^L + \rho r_b^{sf} \tag{16}$$

where

$$R_b = 1 + \frac{\rho K_{db}}{\epsilon} \tag{17}$$

This expression is termed as the retardation factor of biomass.

The reaction terms in equations (11), (14), and (16) can be expressed in terms of the Monod model (see, e.g., Bailey and Ollis [*11*]). The rate of biomass growth in the form of the suspended microorganisms in the liquid phase, r_b^L, is expressed as

$$r_b^L = \mu_m C_b \left(\frac{C_s}{K_s + C_s} \right) \left(\frac{C_o}{K_o + C_o} \right) - k_d C_b \tag{18}$$

where the first term on the right-hand side is for the growth and the second term is for the decay. The rate of biomass growth in the form of microcolonies at the interface, r_b^{sf}, is expressed as

$$r_b^{sf} = \mu_m q_b \left(\frac{C_s}{K_s + C_s} \right) \left(\frac{C_o}{K_o + C_o} \right) - k_d q_b \tag{19}$$

where q_b is the concentration of microcolonies at the interface, based on the mass of the solid phase. Note that as stated in assumption *g*, the concentrations of substrate and oxygen extracted by the microcolonies are equal to those in the bulk of the liquid phase. Similarly, the rate of substrate degradation by the suspended microorganisms in the liquid phase, $-r_s^L$, is

$$(-r_s^L) = \frac{\mu_m}{Y_s} C_b \left(\frac{C_s}{K_s + C_s} \right) \left(\frac{C_o}{K_o + C_o} \right) \tag{20}$$

The rate of substrate degradation by the microcolonies at the interface, $-r_s^{sf}$, is

$$(-r_s^{sf}) = \frac{\mu_m}{Y_s} q_b \left(\frac{C_s}{K_s + C_s} \right) \left(\frac{C_o}{K_o + C_o} \right) \tag{21}$$

The rate of oxygen consumption in the bulk of the liquid phase, $-r_o^L$, and that at the interface, $-r_o^{sf}$, are expressed, respectively, as

$$(-r_o^L) = \frac{\mu_m}{Y_o} C_b \left(\frac{C_s}{K_s + C_s} \right) \left(\frac{C_o}{K_o + C_o} \right) \tag{22}$$

$$(-r_o^{sf}) = \frac{\mu_m}{Y_o} q_b \left(\frac{C_s}{K_s + C_s} \right) \left(\frac{C_o}{K_o + C_o} \right) \tag{23}$$

Substituting the above kinetic expressions and the equilibrium relation of biomass, equation (15), into equations (11), (14), and (16) gives rise, respectively, to (see Appendix II)

$$\frac{\partial C_s}{\partial t} = E \frac{\partial^2 C_s}{\partial x^2} - v \frac{\partial C_s}{\partial x} + \frac{k_s a}{\epsilon} \left(\frac{q_s}{K_{ds}} - C_s \right) - \frac{\mu_m}{Y_s} R_b C_b \left(\frac{C_s}{K_s + C_s} \right) \left(\frac{C_o}{K_o + C_o} \right) \tag{24}$$

$$\frac{\partial C_o}{\partial t} = E \frac{\partial^2 C_o}{\partial x^2} - v \frac{\partial C_o}{\partial x} - \frac{\mu_m}{Y_o} R_b C_b \left(\frac{C_s}{K_s + C_s} \right) \left(\frac{C_o}{K_o + C_o} \right) \tag{25}$$

$$R_b \frac{\partial C_b}{\partial t} = E \frac{\partial^2 C_b}{\partial x^2} - v \frac{\partial C_b}{\partial x} + \mu_m R_b C_b \left(\frac{C_s}{K_s + C_s} \right) \left(\frac{C_o}{K_o + C_o} \right) - k_d R_b C_b \tag{26}$$

These three equations together with equation (12) rewritten as

$$\frac{\partial q_s}{\partial t} = -\frac{k_s a}{\rho}\left(\frac{q_s}{K_{ds}} - C_s\right) \tag{27}$$

constitute the nonequilibrium model.

Dimensional Analysis

To better understand the effects of the model parameters on the solution, it is desirable to rewrite equations (24-27) in dimensionless form. For this purpose, the following dimensionless variables are defined.

$$\theta = \frac{tv}{L} \tag{28}$$

$$X = \frac{x}{L} \tag{29}$$

$$\overline{C}_s = \frac{C_s}{C^*_{sO}} \tag{30}$$

$$\overline{C}_o = \frac{C_o}{C_{of}} \tag{31}$$

$$\overline{C}_b = \frac{C_b R_b}{C^*_{sO} R_s Y_s} \tag{32}$$

$$\overline{q}_s = \frac{q_s}{q_{sO}} = \frac{q_s/K_{ds}}{C^*_{sO}} \tag{33}$$

In these definitions, C_{of} is the concentration of oxygen in the feed solution and C^*_{sO} is the concentration of substrate in the liquid phase which would be in equilibrium with the initial concentration of substrate in the solid phase, q_{sO}. Note that in the definition of the dimensionless concentration of biomass, $\overline{C}_b$, the numerator stands for the total biomass in the forms of both suspended microorganisms in the liquid phase and microcolonies at the interface, and the denominator stands for the maximum quantity of biomass produceable from the available substrate deposited in the bed. Substitution of the dimensionless variables into equations (24-27) results, respectively, in

$$\frac{\partial \overline{C}_s}{\partial \theta} = \frac{1}{\mathrm{Pe}}\frac{\partial^2 \overline{C}_s}{\partial X^2} - \frac{\partial \overline{C}_s}{\partial X} + St_m(\overline{q}_s - \overline{C}_s) - N_{r,1} R_s \overline{C}_b \left(\frac{\overline{C}_s}{\overline{K}_s + \overline{C}_s}\right)\left(\frac{\overline{C}_o}{\overline{K}_o + \overline{C}_o}\right) \tag{34}$$

$$\frac{\partial \overline{C}_o}{\partial \theta} = \frac{1}{\mathrm{Pe}}\frac{\partial^2 \overline{C}_o}{\partial X^2} - \frac{\partial \overline{C}_o}{\partial X} - N_{r,1} W \overline{C}_b \left(\frac{\overline{C}_s}{\overline{K}_s + \overline{C}_s}\right)\left(\frac{\overline{C}_o}{\overline{K}_o + \overline{C}_o}\right) \tag{35}$$

$$\frac{\partial \overline{C}_b}{\partial \theta} = \frac{1}{R_b \mathrm{Pe}}\frac{\partial^2 \overline{C}_b}{\partial X^2} - \frac{1}{R_b}\frac{\partial \overline{C}_b}{\partial X} + N_{r,1}\overline{C}_b \left(\frac{\overline{C}_s}{\overline{K}_s + \overline{C}_s}\right)\left(\frac{\overline{C}_o}{\overline{K}_o + \overline{C}_o}\right) - N_{r,2}\overline{C}_b \tag{36}$$

$$\frac{\partial \overline{q}_s}{\partial \theta} = \frac{St_m}{R_s - 1}(\overline{q}_s - \overline{C}_s) \tag{37}$$

where

$$\mathrm{Pe} = \frac{Lv}{E} \tag{38}$$

$$N_{r,1} = \frac{\mu_m L}{v} \tag{39}$$

$$N_{r,2} = \frac{k_d L}{v} \tag{40}$$

$$St_m = \frac{k_s a L}{v\epsilon} \tag{41}$$

$$R_s = 1 + \frac{\rho K_{ds}}{\epsilon} \tag{42}$$

$$\overline{K}_s = \frac{K_s}{C^*_{sO}} \tag{43}$$

$$\overline{K}_o = \frac{K_o}{C_{of}} \tag{44}$$

$$W = \frac{C^*_{sO} R_s Y_s}{C_{of} Y_o} \tag{45}$$

Among the dimensionless numbers, $N_{r,1}$ and $N_{r,2}$, defined in equations (39) and (40), respectively, are known as the reaction units; the former is for the growth of biomass and the latter is for the decay of biomass. These numbers reflect the magnitudes of reaction rates. R_s, defined in equation (42), is the retardation factor of substrate. W, defined in equation (45), is the ratio of the maximum quantity of biomass produceable from the available substrate to that of biomass produceable from the available oxygen; thus, it can be termed as the oxygen supply number.

For a soil bed with a depth of L and a cross-sectional area of A, the quantity of substrate initially deposited in the liquid phase is $LA\epsilon C^*_{sO}$ and the quantity of substrate initially deposited in the solid phase is $LA\rho q_{sO}$. The sum of these two quantities is the total quantity of the substrate in the bed, $LA\epsilon C^*_{sO} R_s$, where R_s is defined in equation (42). Thus, the maximum quantity of biomass produceable from the substrate is $LA\epsilon C^*_{sO} R_s Y_s$. In case neither substrate nor oxygen flows out of the bed, the maximum quantity of biomass produceable from the substrate is equal to that from the oxygen, which is equal to $t_m v A \epsilon C_{of} Y_o$, where v is the pore velocity of water and t_m is the minimum time required for completing the biodegradation process under the conditions of plug flow and negligible mass transfer resistance. This and equation (45) lead to

$$\frac{t_m v}{L} = \frac{C^*_{sO} R_s Y_s}{C_{of} Y_o} = \mathrm{W} \tag{46}$$

Thus, W can also be defined as the minimum dimensionless time for completing a biodegradation process.

The Damköhler number for bioremediation of contaminated soil, Da, can be defined by dividing equation (39) with equation (41), i.e.,

$$\mathrm{Da} = \frac{N_{r,1}}{St_m} = \frac{\mu_m}{k_s (a/\epsilon)} \tag{47}$$

This number signifies the ratio of the maximum specific growth rate to the maximum substrate transfer rate.

When the aqueous solubility of the substrate in bioremediation of contaminated soil is sufficiently low so that C^*_{s0} is much less than the saturation constant of substrate, K_s, the dimensionless saturation constant of substrate, $\overline{K}_s$, will be much greater than unity. Consequently, a modified Damköhler number, Da′, is defined as follows:

$$\mathrm{Da}' = \frac{\mu_m/\overline{K}_s}{k_s\,(a/\epsilon)} \tag{48}$$

Note that Da′ is inversely proportional to the mass transfer coefficient of substrate, k_s.

SOLUTION ALGORITHM AND NUMERICAL SOLUTION

The model equations developed in the preceding section consist of three convection-dispersion partial differential equations (PDEs) and one ordinary differential equation (ODE). Two major difficulties are encountered in solving these equations. One is that numerical solution of a convection-dispersion PDE is adversely affected by numerical oscillations and excessive numerical diffusion (dissipation) if the convection term is more dominant than the dispersion term [*12, 13*]. The other is that the three PDEs are coupled through the nonlinear reaction terms, and they are also coupled with the ODE. These difficulties have been overcome in the present work by resorting to a recently developed numerical method, the three-point backward finite difference method (TPB method) [*14, 15*]; it is based on the approach proposed by Warming and Beam [*16*]. The TPB method substantially reduces the numerical oscillations and diffusion arising from the low-order discrete approximation of the convection term; it is computationally efficient due to the use of the tridiagonal method to solve the finite difference equations. For a system of PDEs with nonlinear reaction terms, a two-step expansion technique has been developed to linearize the nonlinear finite difference equations and to uncouple the PDEs. The derivation of the numerical procedure for solving equations (34-37) is summarized below.

Equations (34-36) can be compactly rewritten as

$$\frac{\partial \overline{C}_i}{\partial \theta} = P_{1,i}\frac{\partial^2 \overline{C}_i}{\partial X^2} - P_{2,i}\frac{\partial \overline{C}_i}{\partial X} + f_i, \quad i = s, o, b \tag{49}$$

where subscript i refers to component i, and $P_{1,i}$ and $P_{2,i}$ are the coefficients for the dispersion and convection terms, respectively. The nonlinear reaction terms in equation (49), f_i, $i = s, o, b$, can be expressed as

$$f_s\,(\overline{C}_s, \overline{C}_o, \overline{C}_b, \overline{q}_s) = St_m\,(\overline{q}_s - \overline{C}_s) - N_{r,1}R_s\overline{C}_b\left(\frac{\overline{C}_s}{\overline{K}_s + \overline{C}_s}\right)\left(\frac{\overline{C}_o}{\overline{K}_o + \overline{C}_o}\right) \tag{50}$$

$$f_o\,(\overline{C}_s, \overline{C}_o, \overline{C}_b) = -N_{r,1}W\overline{C}_b\left(\frac{\overline{C}_s}{\overline{K}_s + \overline{C}_s}\right)\left(\frac{\overline{C}_o}{\overline{K}_o + \overline{C}_o}\right) \tag{51}$$

$$f_b\,(\overline{C}_s, \overline{C}_o, \overline{C}_b) = N_{r,1}\overline{C}_b\left(\frac{\overline{C}_s}{\overline{K}_s + \overline{C}_s}\right)\left(\frac{\overline{C}_o}{\overline{K}_o + \overline{C}_o}\right) - N_{r,2}\overline{C}_b \tag{52}$$

Application of the TPB temporal differencing to equation (49) yields

$$\frac{3(\overline{C}_i)^{n+1} - 4(\overline{C}_i)^n + (\overline{C}_i)^{n-1}}{2\Delta\theta} = P_{1,i}\left(\frac{\partial^2 \overline{C}_i}{\partial X^2}\right)^{n+1} - P_{2,i}\left(\frac{\partial \overline{C}_i}{\partial X}\right)^{n+1} + (f_i)^{n+1} + 0(\Delta\theta^2)$$

$$= P_{1,i}\left(\frac{\partial^2 \overline{C}_i}{\partial X^2}\right)^{n+1} - P_{2,i}\left(\frac{\partial}{\partial X}\right)(\Delta\overline{C}_i)^n - P_{2,i}\left(\frac{\partial \overline{C}_i}{\partial X}\right)^n + (f_i)^{n+1}, \quad i = s, o, b \tag{53}$$

where superscript n refers to the n-th time step, and the "delta" form, $(\Delta\overline{C}_i)^n$, is defined as [*16*]

$$(\Delta\overline{C}_i)^n = (\overline{C}_i)^{n+1} - (\overline{C}_i)^n \tag{54}$$

Approximation of the first term on the right-hand side of equation (53) by the central differencing, the second term by the upstream differencing and the third term by the TPB spatial differencing results in a finite difference equation of the following form:

$$\frac{3(\overline{C}_i)_j^{n+1} - 4(\overline{C}_i)_j^n + (\overline{C}_i)_j^{n-1}}{2\Delta\theta} = P_{1,i}\left(\frac{(\overline{C}_i)_{j+1}^{n+1} - 2(\overline{C}_i)_j^{n+1} + (\overline{C}_i)_{j-1}^{n+1}}{\Delta x^2}\right) - P_{2,i}\frac{\Delta(\overline{C}_i)_j^n - \Delta(\overline{C}_i)_j}{\Delta x} - P_{2,i}\frac{3(\overline{C}_i)_j^n - 4(\overline{C}_i)_{j-1}^n + (\overline{C}_i)_{j-2}^n}{2\Delta X} - f_{i,j}^{n+1} + 0(\Delta\theta^2 + \Delta X^2), \quad i = s, o, b \tag{55}$$

where subscript j refers to the j-th grid point. Rewriting this equation and ignoring the truncational error give

$$(-r_{1,i} - 2r_{2,i})\,(\overline{C}_i)_{j-1}^{n+1} + (3 + 2r_{1,i} + 2r_{2,i})\,(\overline{C}_i)_j^{n+1} - r_{1,i}\,(\overline{C}_i)_{j+1}^{n+1} = -r_{2,i}\,(\overline{C}_i)_{j-2}^n + 2r_{2,i}\,(\overline{C}_i)_{j-1}^n + (4 - r_{2,i})\,(\overline{C}_i)_j^n - (\overline{C}_i)_j^{n-1} + 2\Delta\theta\, f_i^{n+1}, \quad i = s, o, b \tag{56}$$

where

$$r_{1,i} = \frac{2\Delta\theta\, P_{1,i}}{\Delta X^2} \tag{57}$$

$$r_{2,i} = \frac{\Delta\theta\, P_{2,i}}{\Delta X} \tag{58}$$

Equation (56) is a system of nonlinear equations due to the existence of the nonlinear reaction term, f_i^{n+1}. However, if f_i^{n+1} can be approximated in terms of f_i^n and f_i^{n-1}, equation (56) can be solved with the tridiagonal method, which is highly efficient for solving a system of linear equations having a tridiagonal coefficient matrix. This can be accomplished through the two-step Taylor expansion technique.

According to the Taylor expansion,

$$f_i\,(\theta + \Delta\theta) = f_i\,(\theta) + f'_i\,(\theta)\,\Delta\theta + \frac{1}{2}f''_i\,(\theta)\,\Delta\theta^2 + 0(\Delta\theta^3) \tag{59}$$

$$f_i\,(\theta - \Delta\theta) = f_i\,(\theta) - f'_i\,(\theta)\,\Delta\theta + \frac{1}{2}f''_i\,(\theta)\,\Delta\theta^2 - 0(\Delta\theta^3) \tag{60}$$

Subtracting the second from the first yields

$$f_i(\theta + \Delta\theta) = f_i(\theta - \Delta\theta) + 2f'_i(\theta)\,\Delta\theta + 0(\Delta\theta^3) \quad (61)$$

$$f_i^{n+1} = f_i^{n-1} + 2\left(\frac{\partial f_i^n}{\partial\theta}\right)\Delta\theta + 0(\Delta\theta^3) \quad (62)$$

Note that the magnitude of truncational error from this expansion is one order higher than that from equation (56); thus, this error does not significantly affect the accuracy of the solution. Also note that substitution of equation (62) into equation (56) uncouples all PDEs, equations (34-36), so that they can be solved separately at each time step. The expressions for the derivatives of f'_i's with respect to θ in equation (62) are obtained as follows:

$$\frac{\partial f_s}{\partial\theta} = \frac{\partial f_s}{\partial\overline{C}_s}\frac{\partial\overline{C}_s}{\partial\theta} + \frac{\partial f_s}{\partial\overline{C}_o}\frac{\partial\overline{C}_o}{\partial\theta} + \frac{\partial f_s}{\partial\overline{C}_b}\frac{\partial\overline{C}_b}{\partial\theta} + \frac{\partial f_s}{\partial\overline{q}_s}\frac{\partial\overline{q}_s}{\partial\theta} \quad (63)$$

$$\frac{\partial f_o}{\partial\theta} = \frac{\partial f_o}{\partial\overline{C}_s}\frac{\partial\overline{C}_s}{\partial\theta} + \frac{\partial f_o}{\partial\overline{C}_o}\frac{\partial\overline{C}_o}{\partial\theta} + \frac{\partial f_o}{\partial\overline{C}_b}\frac{\partial\overline{C}_b}{\partial\theta} \quad (64)$$

$$\frac{\partial f_b}{\partial\theta} = \frac{\partial f_b}{\partial\overline{C}_s}\frac{\partial\overline{C}_s}{\partial\theta} + \frac{\partial f_b}{\partial\overline{C}_o}\frac{\partial\overline{C}_o}{\partial\theta} + \frac{\partial f_b}{\partial\overline{C}_b}\frac{\partial\overline{C}_b}{\partial\theta} \quad (65)$$

The derivatives of f_i's with respect to $\overline{C}_i$ in equations (63-65) are obtained analytically from equations (50-52); $\partial\overline{C}_i/\partial\theta$ can be calculated from the finite difference approximation of equations (34-36). Meanwhile, the evaluation of $\partial\overline{q}_s/\partial\theta$ in equation (63) can be directly obtained from equation (37). With all these derivatives available, f_i^{n+1} can be evaluated from equation (62); subsequently, $\overline{C}_i^{n+1}$ is obtained with the tridiagonal method from equation (56).

After equations (34-36) are solved with the TPB method at each time step, the ODE among the model equations, equation (37), can be solved for $\overline{q}_s^{n+1}$ with the second order Runge-Kutta method. The resultant scheme is

$$\overline{q}_s^{n+1} = b_1\overline{C}_s^{n+1} + b_2\overline{C}_s^{n} + b_3\overline{q}_s^{n} \quad (66)$$

where

$$b_1 = \frac{\Delta\theta\, St_m}{2\overline{K}_{ds}} \quad (67)$$

$$b_2 = \frac{\Delta\theta\, St_m}{2\overline{K}_{ds}}\left(1 - \frac{\Delta\theta\, St_m}{\overline{K}_{ds}}\right) \quad (68)$$

$$b_3 = 1 - \frac{\Delta\theta\, St_m}{\overline{K}_{ds}} + \frac{(\Delta\theta\, St_m)^2}{2\overline{K}_{ds}^2} \quad (69)$$

Note that the TPB method is a two-step method; thus, a starting algorithm is needed to calculate $\overline{C}_i$ at time step $n = 1$. This algorithm can be generated through the combination of the Crank-Nicolson method and the two-step expansion [*14, 15*].

Two classes of numerical simulation have been conducted with the developed algorithm. One is for the once-through operation for which the initial and boundary conditions are

$$\text{At } \theta = 0,\quad \overline{C}_s(0,X) = 1.00,\quad \overline{q}_s(0,X) = 1.00$$
$$\overline{C}_o(0,X) = 0.05,\ \overline{C}_b(0,X) = 0.01$$

$$\text{At } X = 0,\ \overline{C}_i(\theta,0) = (\overline{C}_i)_{o+} - \frac{1}{\mathrm{Pe}}\left(\frac{\partial\overline{C}_i}{\partial X}\right)_{o+},\quad i = s, o, b$$

where

$$\overline{C}_s(\theta,0) = 0.00$$
$$\overline{C}_o(\theta,0) = 1.00$$
$$\overline{C}_b(\theta,0) = 0.01$$

$$\text{At } X = 1,\quad \frac{\partial\overline{C}_i}{\partial X} = 0,\quad i = s, o, b$$

The other is for the recycle operation, in which the effluent containing unreacted substrate is recycled to the top of the bed to eliminate the substrate, i.e., contaminants, to the maximum extent possible. For this operation, the initial conditions and the boundary conditions at $X = 1$ are the same as those for the once-through operation. The boundary conditions at the inlet of the bed are

$$\text{At } X = 0,\quad \overline{C}_i(\theta,0) = (\overline{C}_i)_{o+} - \frac{1}{\mathrm{Pe}}\left(\frac{\partial\overline{C}_i}{\partial X}\right)_{o+},\quad i = s, o, b$$

where

$$\overline{C}_s(\theta,0) = \overline{C}_s(\theta - \Delta\theta, 1)$$
$$\overline{C}_o(\theta,0) = 1.00$$
$$\overline{C}_b(\theta,0) = \overline{C}_b(\theta - \Delta\theta, 1)$$

where the residence time of the recycle stream is assumed to be very short and equal to $\Delta\theta$, the dimensionless temporal step size for the numerical integration. It is also assumed that no reaction takes place in the recycle stream. The parameters used in the simulation are given in Table 1.

TABLE 1. PARAMETER VALUES FOR THE NUMERICAL SIMULATION

$N_{r,1}$	= 12.0	$N_{r,2}$	= 0.2
K_s	= 3.0	K_o	= 0.05
Pe	= 100	W	= 6, 12.5
R_s	= 20, 60, 80	R_b	= 50
St_m	= 4, 8, 40	D'_a	= 0.1, 0.5, 1

RESULTS AND DISCUSSION

The results have been obtained from simulating both once-through and recycle operations. Analysis of the dynamics of the once-through operation enables us to determine the effects of various model parameters on the rate of biodegradation. Insight into the *in situ* bioremediation process can be gained through understanding the dynamics of the recycle operation.

Dynamics of the Once-Through Operation

The effects of model parameters on the rate of biodegradation have been analyzed by focussing on the modified Damköhler number, Da′, the retardation factor of substrate, R_s, and the oxygen supply number, W.

Figures 2 through 4 reveal the effect of Da′ on the rate of biodegradation. Da′ reflects the ratio of the maximum specific growth rate to specific substrate transfer rate. When the maximum specific growth rate is fixed, the larger the Da′, the smaller the transfer rate, or the larger the resistance to substrate transport. When Da′ is equal to 1, $\overline{C}_s$ is much lower than $\overline{q}_s$ (see Figure 2). The difference between $\overline{C}_s$ and $\overline{q}_s$ represents the departure of the state of the system from its equilibrium state, which is determined by the rate of substrate transport. When Da′ decreases to 0.5, the rate of substrate transport increases, but the difference between $\overline{C}_s$ and $\overline{q}_s$ continues to be appre-

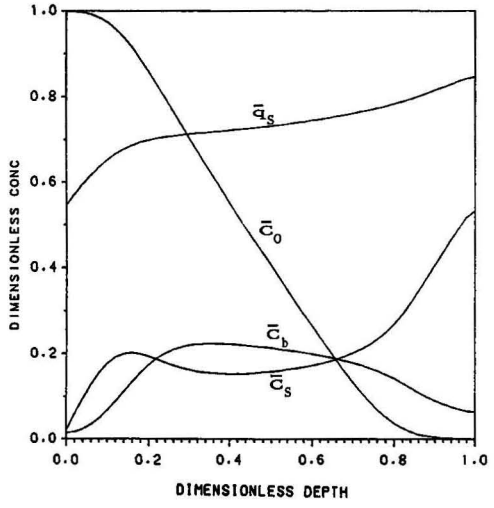

Figure 2. Concentration profiles for the once-through operation at $\theta = 3$: Da′ = 1, $R_s = 20$, and $W = 12.5$.

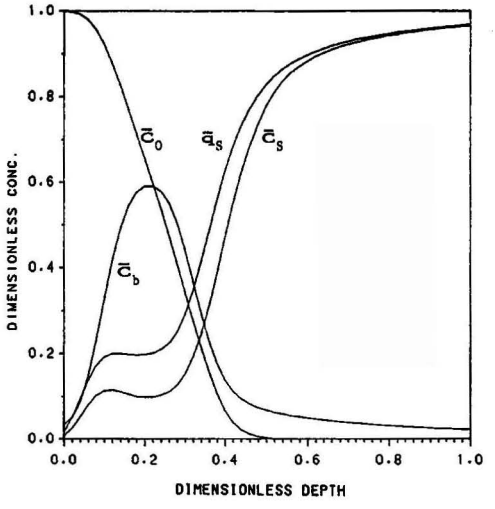

Figure 4. Concentration profiles for the once-through operation at $\theta = 3$: Da′ = 0.1, $R_s = 20$, and $W = 12.5$.

ciable (see Figure 3). When Da′ further decreases to 0.1, the rate of substrate transport becomes so fast that $\bar{C}_s$ approaches to $\bar{q}_s$. A comparison between Figures 2 and 4 shows the smaller the Da′, the faster the rate of biodegradation.

The rate of biodegradation is also affected by the retardation factor of substrate, R_s. By definition, R_s signifies the magnitude of the equilibrium constant of substrate, K_{ds}. The larger the R_s, the larger the K_{ds}, and, from equation (7) or (9), the smaller the concentration gradient or mass transfer driving force. A comparison between Figures 4 and 5 indicates that when R_s increases from 20 to 60 and Da′ remains at 0.1, the difference between $\bar{C}_s$ and $\bar{q}_s$ increases, or the nonequilibrium behavior is enhanced. This is because the rate of substrate transport is decreased. R_s in bioremediation of contaminated soil may be larger than 60. The larger the R_s, the slower the rate of substrate transport, and thus, the slower the rate of biodegradation.

The oxygen supply number, W, is another factor affecting the rate of biodegradation; as defined in equation (45), it signifies the ratio of the maximum quantity of biomass produceable from the available substrate to that from the available oxygen. The larger the W, the lesser the available oxygen. Figures 3 through 5 indicate that when W is 12.5 and Da′ or R_s is small, the oxygen in the liquid phase is rapidly consumed and the insufficient oxygen supply through the liquid phase becomes rate-limiting. A comparison between Figures 3 and 6 reveals that when W decreases to 6 from 12.5, the effect of insufficient oxygen supply becomes less profound and the resistance to substrate desorption becomes increasingly dominant. Note that the increase in R_s can change the rate-limiting step for the same W. For instance, as R_s increases from 20 to 80 and W remains 12.5, we see from Figures 3 and 7 that the difference between $\bar{C}_s$ and $\bar{q}_s$ increases significantly and the value of $\bar{C}_s$ becomes very low, indicating that the resistance to the substrate desorption is rate-limiting.

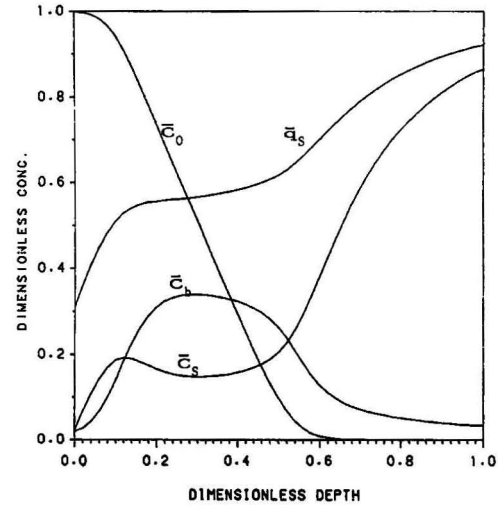

Figure 3. Concentration profiles for the once-through operation at $\theta = 3$: Da′ = 0.5, $R_s = 20$, and $W = 12.5$.

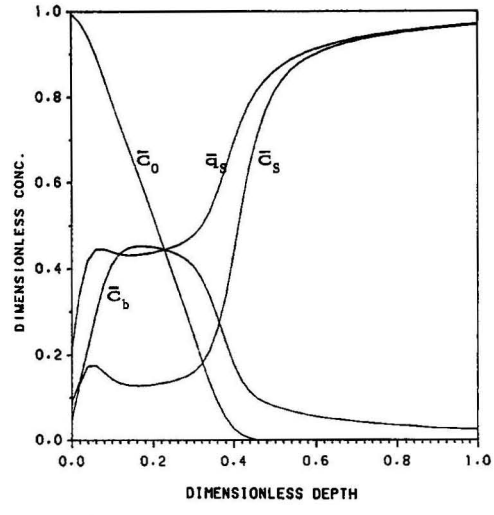

Figure 5. Concentration profiles for the once-through operation at $\theta = 3$: Da′ = 0.1, $R_s = 60$, and $W = 12.5$.

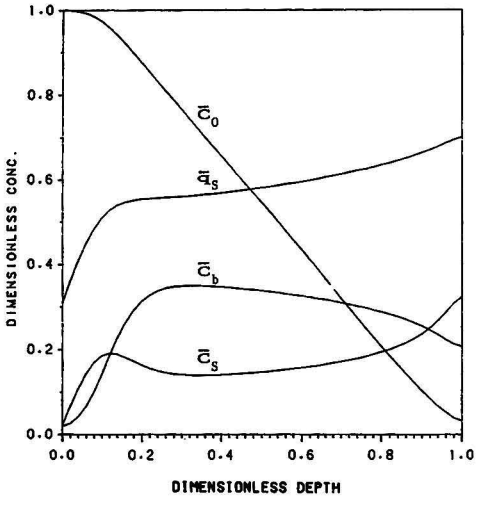

Figure 6. Concentration profiles for the once-through operation at $\theta = 3$: $Da' = 0.5$, $R_s = 20$, and $W = 6$.

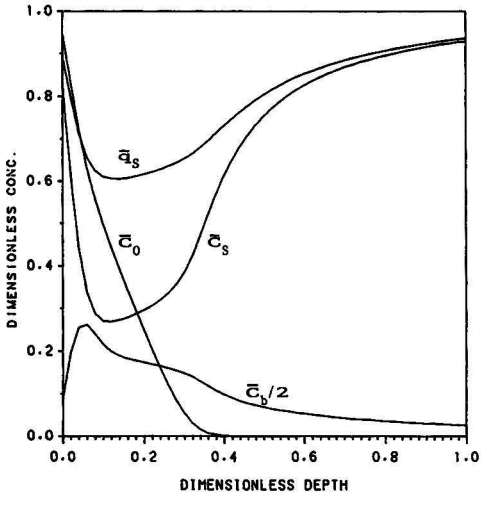

Figure 8. Concentration profiles for the recycle operation at $\theta = 2$: $Da' = 0.2$, $R_s = 20$, and $W = 8$.

Dynamics of the Recycle Operation

The once-through operation discussed in the preceding subsection has demonstrated the effects of substrate transport resistance and insufficient oxygen supply on the rate of biodegradation. However, the once-through operation is seldom employed because the contaminants would flow into the groundwater underneath the bed. The recycle operation provides a means to eliminate the substrate, i.e., contaminants, to the maximum extent possible.

The simulated concentration profiles are plotted at different dimensionless times in Figures 8 through 11. At θ equal to 2 and 4, three distinct reaction zones are observed in the bed (Figures 8 and 9). In the upper zone, the concentrations of both oxygen and recycled substrate are high, thereby exhibiting a high rate of biodegradation and steep decline in the concentration profiles. In the middle zone, the rate of biodegradation becomes moderate because it is constrained by the low concentrations of oxygen and/or substrate in the liquid phase; thus, the concentration profiles become rather flat. Oxygen is totally consumed in the lower zone, and thus, degradation of substrate ceases. Figure 10 demonstrates that at θ equal to 6, the middle zone expands substantially as the result of degradation of substrate; meanwhile, the lower zone shrinks significantly. The concentration profiles at $\theta = 8$ (Figure 11) indicate that the biodegradation process is almost complete. The fact that the oxygen supply number, W, is also equal to 8 is consistent with equation (46), which indicates that W can also be defined as the minimum dimensionless time for completing a biodegradation process. Note that how close the dimensionless biodegradation time is to W depends on both the mass transfer resistance and hydraulic dispersion. The larger the mass transfer resistance and hydraulic dispersion, the longer the dimensionless biodegradation time. If they are negligible, the dimensionless time will be equal to W.

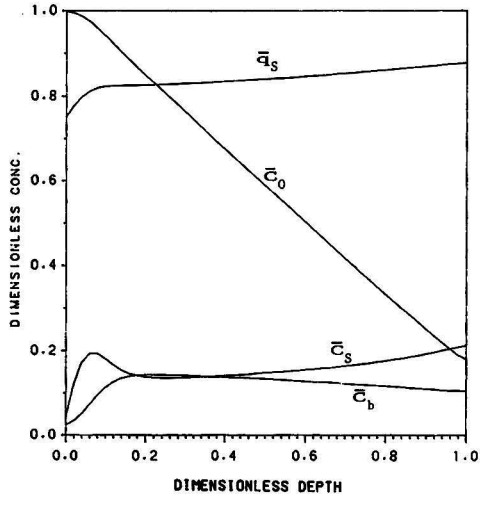

Figure 7. Concentration profiles for the once-through operation at $\theta = 3$: $Da' = 0.5$, $R_s = 80$, and $W = 12.5$.

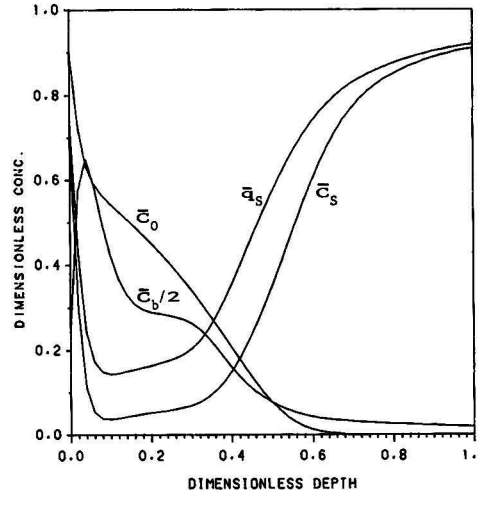

Figure 9. Concentration profiles for the recycle operation at $\theta = 4$: $Da' = 0.2$, $R_s = 20$, and $W = 8$.

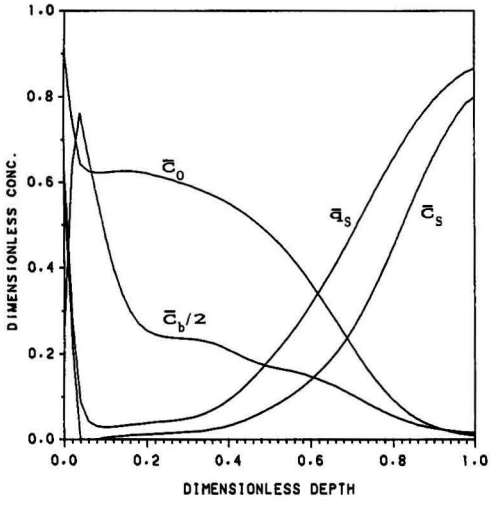

Figure 10. Concentration profiles for the recycle operation at $\theta = 6$: $Da' = 0.2$, $R_s = 20$, and $W = 8$.

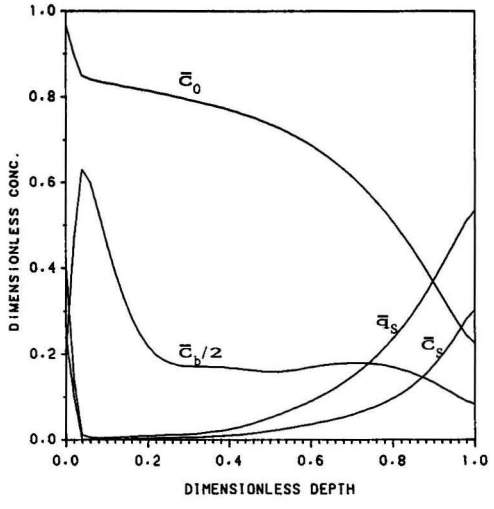

Figure 11. Concentration profiles for the recycle operation at $\theta = 8$: $Da' = 0.2$, $R_s = 20$, and $W = 8$.

CONCLUSION

A mathematical model for biodegradation of contaminants deposited in a soil bed has been developed. The transport resistance to contaminant migration within the pore network in soil particles is considered. The model equations comprise three convection-dispersion partial differential equations and one ordinary differential equation. The effects of insufficient oxygen supply, growth of biomass and resistance to contaminant migration on the rate of biodegradation have been examined with the model.

To simulate *in situ* biodegradation, the model equations have been solved by a recently developed numerical method, the three-point backward finite difference method (TPB method). This method approximates the first order temporal and spatial derivatives in convection-dispersion PDEs through the three-point backward finite differencing, and resorts to the two-step Taylor expansion technique to linearize the finite difference equations containing nonlinear reaction terms. This has resulted in high computational efficiency and substantial reduction in numerical oscillations and diffusion.

The numerical simulation of the once-through operation has revealed the effects of model parameters on the solution and has demonstrated that a nonequilibrium model is more appropriate than an equilibrium model; the rate of biodegradation may be limited not only by insufficient oxygen supply, but also by the transport resistance to substrate desorption. Under certain circumstances, the latter is even more dominant than the former.

The simulation of the operation involving the recycle of unreacted substrate, i.e., contaminants, has indicated that biodegradation takes place mainly in the upper zone of the bed and that the oxygen supply factor, W, can serve as an estimate of the dimensionless biodegradation time if the mass transfer is relatively fast.

APPENDIX I. DERIVATION OF THE EQUILIBRIUM MODEL

In this model, the concentration of each component in the liquid phase is in equilibrium with that of the corresponding component in the solid phase. Thus, for component i,

$$q_i = K_{di} C_i \tag{AI.1}$$

where a linear equilibrium isotherm is assumed. Substituting this equation into equation (4) in the text results in

$$\rho K_{di} \frac{\partial C_i}{\partial t} = a j_i^s \tag{AI.2}$$

Combining this equation with equation (6) in the text gives

$$\epsilon \frac{\partial C_i}{\partial t} + \rho K_{di} \frac{\partial C_i}{\partial t} = \epsilon E \frac{\partial^2 C_i}{\partial x^2} - \epsilon v \frac{\partial C_i}{\partial x} + \epsilon r_i^L + \rho r_i^{sf} - a J_i^s + a J_i^s \tag{AI.3}$$

or

$$\epsilon \left(1 + \frac{\rho K_{di}}{\epsilon}\right) \frac{\partial C_i}{\partial t} = \epsilon E \frac{\partial^2 C_i}{\partial x^2} - \epsilon v \frac{\partial C_i}{\partial x} + \epsilon r_i^L + \rho r_i^{sf} \tag{AI.4}$$

This expression is the governing equation for the equilibrium model; note that no mass transfer term is involved.

APPENDIX II. DERIVATION OF EQUATIONS (24) THROUGH (26)

The procedures for deriving equations (24) through (26) in the text are the same. Thus, only equation (24) is derived here for illustration.

Substitution of equations (20) and (21) into equation (11) in the text gives

$$\epsilon \frac{\partial C_s}{\partial t} = \epsilon E \frac{\partial^2 C_s}{\partial x^2} - \epsilon v \frac{\partial C_s}{\partial x} + a k_s \left(\frac{q_s}{K_{ds}} - C_s\right) - \frac{\mu_m}{Y_s} \epsilon C_b \left(\frac{C_s}{K_s + C_s}\right)\left(\frac{C_o}{K_o + C_o}\right) - \frac{\mu_m}{Y_s} \rho q_b \left(\frac{C_s}{K_s + C_s}\right)\left(\frac{C_o}{K_o + C_o}\right) \tag{AII.1}$$

Substituting equation (15) in the text into this equation and dividing both sides of the resultant expression by ϵ yield

$$\frac{\partial C_s}{\partial t} = E\frac{\partial^2 C_s}{\partial x^2} - v\frac{\partial C_s}{\partial x} + \frac{k_s a}{\epsilon}\left(\frac{q_s}{K_{ds}} - C_s\right) - \frac{\mu_m}{Y_s}\left(1 + \frac{\rho K_{db}}{\epsilon}\right) C_b \left(\frac{C_s}{K_s + C_s}\right)\left(\frac{C_o}{K_o + C_o}\right)$$

or

$$\frac{\partial C_s}{\partial t} = E\frac{\partial^2 C_s}{\partial x^2} - v\frac{\partial C_s}{\partial x} + \frac{k_s a}{\epsilon}\left(\frac{q_s}{K_{ds}} - C_s\right) - \frac{\mu_m}{Y_s} R_b C_b \left(\frac{C_s}{K_s + C_s}\right)\left(\frac{C_o}{K_o + C_o}\right) \quad \text{(AII.2)}$$

which is equation (24) in the text.

ACKNOWLEDGMENT

Although the research described in this article has been funded in part by the United States Environmental Protection Agency under assistance agreement R-815709 to the Hazardous Substance Research Center for U.S. EPA Regions 7 and 8 with headquarters at Kansas State University, it has not been subjected to the Agency's peer and administrative review and therefore may not necessarily reflect the views of the agency and no official endorsement should be inferred. This research was partially supported by the Kansas State University Office of Hazardous Waste Research.

NOTATION

a interfacial area per unit volume of the soil bed, L^2/L^3
C_i concentration of component i in the liquid phase, M/L^3
C_{of} concentration of oxygen in the feed solution, M/L^3
$\overline{C_i}$ dimensionless concentration of component i
E dispersion coefficient, L^2/t
j_i^L transport flux from the liquid phase to the interface, $(M/L^2)/t$
j_i^s transport flux from the interface to the bulk of the solid phase, $(M/L^2)/t$
k_d reaction rate constant for the decay of biomass, t^{-1}
k_s mass transfer coefficient of substrate, L/t
K_o saturation constant of oxygen, M/L^3
K_s saturation constant of substrate, M/L^3
K_{di} linear isotherm partition coefficient of component i
L depth of the contaminated soil bed, L
q_i concentration of component i in the solid phase, M/M dry soil
$\overline{q_i}$ dimensionless concentration of component i in the solid phase
r_i^L reaction rate in the liquid phase, $(M/L^3)/t$
r_i^{sf} reaction rate at the interface, $(M/M$ dry soil$)/t$
$R_i = 1 + \frac{\rho K_{di}}{\epsilon}$ = retardation factor for component i
v pore velocity of the liquid, L/t
t time, t
x vertical position, L
X dimensionless depth
Y_o yield factor of oxygen
Y_s yield factor of substrate

Greek Letters

ρ bulk density of the soil bed, M dry soil/L^3
ϵ void fraction of the soil bed
μ_m maximum specific growth rate of biomass, t^{-1}
θ dimensionless time

Superscript

n n-th time step
L liquid phase
s solid phase
sf interface

Subscripts

i s, o, b for substrate, oxygen, and biomass, respectively
j j-th grid point

LITERATURE CITED

1. Bouwer, E. J. and P. L. McCarty, "Modeling of Trace Organics Biotransformation in the Subsurface," *Ground Water*, **22**, 433, 1984.
2. Borden, R. C. and P. B. Bedient, "Transport of Dissolved Hydrocarbons Influenced by Oxygen-Limited Biodegradation, 1. Theoretical Development," *Water Resources Res.*, **22**, 1973, 1986.
3. Molz, F. J., M. A. Windowson, and L. D. Benefield, "Simulation of Microbial Growth Dynamics Coupled to Nutrient and Oxygen Transport in Porous Media," *Water Resources Res.*, **22**, 1207, 1986.
4. Lee, M. D., J. M. Thomas, R. C. Borden, P. B. Bedient, C. H. Ward, and J. T. Wilson, "Biodegradation of Aquifers Contaminated with Organic Compounds," *CRC Critical Reviews in Environmental Control*, **18**, 29, 1988.
5. Kosson, D. S., G. C. Agnihotri, and R. C. Ahlert, "Modeling and Simulation of a Soil-Based Microbial Treatment Process," *Journal of Hazardous Materials*, **14**, 191, 1987.
6. Windowson, M. A., F. J. Molz, and L. D. Benefield, "A Numerical Transport Model for Oxygen- and Nitrate-Based Respiration Linked to Substrate and Nutrient Availability in Porous Media," *Water Resources Res.*, **24**, 1553, 1988.
7. Baveye, P. and A. Valocchi, "An Evaluation of Mathematical Models of the Transport of Biologically Reacting Solutes in Saturated Soils and Aquifers," *Water Resources Res.*, **25**, 1413, 1989.
8. Mackay, D. M. and J. A. Cherry, "Groundwater Contamination: Pump-and-Treat Remediation," *Environ. Sci. Technol.*, **23**, 630, 1989.
9. Iwata S., T. Tabuchi, and B. P. Warkentin, *Soil-Water Interaction, Mechanisms and Applications*, pp. 221-276, Marcel Dekker, New York, 1988.
10. Valocchi, A. J., "Validity of the Local Equilibrium Assumption for Modeling Sorbing Solute Transport through Homogeneous Soil," *Water Resources Res.*, **21**, 808, 1985.
11. Bailey, J. E. and D. F. Ollis, *Biochemical Engineering Fundamentals*, pp. 373-456, McGraw-Hill, New York, 1987.
12. Finlayson, B. A., *Nonlinear Analysis in Chemical Engineering*, pp. 231-265, McGraw-Hill, New York, 1980.
13. Oran, E. S. and J. P. Boris, *Numerical Simulation of Reactive Flow*, pp. 79-133, Elsevier, New York, 1987.
14. Wu, J. C., *Modeling of In Situ Neutralization and Biodegradation Processes and Numerical Simulation with the Three-Point Backward Finite Difference Method*, M.S. Thesis, Kansas State University, Manhattan, KS, 1989.
15. Wu, J. C., L. T. Fan, and L. E. Erickson, "Three-Point Backward Finite Difference Method for Solving a System of Mixed Hyperbolic-Parabolic Partial Differential Equations," Submitted to *Computers & Chemical Engineering*, 1989.
16. Warming, R. F. and R. M. Beam, "On the Construction and Application of Implicit Factored Scheme for Conservation Laws," *SIAM-AMS Proceedings*, **11**, 85, 1978.

Design Considerations and Metals Disposition in Fluidized-Bed Incineration of Refinery Wastes

Robert G. Corry
CH2M Hill, 6060 S. Willow Dr., Greenwood Village, CO 80111-5112

and

George P. Rasmussen
Waste-Tech Services, Inc.

Disposal of refinery biotreatment sludges through land application is being strictly controlled and, in many cases, eliminated by regulatory constraint. An alternative to land application of sludges is incineration. This paper discusses fluidized-bed incineration pilot studies conducted on refinery sludges obtained from two different refineries. Destruction of hazardous organic constituents, as well as the fate of inorganic metals, is discussed. Metal emissions are examined and the impact of the new EPA metals emissions limits is investigated. Installation of a waste heat recuperator to preheat combustion air is explored as an alternative to a high-pressure sludge dewatering process.

REGULATORY FRAMEWORK

Land application of refinery biotreating sludges is being stringently restricted by EPA regulations. As a result, various alternatives are being discussed in the literature. These include incineration, stabilization, sludge biotreatment, and solvent extraction to remove or mitigate organic contaminants. In all cases, a residue that requires suitable disposal is produced. Depending on the sludge's ash content, incineration of refinery sludges can reduce volume by 80 to 90%. The potential exists for delisting the incinerator ash to reduce future liability and landfill costs.

Incineration of refinery and biological sludges is a well-known commercial practice. Many incinerators, such as the Amoco incinerators in Whiting, Indiana, and Mandan, North Dakota, are fluidized-bed incinerators. They work particularly well with sludges because of their ability to break up the sludge droplets and expose the waste to oxidizing conditions. The results obtained in a series of fluidized-bed incineration experiments using actual refinery sludges under a range of controlled conditions are discussed below.

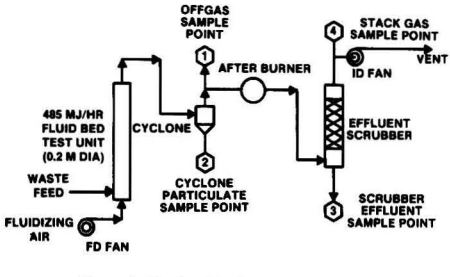

Figure 1. Fluidized-bed incineration unit.

FLUIDIZED-BED INCINERATION TEST UNIT

A series of seven test burn runs were conducted in a 0.2 meter, 485 million joules-per-hour (mJ/hr) fluidized-bed test unit owned by Waste-Tech Services in Golden, Colorado. A process flow diagram for the unit is shown in Figure 1. Air is forced into the fluidized-bed media at a slight positive pressure by the forced draft (FD) fan. Superficial gas velocities of 1.2 to 3.7 meters per second are commonly used, which results in good to high energy release in the unit. Waste feed sludge is injected into the fluidized-bed using a positive displacement pump and air assist.

TABLE 1. ULTIMATE ANALYSES OF REFINERY SLUDGES

Ultimate Analyses (wt %)	Sludges A	Sludges B
Carbon	12.3	12.8
Hydrogen	1.6	1.8
Oxygen (by difference)	3.4	7.9
Nitrogen	0.1	0.8
Sulfur	1.1	0.3
Halides	<0.1	<0.1
Water	61.5	64.9
Ash	20.0	11.5
TOTAL	100.0	100.0
Higher Heating Value (HHV), Btu/lb	2,400	2,440

Gases exiting the shallow (0.5 to 1.0 meter) fluidized-bed region enter the integral, Secondary Reaction Chamber (SRC). The SRC is an unfired, refractory-lined chamber with 2 to 3 seconds of residence time that serves to complete combustion. Coarse (10 micrometer [μm] or larger) particulates are removed in a cyclone from the gas stream at the end of the SRC. Incinerator off gas is tested at the cyclone exit for organics, particulates, and combustion products.

An afterburner is installed in the unit after the cyclone exit gas sample point to ensure complete destruction of the principal organic hazardous constituents at research test conditions before venting. Commercial fluidized-bed incinerators of this type do not require and are not equipped with an afterburner. The pilot unit afterburner gases are scrubbed in a caustic wash, packed-bed scrubber, followed by a mist eliminator. Combustion gases are removed by the induced draft (ID) fan. The process unit above the fluidized-bed is maintained at a slight vacuum by the ID fan to control fugitive emissions. A stack gas sample point upstream of the ID fan is used to test for stack particulate and metal emissions.

WASTE FEED COMPOSITIONS

The refinery sludges used in this test program were obtained from two refineries owned by different companies. Both refineries had lagoon-type biotreatment systems. The lagoon sludges from each refinery were composites blended from several streams within each refinery. The individual streams were blended based on their annual production rate to produce an "average" waste feed composition to be processed at an incineration facility at the site. The waste feed ultimate analyses of the two composite sludges are very similar (Table 1). The higher heating values of the two sludges are almost the same. The higher heating value is the heat of combustion measured when water in the combustion gas is condensed to the liquid phase.

The sludges were analyzed for hazardous components as listed in *40 CFR*, Part 261, Appendix VIII. Principal organic hazardous components (POHCs) were determined by gas chromatograph mass spectroscopy (GS-MS) analysis. The sludge POHCs were petroleum compounds or those used in refinery processing: toluene, other alkylbenzenes, naphthalene, other polynuclear aromatics, and phenol. The sludges were analyzed for eight Appendix VIII hazardous metals by atomic adsorption (AA). Lead and chrome were found in both samples, presumably residues from gasoline additives and water treatment chemicals. Nickel, probably from petroleum and catalyst, was found in some samples. Some nickel and chrome are leached from refinery piping. The significant levels of chromium and lead found in these samples should decline at these and other refineries because of the discontinuation of chromium-based water treatment chemicals and the phaseout of lead additives.

INCINERATOR TEST BURN RESULTS

Seven fluidized-bed incineration pilot tests were made with the A and B sludge composites. The operating conditions and organic destruction results are reported in Table 2. Five of the pilot tests were made with Sludge Composite A, and two with sludge Composite B. The incinerator exit oxygen content was measured with an on-line Ametek WDG-11C oxygen analyzer, calibrated before each pilot test, and averaged over the 2- to 10-hour test period.

The exit gases contained 7.9 to 11.2 volume percent (vol %) oxygen measured on a wet basis. These oxygen concentrations translate into approximately 50 to 100% excess air. The average incinerator temperature, based or six thermocouples distributed throughout the vessel, ranged from 645° to 756°C.

The sludge composites were spiked with 1 to 2 weight percent of each of two POHCs to be studied during the tests. Waste feed spiking was required to allow measurement of the POHCs in the incinerator off gas. Sludge A was spiked with toluene and naphthalene. Sludge B was spiked with naphthalene and phenol. The organic destruction and removal efficiencies (DRE) shown in Table 2 were measured at the afterburner inlet and are the result of two incinerator off-gas organic content analyses measured using a liquid adsorption technique [*1*]. The destruction and removal efficiencies are defined as follows:

$$\text{DRE} = \frac{\text{wt POHC in feed} - \text{wt POHC in off gas}}{\text{wt POHC in feed}} \times 100 \text{ weight percent}$$

The POHC destruction shown in Table 2 suggests that toluene, naphthalene, and phenol have comparable destruction results at a given set of operating conditions. A

TABLE 2. REFINERY SLUDGE INCINERATION TEST BURN RESULTS

Run No.	Sludge Feed	Excess O_2 at Vessel Exit, Wet (vol %)	Incinerator Temperature (°C)	POHC DRE, wt % Toluene	Naphthalene	Phenol
1	A	7.9	665	99.973	99.866	—
2	A	10.2	645	99.931	99.986	—
3	A	11.2	653	99.931	99.997	—
4	A	8.4	680	99.965	99.994	—
5	A	9.8	691	99.992	99.996	—
6	B	8.5	756	—	99.395	99.963
7	B	9.5	745	—	99.999	99.999

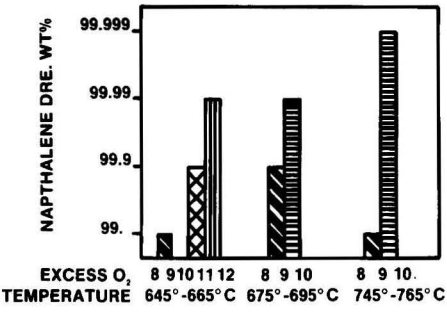

Figure 2. Naphthalene destruction as a function of temperature and excess oxygen.

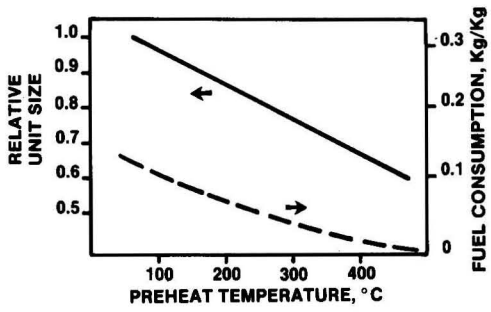

Figure 4. Waste heat recuperation significantly reduces incinerator size.

plot of naphthalene destruction results is shown in Figure 2 as a function of incineration temperature and exit gas oxygen content.

As expected, POHC destruction increases as the temperature and oxygen content increase. The EPA-required POHC 99.99 weight percent DRE was met at a comparatively low temperature of 691°C. A rough correlation can be made with the limited number of data points in Table 2, which suggests that an incinerator temperature increase of 30°C allows the exit oxygen content to be reduced by 1 vol percent at constant POHC DRE. Energy balances based on this correlation show that the higher temperature is more fuel efficient than the addition of more excess air.

SLUDGE DRYING AND HEAT RECUPERATION FOR IMPROVED PERFORMANCE

A series of computer-modeled incinerator design cases were made using the refinery sludge compositions in Table 1 at 704°C and 75% excess air. In the first series of computer simulations, water was removed from the sludge to simulate a high-pressure sludge dewatering press without hydrocarbon loss. The results of these simulations are shown in Figure 3. Dewatering reduces both the required incinerator size and the supplemental fuel consumption.

An optimum water content is reached at approximately 40 weight percent where the unit size has been reduced 10% and no supplemental fuel is required to maintain incineration temperature. Unit size increases at refinery sludge water contents less than 40 weight percent if unit temperature is held constant due to the addition of quenching air. In commercial practice, the incineration temperature would be allowed to rise and the unit size would stay constant.

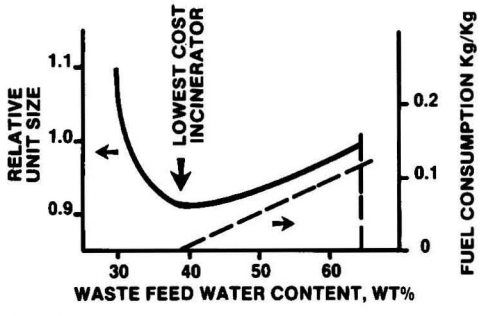

Figure 3. Sludge dewatering reduces unit size and auxiliary fuel requirements.

A second set of computer simulation results is shown in Figure 4 at constant refinery waste feed water content (64 weight percent), 70°C temperature, and 75% excess air. Incinerator size and fuel consumption are shown as a function of inlet air temperature simulating the presence of a heat recuperator in the incinerator system used to heat combustion air. Both unit size and fuel consumption decline nearly linearly as preheat temperature is increased. At a 370°C preheat, a reasonably conservative heat recuperation temperature, the incinerator size is reduced 30% below the 70°C temperature obtained at the FD fan exit without heat recuperation. Auxiliary fuel consumption at 370°C preheat is reduced 80%.

A heat recuperator to preheat combustion air may be more cost-effective in some cases than waste feed dewatering. Capital costs for either option are comparable, but the heat recuperator significantly reduces the incinerator size. The operating costs with refinery sludges may be lower with heat recuperation, since the use of filter aids for some dewatering processes is expensive and increases incinerator ash production with the associated disposal costs.

METAL DISPOSITION RESULTS

During the refinery sludge pilot incineration test, five sets of chromium and four sets of lead material balances were made. During these tests, there were three stack emission tests for chromium and two for lead. The average results from these balances are shown in Table 3. The range of material balance closures is shown in Table 3 as well.

The results in Table 3 show that about 80% of the chrome and over 90% of the lead were captured in the cyclone on the larger 10 μm+ particulates exiting the fluidized-bed pilot unit. Less than 10% of either metal was retained in the fluidized-bed media. The fluidized-bed media was coated with a layer of residue during the test burn. This residue was observed to be removed during periods between tests when the unit was operated on fuel oil only. Based on this observation, it is expected that during prolonged operation the metal content on the fluid-

TABLE 3. DISPOSITION OF METALS DURING REFINERY SLUDGE INCINERATION

Disposition	Chromium	Lead
Wt % Captured in the Fluid Bed	8	1
Wt % Captured in the Cyclone	83	96
Wt % Captured in the Scrubber	3	2
Wt % Emitted to the Stack	1	2
Wt % Material Balance Closure, Range	79–103	60–127

TABLE 4. ALLOWABLE INCINERATOR SIZE BASED ON EPA GUIDANCE

	Chromium	Lead
Metal in Waste Feed, WPPM	100–1,500	30–300
Allowable Emission/Feed Rate (g/sec)	4×10^{-3}	0.4
Tier I Waste Feed Rate		
Maximum (kg/hr)	144	48,000
Minimum (kg/hr)	10	4,800
Tier II Waste Feed Rate		
Maximum (kg/hr)	14,400	2.4×10^{6}
Minimum (kg/hr)	1,000	2.4×10^{5}

Basis: Rural noncomplex terrain, 65-meter effective stack height.

ized-bed media will reach a steady-state level and not accumulate further metal except as large particulates.

Two to three percent of the lead and chrome were found in the scrubber. Only one to two percent of the lead and chrome exited the incinerator via the stack. The balance of metal is caught in the cyclone and vent scrubber. The percent metals emitted from the stack are comparable, but lower than those observed by others [2] during sewage sludge incineration in fluidized-bed incinerators.

AIR EMISSIONS OF METALS

Metal emissions from incinerator stacks have become a major area of regulatory concern. In September 1988, the EPA issued a draft final guidance manual for metals and hydrogen chlorine emissions from hazardous waste incinerators [3]. The new guidelines have a three-tier system to determine permitted metal and hydrogen chloride emissions, based on health standards.

In Tiers I and II, absolute emission limits in grams per second are tabulated as a function of stack height, terrain, and population density. In Tier I, all hazardous metals in the waste feed are assumed to exit with the stack gas, and a permitted waste feed rate can be back calculated from the emission limit. In Tier II, allowance is given for air pollution control equipment and metals removal in the captured ash streams.

The Tier III emissions limits are set on site-specific modeling and health-based standards. The permitting process moves from one tier to the next tier and to the higher level of complexity, as required by the incinerator emission level. If incinerator emissions cannot be permitted at Tier III, then additional engineering or operating controls must be installed to meet the Tier III emission limits.

Table 4 shows the effect of the new incinerator metal emission guidelines on a scale up of the pilot unit results with refinery sludges. Based on the assumed case of an incinerator located in a rural area with noncomplex terrain and an effective stack height of 65 meters, the allowable emissions of chromium and lead were obtained from the guidance document. These allowable emissions limits, obtained from the guidance document, are 4×10^{-3} grams per second (g/sec) for chromium and 0.4 g/sec for lead, as shown in Table 4. The waste feed content of lead and chromium is also shown in Table 4 and can be used to calculate the incinerator feed rate under Tier I.

The Tier I assumption that all the waste feed metals are vented from the stack shows that chromium emissions restrict the unit to a nonuseful size of 10 to 144 kg/hr. Examination of the metals emissions limits based on the Tier II guidelines, which credit metal capture in APC equipment, allows the incinerator to be an economical size of 1,000 kg/hr to 14,400 kilograms per hour (kg/hr), as shown in Table 4. The Tier II estimates are based on the 1% stack emission of chromium in the waste feed and 2% emission of lead, as shown in Table 3.

Meeting the new Tier II metals missions guidelines in fluidized-bed incinerators with refinery sludges will require additional investment for improved air pollution control equipment and higher stacks. However, it can be done with readily available equipment and with a reasonable level of operating control.

CONCLUSIONS

Two refinery lagoon sludges from different locations were incinerated in a fluidized-bed pilot test unit. The composite sludges from both locations were similar in composition and contained the following hazardous constituents:

- Toluene
- Other alkyl benzenes
- Naphthalene
- Other polynuclear aromatics
- Phenol
- Lead
- Chromium
- Nickel

Acceptable regulatory destruction and removal efficiency (99.99 weight percent) were obtained at the comparatively mild temperature of 691°C. Sludge dewatering to 40 weight percent water reduced the incinerator size by 10% and eliminated auxiliary fuel requirements. Use of a waste heat recuperator to preheat conversion air reduced unit size by 30% and auxiliary fuel requirements by 80% at conservative preheat temperatures. Unit metal emissions of lead and chromium can meet potential regulatory requirements. Fluidized-bed incineration is a proven and effective means of treating refinery wastes to comply with present and proposed environmental regulations.

ACKNOWLEDGMENTS

The authors of this paper wish to recognize the contributions of the following people whose help was instrumental in this work: Chuck Bartholomew, Bob Benedict, Alan Dump, Eliot Cooper, Doug Georgic, Paul Hansen, Tamara Muhic, Kelly Toller, and Craig Young.

LITERATURE CITED

1. Young, C. and L. Trejo, "Evaluation of 2-Propanol vs. Liquid Absorbent for Hazardous Pollutants," Proc. Symp. on Recent Advances in Pollutant Monitoring of Ambient Air and Stationary Sources, Raleigh, North Carolina (May, 1982).
2. Gersle, R., "Emissions of Trace Metals and Organic Compounds from Sewage Sludge Incineration," 81st APCA Meeting, Dallas, Texas (June, 1988).
3. U.S. Environmental Protection Agency, "Guidance on Metals and HCL for Hazardous Waste Incinerations—Draft Final Report" (September, 1988).

Fluidized Bed Combustion of Aluminum Smelting Waste

R. S. Tabery and K. Dangtran
Turnpoint Engineering Corporation, Austin, Texas 78746

Pilot tests by Fluidized Bed Combustion (FBC) have successfully destroyed Spent Potliner (SPL), a hazardous waste by-product from aluminum smelters. Well known technical challenges such as ash agglomeration, ash leachate control, and off-gas emission control have been studied and overcome by additives and by special combustion chamber design.

Economic evaluation of a 20,000 tons per year (9 megawatt) facility indicates that disposal costs are competitive with land-based disposal.

A 0.5 MW Fluidized Bed Combustor of this design is under construction by Turnpoint Engineering Corporation.

NATURE OF THE ALUMINUM SMELTING WASTE

Commercially smelted aluminum metal was first produced and is still produced by reducing aluminum from its oxide by an electrolysis technique called the Hall-Heroult process. The process consists of dissolving alumina in a bath of molten salts, cryolite (Na_3AlF_6) and aluminum fluoride (AlF_3) in an electrolysis pot lined with refractory and carbon (cathode). An electric current passes between the anode and the cathode. Figure 1 shows the cross section of a typical aluminum reduction pot. The carbon anodes, inserted directly in the molten bath are consumed during the operation and must be replaced periodically. The thick carbon lining cathode, or potliner, is not consumed, but must be removed and replaced after 3-5 years or longer due to the loss of its integrity by migration of cryolite bath, molten aluminum, salts, and other chemicals. From 40-60 tons of waste are discarded as spent potliner (SPL) per replacement, depending on the size of the pot.

The quantity of SPL generated annually in the United States has exceeded 200,000 tons. In addition, over 1,200,000 tons are presently found in recoverable storage and more are festering in landfills. Table 1 shows the compositions of typical spent potliner from two US aluminum producers. Because of high concentrations of fluorine and cyanide, SPL was recently listed as "hazardous" (EPA hazardous waste # K088 [*1*]).

SCOPE

Several management alternatives to land-based disposal of SPL have been suggested [2]. The complexity, cost, disposal of residuals, and engineering problems of most of these alternatives make them economically unacceptable.

Perhaps the most promising solution is Fluidized Bed Combustion. During the last decade, FBC has been widely adopted for burning low-grade fuels and gained commercial acceptance for the disposal of a growing number of solid and liquid wastes [*3, 4, 5, 6*]. The advantages of this process are well established: High turbulence and residence time of the waste in the combustion chamber allow complete combustion at a moderate temperature. FBC has also demonstrated the capability to dry-scrub acid gases evolved from the combustion of halogenated, sulfurous and phosphorous containing waste by injecting sorbents in the combustion chamber.

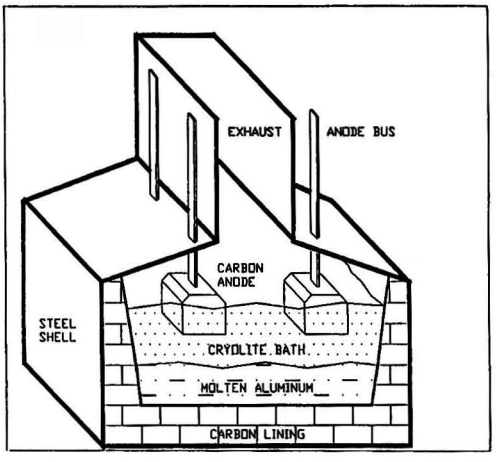

Figure 1. Aluminum reduction pot cross section.

A number of attempts to apply FBC to SPL have been made [7, 8]. However, technical and environmental feasibility was not satisfactorily demonstrated. Three primary difficulties need to be overcome, namely:

Agglomeration: Ash resulting from combustion forms a low-melting eutectic causing the entire bed mass to agglomerate, thereby requiring shutdown of the process. Published data on the agglomeration behavior of SPL in fluidized bed is non–existent. However, agglomeration studies of low–grade anthracite and lignite by Fluidized Bed Combustion and Gasification can be found in recent literature [9, 10]. In those studies, agglomeration was attributed to the interaction between acidic and basic oxides (SiO_2 and K_2O) at operating temperature.

Ash Leachability: Fluoride, cyanide and metal ion concentrations in the ash leachate must be low enough to satisfy regulatory authorities that no harm will come from proper disposal of the ash. Cyanide is relatively easy to destroy at FBC temperature (850°C) if agglomeration is controlled. Fluoride and metals are contaminants of chief concern.

Off-gas Emissions: Satisfactory control of hydrogen fluoride (HF) emissions as well as other combustion products is necessary. HF emissions can be controlled by limestone addition. This, however, can aggravate the problems of agglomeration [1, 6, 7].

These major problems have been investigated in two small-scale combustors, a spouted bed and a deep bubbling bed and presented in the first part of his paper. The effect of additives on agglomeration, leachability of the ash, and on the emission of acid gases was investigated. X-ray diffraction and scanning electron micrograph (SEM) techniques were used to study the nature of interstitial glue holding agglomerates together. The effect of design was also studied; a special combustion chamber design specifically for burning SPL and similar hard-to-handle wastes is proposed.

In the second part of this paper, results from test burns investigated in the first part are used to develop an economic model. In this study, a fluidized bed combustor with a capacity of 20,000 tons SPL per year is fitted to an existing cement kiln for generating 9000 KW.

TABLE 1. COMPOSITION OF TYPICAL SPENT POTLINER FROM TWO MAJOR US ALUMINUM PRODUCERS.

Composition	Alcoa (%)	Reynolds (%)
Carbon	28.6	42.70
Aluminum	14.20	4.70
Silicon	4.76	0.11
Iron	3.23	0.27
Sodium	13.90	20.00
Fluorine	18.20	17.60
Cyanide	0.09	0.13

EXPERIMENTAL

Materials

Spent potliner from an ALCOA smelter was selected for use in testing (see Table 1 for its composition). The heating value of the SPL is low (2222 cal/gram). For self-sustained combustion, an additive with high heating value has been used as auxiliary fuel and, more importantly, for increasing the fusion temperature of the ash to above the FBC operating temperature. (We would like to share with you the nature of this ingredient, but unfortunately this innovative process is not completely protected as yet. To avoid confusion, this ingredient will be called additive (A) in this work.) SPL and additive samples were sieved to less than 10 mm prior to injection into the reactor chamber. Central Texas limestone with a narrow particle size distribution around 6 mm was used as sorbent (S).

Equipment

Test burns were conducted in two small–scale reactors, a spouted bed and a fluidized bed combustor.

Spouted Bed Combustor: Figure 2 shows the schematic of the 5 cm diameter, 90 cm high spouted bed used. The reactor, constructed of Hastelloy B. Bed material, was brought to 700°C by a 10,000 Hz inductive heating coil prior to manual feeding of fuel blend through the top of the bed. The air was measured via rotameter before

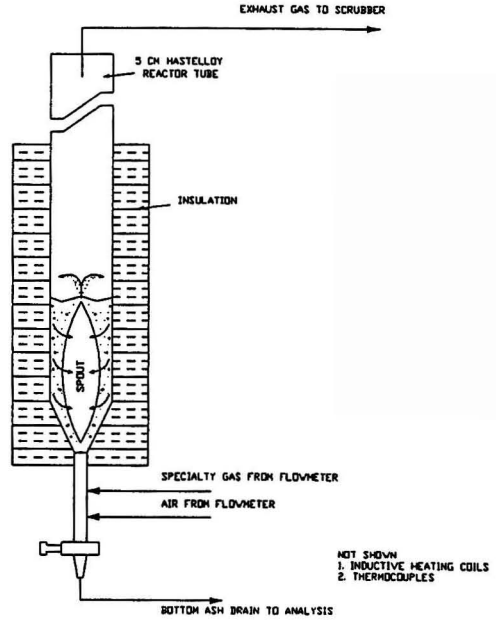

Figure 2. Spouted bed combustor.

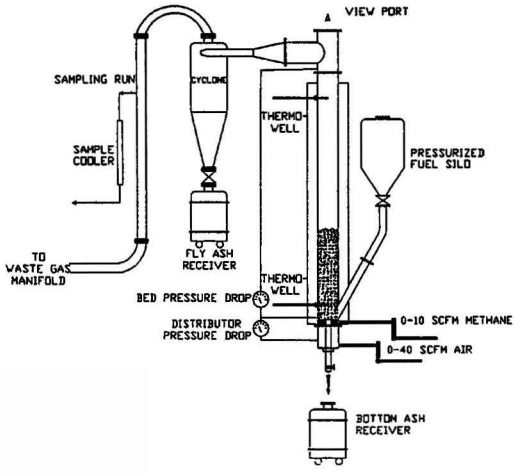

Figure 3. 15 cm FBC reactor.

entering the combustion chamber. Bed temperature was recorded by a small thermocouple suspended at different locations in the bed.

Fluidized Bed Combustor: Experiments were performed in a 15 cm diameter, 210 cm high atmospheric fluidized bed combustor configured for continuous operation at a feed rate of 10 kg/hr. The reactor and most major components of the plant were constructed of type 309 stainless steel. The major components of the pilot reactor are illustrated in Figure 3.

The air required for combustion and fluidization was supplied volumetrically and distributed homogeneously through the typical 30 cm bed via a windbox and a perforated plate covered with alumina balls. Methane was used for preheating the bed to 600°C, which was generally sufficient to ignite the reactive fuel blend.

Fuel blends (A, SPL, and S) were premixed and placed in an airtight hopper prior to injection into the combustion chamber at a height of 5 cm above the distributor plate. Flue gas entered a cyclone where entrained particles were collected for analysis and disposal. The exhaust stream from the cyclone was introduced either to the sampling line for analysis or directly to a waste gas manifold.

Bed solid was drained intermittently via a central 4 cm duct to maintain constant bed height. Samples were collected routinely for analysis. Temperature and pressure were measured in the reactor via thermocouples and pressure taps.

TABLE 2. SUMMARY OF ADDITIVE (A), SORBENT (S), AND SPL PROPORTIONS USED IN SPOUTED AND FLUIDIZED BED TEST RUNS. THIS TABLE SHOWS ALSO THE TEMPERATURE OF AGGLOMERATION ENCOUNTED.

Test #	A/SPL (weight)	S/SPL (weight)	Ca/F (molar)	Agglom. T(°C)	Technique Used
1	0	0.00	0.00	770	SB
2	4	0.12	0.12	>900*	SB
3	10	0.30	0.30	>900*	SB
4	4	0.40	0.40	>950*	SB
5	1	1.00	1.00	800-900	FB
6	3	1.00	1.00	950	FB
7	8	1.00	1.00	>950*	FB
8	3	0.50	0.50	950	FB
9	3	0.90	0.90	950	FB
10	3	1.15	1.15	950	FB

SB: Spouted Bed
FB: Fluidized Bed
* No Agglomeration Observed

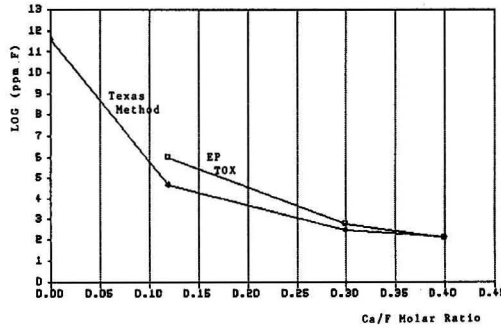

Figure 4. Fluorine leachability versus Ca/F molar ratio.

RESULTS AND DISCUSSIONS

A series of four spouted bed and six fluidized bed tests were conducted at different A/SPL and S/SPL weight ratios (Table 2).

In the spouted bed, the initial bed material fed to the reactor was 600 grams of alumina. When the bed temperature reached 700°C, fuel blend was gravity fed. The feeding rate, initially very low, was incrementally increased from 1 gram/min to 6 gram/min. Temperature of the bed was raised from 700°C to 900°C or higher after one bed equivalent of fuel blend had been fed. A superficial air velocity of 46 cm/sec was maintained constant during all these tests.

In the 15 cm fluidized bed combustor, a 20 cm static height of alumina was used initially and fluidized at a superficial air velocity of 75 cm/sec.

Effect of A/SPL Weight Ratio on Agglomeration Temperature: Ash agglomeration temperature is presented versus additive/SPL ratio in Table 2. Results show an increase of the ash agglomeration temperature with the A/SPL weight ratio in both spouted and fluidized beds. Without additive (run 1), bed solids started to agglomerate at 770°C. Table 2 shows also that a weight ratio of A versus SPL of approximately 3:1 is necessary to increase the agglomeration temperature to 950°C.

Effect of S/SPL Weight Ratio on Fluoride Leachability: Fluoride concentration in both water and acid leachates decreases sharply with Ca/F molar ratio. By increasing from 0 to 0.4 S/SPL weight ratio (which corresponds to 0 to 0.4 Ca/F molar ratio), a decrease in fluoride concentration from 10.5% to 8 ppm is noted. This sharp decrease is shown in Figure 4, in which concentration of fluoride in the leachates is plotted in logarithmic scale versus the molar ratio of Ca/F.

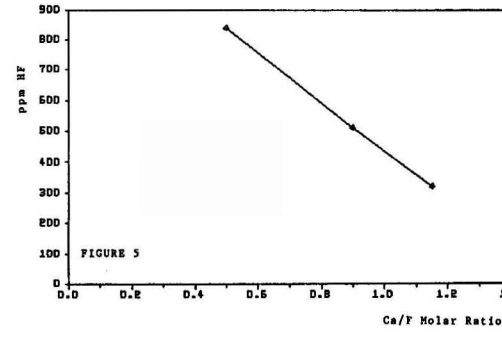

Figure 5. HF emission versus Ca/F molar ratio.

TABLE 3. FLY ASH AND BOTTOM ASH ANALYSIS AND LEACHABILITY.

Sample Identification		Fly Ash Run 13	Bottom Ash Run 13	Fly Ash Run 14	Bottom Ash Run 14
Ash Analysis (mg/kg)					
Total cyanide		5.60	1.20	4.70	1.20
Free cyanide		1.60	<0.5	1.80	<0.50
Total fluoride		72.00	50.30	74.80	50.40
Total Sulfide		<20.00	160.00	<20.00	300.00
Total organic carbon		1240.00	220.00	1210.00	57.00
Total arsenic		19.00	36.00	7.00	5.00
Total barium		200.00	<100.00	400.00	400.00
Total cadmium		4.00	<10.00	3.00	2.00
Total chromium		80.00	<50.00	50.00	25.00
Total lead		35.00	<50.00	30.00	30.00
Total mercury		0.01	<0.01	0.01	<0.01
Total selinium		2.80	1.40	1.20	1.10
Total silver		7.00	<20.00	5.00	8.00
Total nickel		35.00	<50.00	35.00	25.00
ASTM DI Cyanide Leach (mg/l)		0.11	0.03	0.08	0.03
	Drinking Water Standards				
E.P. TOX Leach (mg/l)					
Fluoride	1.4-2.4	5.60	7.00	6.20	7.40
Arsenic	0.05*	<0.1	<0.10	<0.10	<0.10
Barium	1.00*	<1.00	<1.00	<1.00	<1.00
Cadmium	0.01*	<0.10	<0.10	<0.10	<0.10
Chromium	0.05*	<0.50	<0.50	<0.50	<0.50
Lead	0.05*	<0.50	<0.50	<0.50	<0.50
Mercury	0.002*	<0.004	<0.004	<0.004	<0.004
Selenium	0.01*	<0.05	<0.05	<0.05	<0.05
Silver	0.05*	<0.20	<0.20	<0.20	<0.20
Nickel	0.35	<0.50	<0.50	<0.50	<0.50
7-Day Water Leach (Texas Method) (mg/l)					
Arsenic	0.05*	0.650	0.5650	0.4000	<0.1137
Barium	1.00*	<0.1000	<0.1000	<0.1000	<0.5750
Cadmium	0.01*	0.0267	0.0175	0.0375	0.0325
Chromium	0.05*	0.1670	<0.0500	0.0625	0.1625
Lead	0.05*	0.2170	0.1125	0.2000	0.1625
Mercury	0.002*	<0.0002	<0.0002	<0.0002	<0.0005
Selenium	0.01*	0.2234	0.1575	0.1775	<0.0625
Silver	0.05*	0.0934	0.0500	0.0850	<0.0275
Nickel	0.35	0.3333	0.1250	0.3250	0.2125

* RCRA limit is 100 times this value.

Effect of S/SPL Weight Ratio on HF Emission: Exhaust gas was sampled and analyzed at variable S/SPL weight ratios (runs 8-10, see Table 2), in which A/SPL weight ratio was kept constant and equal to 3:1.

As expected, increasing the molar ratio of calcium to fluorine lowered HF emission. The capture of HF by limestone can be described simply as:

$$CaCO_3 \xrightarrow{850°C} CaO + CO_2 \quad (1)$$

$$CaO + 2\,HF \rightarrow CaF_2 + H_2O \quad (2)$$

HF concentration in the exhaust gas is plotted versus Ca/F molar ratio in Figure 5. HF emission decreases more or less linearly with increasing Ca/F molar ratio. This is not surprising for a diffusion–limited process in which the reaction rate is proportional to the availability of CaO reactive sites.

The high lime requirements for control of fluoride ion leachability implies, as an ineluctable consequence, excellent HF emission control. (See Ash Analysis below.)

Ash Analysis: Fly ash and bottom ash samples from two representative FBC runs (at 850°C, A/SPL and S/SPL weight ratios of 3:1 and 1:1, respectively) were collected for analysis. Results from this analysis is presented in Table 3, in which the analytical analysis of ash samples are presented in the first part, and the leachability analysis of different contaminants is presented in the second. Various leach techniques were employed including EP Toxicity, ASTM, and Texas distilled water leaches. Results from the Texas method represent the average of 4 samples. The EPA drinking water standards and RCRA limits for each concentration are also presented. One can note clearly that:

1. From the analytical analysis of the ash, concentration of all components, except sulfide are higher in the fly ash than in the bottom ash. This could be attributed to elutriation of unburned fine particles. Recycling of these particles or increasing the residence time of the waste in the bed can improve already acceptable concentrations.
2. Fluoride, cyanide and metals concentration in the ash leachate are well below RCRA standards. (Lime is thought to play a role in immobilizing metals.)
3. Concentration of metals are generally higher in the EP leachates than in the Texas leachates. This may be due to the requirement in the test for adjustment to a pH of 5 prior to steeping.

Nature of Agglomerate Interstitial Glue: The agglomerate produced by run 1 (without additive, see Table 2) was studied by x-ray diffraction and SEM. Analysis shows that the glue is composed of approximately 51% F, 30% Na, 16% Al, and traces of Ca and others, suggesting

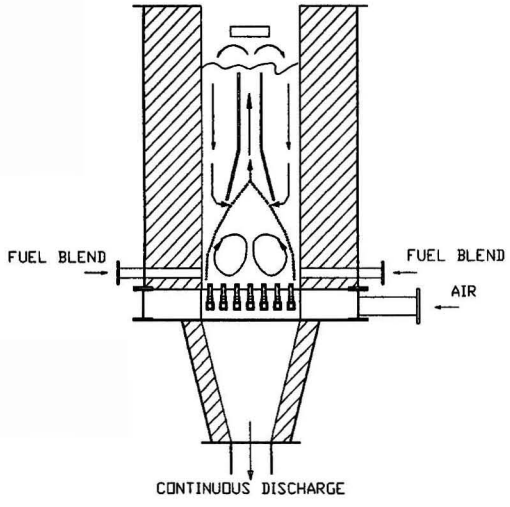

Figure 6. Internal circulating bed and continuous removal of oversized materials.

that F, Na, and Al are the most important components causing bed agglomeration.

COMBUSTION CHAMBER DESIGN STUDY

Fluidized Bed Combustion chamber design is particularly important when burning SPL and low-grade fuels with similar softening characteristics.

The cause of ash agglomeration can be described as a consequence of localized excessive temperature within the combustion zone compared to the ash fusion temperature. Of course, poor design of the combustion chamber can lead to an excursion of temperature. In such a system a waste particle, when injected, instead of being rapidly dispersed in the support solid, can sink and build up near the bottom of the bed creating a zone in which heat generated by combustion of the fuel element is higher than the heat transfer rate to the surrounding area via incomplete mixing, leading to hot spots. The localized exotherm causes fusion of the ash.

Good mixing of fresh fuel, waste, additive, and spent ash particles in the combustion chamber is evidently of primary importance in firing SPL. Segregation of these particles—on the contrary—is believed to be a major contributing cause of agglomeration. To minimize the agglomeration problem, a combination of internal circulation of the dense phase—allowing good mixing and even distribution of fresh feed—and an effective *in situ* agglomerate withdrawal system should be considered.

Internal Circulating Bed: Despite successful small-scale test burns in a spouted bed, the later is not recommended for commercial application. The main disadvantage of a spouted bed is, that despite its highly turbulent central zone, the remaining part is relatively stagnant. This poor gas-solid contacting zone can be devastating for such low-fusion-temperature fuels as SPL. For this purpose, an advanced fluidized bed, within which coexist good gas–solid contacting of a smoothly bubbling bed and an intensely active zone similar to a spouted bed is required. To enhance the degree of mixing of fresh waste particles and promote smooth dense–phase circulation of the bed materials, installation of a central fast riser within the bed is proposed.

It is well established that bubble behavior is the main phenomena governing solid mixing in a fluidized bed layer. Solids are carried upward by the wake and drift of a rising bubble. The downward movement of solid consequently occurs elsewhere, in bubble–free regions. It is also well known that bubble distribution is not uniform across a horizontal section. It has been found that they form preferentially close to the wall and gather upward toward the central axis by oblique coalescence at approximately one bed diameter from the distributor. This natural hydrodynamic property of bubbles induces in a deep bed an upward movement of the dense–phase along the central axis between approximately one bed diameter from the distributor and the top of the bed. Once the bubble bursts the surface, solids are spread out and start descending in the bubble–free region close to the wall. At approximately one bed diameter from the distributor, the downward flow of emulsion moves inward and solids are redistributed. In the bed area below the riser, solids move in an inward circulating pattern. The overall circulation pattern of solids is better known as "gulf stream" effect [*11, 12*]. Superimposed on this overall effect is significant random motion due to passing bubble–a characteristic of fluidization.

To take advantage of this hydrodynamic effect, a relatively deep bed must be used. A central fast riser with a divergent bottom has proven to enhance the "gulf stream" effect and accelerate circulation. Figure 6 shows the central fast riser with the preferential bubble and solid patterns. Different shapes and designs of the riser are proposed. Design and installation detail can be found elsewhere [*13*].

Continuous Removal of Oversized Materials: If agglomerates are formed during operation their difference in size and density, when compared to the bed material, will cause segregation. These agglomerates need to be removed as they are formed. An effective withdrawal system is required. A system of air distribution by parallel air headers with approximately 50% opening is presented in Figure 6. Pressurized air is first introduced to an annular air plenum, then through parallel air headers, and finally is released to the combustion layer via standpipes. The high percentage of opening assures efficient (instantaneous and even) removal of agglomerates. Spacing between air headers is also an important parameter: It must be large enough to allow passage of any agglomerate formed but small enough to ensure homogeneous repartition of the fluidizing air.

ECONOMIC STUDY

The process of incinerating SPL by FBC and offering the ash to a cement kiln is particularly attractive. Beside the benefits provided by FBC discussed in the first part of this work (recovery of energy while destroying the waste) the byproduct ash generated through this process may also have viable asset value. When used as an additive in cement manufacturing, the byproduct ash presented multiple benefits:

Fuel Saving: The byproduct ash can lower the clinkering temperature (the operating temperature of the kiln). Moreover, limestone from the FBC is precalcined prior to kiln entry, further lowering the energy requirement.

Increased Product Throughput: Byproduct ash accelerates clinker formation and calcination reactions, thereby more product can be made per unit of fuel consumed.

Fluoroaluminate Content: The high fluoride and alumina content of the ash provided allows the cement manufacturer to take advantage of the fluoroaluminate phase for cement with high early–strength development.

An economic model was developed to ascertain the economics of a FBC facility serving an existing cement kiln for SPL management. In this model SPL, additive,

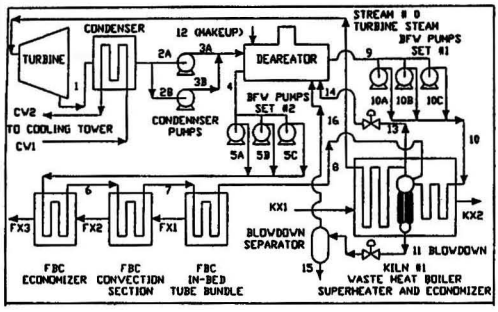

Figure 7. Facility steam loop schematic.

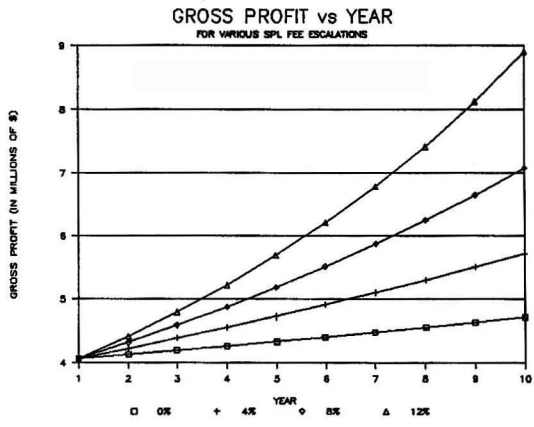

Figure 8. Gross profit versus year for various SPL fee escalations.

and sorbent are incinerated by FBC. Byproduct ash from FBC is provided free to the cement kiln. Heat from the FBC and from the cement kiln is recovered for generating electricity through a turbine generator. A steam loop schematic of the facility is presented in Figure 7. All facility equipment is assumed new except the existing kiln. The heat balance of this facility is presented in Table 4. Assuming a turbine generator efficiency is 75%, 122,400 MJ/hr is needed (of which 57,300 MJ/hr is supplied from the FBC) for generating 9.44 MW electricity.

A complete investigation of this economic model has been performed, based on a weight ratio of additive and sorbent versus SPL of 3:1 and 1:1 respectively.

Assumptions have been made as close as possible to data given by a cement kiln. Two major parameters of this economic model are: (1) the commodity annual cost escalation, and (2) the SPL management cost escalation. While the first one is relatively easy to assign, the second one, directly associated to the degree of severity in applying the newly-established law declaring SPL as hazardous, is more subtle to suppose.

Expenses, revenues, and profits of this FBC facility and kiln, versus kiln alone, are calculated for 10 years assuming annual escalation cost of 4%. Results show that the major source of revenue is from the generation of electrical power. In Figure 8, total profit is plotted versus year for various SPL annual management cost escalators (with fixed commodity escalation factors = 4%). From this figure, profit of this process is clear. Even with a 0% increase in the management cost of SPL, the profit is still substantial.

TABLE 4. CEMENT PLANT HEAT BALANCE.

Stream #	Mass Rate (Kg/Hr)	Enthalpy (KJ/Kg)	Press (10^3 Pa)	Temp (°K)	Energy (10^3 MJ/Hr)
0 Super heated	36343	3367.9	6205	755	122.4
1 Turbine Exhaust	36343	2583.7	10	320	93.9
2 Condensate	36343	195.4	10	320	7.1
3 Deaerator Feed	36343	195.4	138	320	7.1
4 FBC BFW Low Pr	22680	458.5	138	382	10.4
5 FBC BFW High Pr	22680	467.4	8618	384	10.6
6 Economiser Exit	22680	784.8	8446	460	17.8
7 Convection Exit	22680	1278.7	7584	578	29.0
8 FBC Tube Bundle	22680	2526.4	6550	554	57.3
9 Kiln BFW Low	18416	456.1	138	382	8.4
10 Kiln BFW High	18416	461.5	6550	384	8.5
11 Blowdown	454	1101.3	6550	551	0.5
12 Makeup Water	324	92.6	138	300	0.03
13 De-Air Stm High	4300	2767.4	6550	554	11.9
14 De-Air Stm Low	4300	2139.5	138	382	9.2
15 Blowdown Liquid	324	455.9	138	382	0.1
16 Blowdown Vapor	130	2307.7	138	382	0.3
0 Theoretical	36343	3367.9	6205	755	122.4
KX1 Kiln 1 Exhaust	164844			839	
KX2 Boiler Exhaust	164844			478	
FX1 FBC Exhaust	23586			1089	
FX2 Conv. Exhaust	23586			700	
FX3 Econ. Exhaust	23586			433	
FBC Economiser Thermal Output					7.2
FBC Convective Thermal Output					11.2
In-Bed Bundle Thermal Output					28.3
Kiln 1 Boiler etc. Thermal Output					69.3
Condenser Pump Work					0.004
Condenser Heat Duty (calculated)					86.9
BFW Pump Set 1 Work					0.14
BFW Pump Set 2 Work					0.24
Percent Breakdown			0.89%		
Assumed Turbine-Generator Efficiency			75.00%		
Electrical Output			9444.634 KW		

CONCLUSIONS

Experimental data from bench–scale studies indicate that SPL can be destroyed safely by spouted bed and by fluidized bed combustors via modification of ash chemistry.

X-ray and electron micrographs reveal that the "glue" found in agglomerates formed during combustion of SPL is composed of approximately 51% F, 30% Na and 16% Al. These components are thought to cause bed agglomeration.

The ash agglomeration temperature is increased from 770°C to 950°C by using an appropriate additive in an additive: SPL weight ratio of 3:1.

As expected, increasing the molar ratio of calcium to fluorine lowered HF emissions. HF emissions decreases more–or–less linearly with increasing Ca/F molar ratio.

Fluoride concentration in the leachate decreases sharply with increasing Ca/F molar ratio.

Beside the important role of additives and ash chemistry, hydrodynamics of the FBC should not be neglected in burning SPL and similar low–melting wastes. A combination of an internal dense–phase recirculation system (allowing mixing and even distribution of the fresh feed), and an effective withdrawal system (allowing elimination of agglomerates as they are formed) is considered critical in system design.

The advantage of applying FBC of SPL to a cement kiln is clear. While the benefit from byproduct ash is not considered, the economic model shows that the main resource is from generation of electrical power.

ACKNOWLEDGMENT

The authors acknowledge support of Turnpoint Engineering Corporation and the U.S. Department of Energy.

LITERATURE CITED

1. Environmental Protection Agency, *Federal Register*, **40**, CFR Parts 261 and 302, September, 1988.
2. Blayden, L. C., and S. G. Epstein, "Spent potlining symposium", *Journal of Metals*, **36**, 22 (1984).
3. Yaverbaum, L., *Fluidized Bed Combustion of Coal and Waste Materials*, Noyes Data Corporation, USA (1977).
4. Liao, P. B., *Journal WPCF*, **46**, No. 8, 1895 (1974).
5. Ho, T. C., Paul Ku, and J. R. Hopper, *AIChE Symp. Ser.*, 262, **84**, 126 (1988).
6. Cammarota, A., *M. D'Amore, G. Donsi, and L. Massimilla, 18th Symposium on Combustion*, The Combustion Institute, Pittsburgh, PA, 257 (1980).
7. Drake, R. N., "Fluidized Bed Combustion of Spent Potlining", Final report to The Aluminum Association, GA Technologies (1984).
8. GA Technologies, "Circulating Bed Combustion of Spent Potlining." Test report prepared for The Aluminum Association. GA Project 2555 (1985).
9. Rozelle, P. L., and A. W. Scaroni, "Bed Agglomeration and Ash Disposal for Anthracite–fired Fluidized Bed Combustors," *The 9th International Conference on Fluidized Bed Combustion* (1987).
10. Vora, M. K., W. A. Sandstrom, and A. G. Rehmat, "Ash agglomeration in Fluidized bed," *6th Natl. Conf. on Energy and Env.*, Pittsburgh, Pa (1979).
11. Masson, H. A., *Fluidized Bed Combustion*, Ed Radovanovic, Hemisphere Publishing Corporation (1986).
12. Grace J. R., *Fluidized Bed Boilers: Design and Application*, Ed. Prabir Basu, Pergamon Press (1984).
13. Tabery, R. S., and K. Dangtran, "Fluidized Bed Combustion of Aluminum Smelting Waste," U.S. Patent serial number 242,526, Submitted Sept. 1988.

International Conference on Pollution Prevention: Clean Technologies and Clean Products—The Environmental Challenge of the 1990s

A 3-day international conference examining the issues and technologies related to pollution prevention. Innovative technologies will be featured. The current status and future directions of various efforts by government and industry will be presented and explored.

June 10-13, 1990, the Omni Shoreham Hotel, Washington, DC.

Organized by the U.S. Environmental Protection Agency (EPA) and the International Association for Clean Technology (IACT).

Co-sponsored by major national and international agencies and organizations including the U.S. Department of Energy (DOE), the U.S. Department of Defense (DOD), the United Nations Environment Programme (UNEP), and the United Nations Industrial Development Organization (UNIDO).

Major Topics for the Conference

- National and International Policy and Regulatory Issues
- Research and Development and Applications
  - Clean Products
  - Clean Technologies
  - Source Reduction
  - Recycle and Reuse
  - Product Modification and Materials Substitution
- Incentives for Pollution Prevention
- Education and Information Exchange
- Role of National and International Organizations
- Global Pollution Prevention Issues
- Reduction of Radioactive Wastes and Radioactive/Hazardous—Mixed Wastes
- Technology Application and Case Histories

Help fill 100 Million vacancies by 1992.

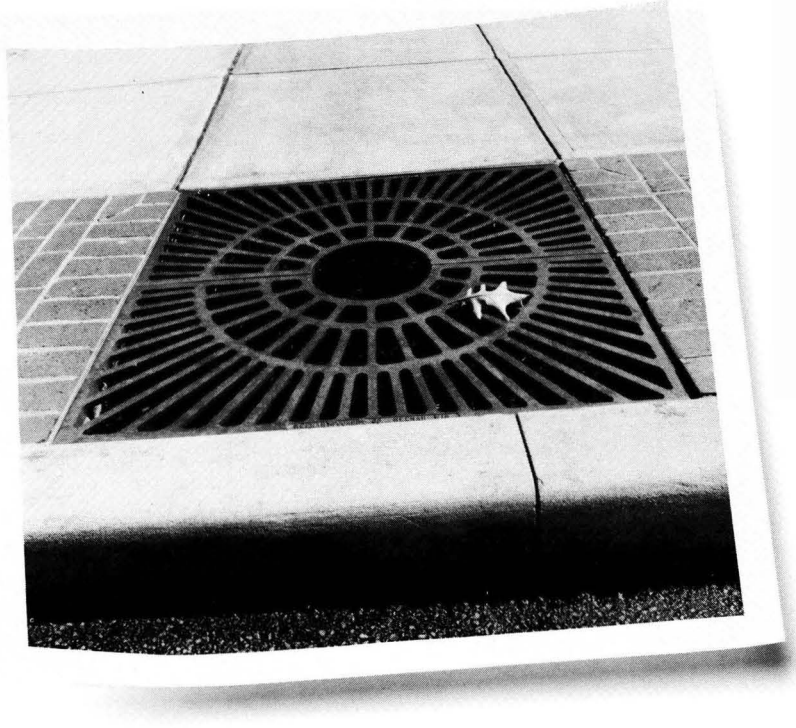

What can you do to help solve environmental problems? Join other Americans across the country in planting trees. You'll be shading your community and reducing heat-trapping CO_2 build-up in the earth's atmosphere. And, you'll be doing your part for Global ReLeaf.

There are at least 100 million tree planting sites available around our homes, towns and cities. And it's time these vacancies were filled. Planting trees is something you can do, right now, to make a difference in your community and the world.

This is just one of the goals of our Global ReLeaf campaign. Can it be done? Certainly. But not without *your* support. For more information on how you can help, write Global ReLeaf, American Forestry Association, P.O. Box 2000, Dept. GR1, Washington, DC 20013.

GLOBAL RELEAF

You can make a world of difference.

find information fast

document delivery

fast precise searches

ESL information services

save time and money

online information retrieval

comprehensive bibliographies

ESL Information Services addresses the special needs of the Engineering and Technological community. Through the DIALOG information retrieval system, we can survey 'online' 15 years of the worldwide engineering and scientific literature in a few minutes at costs that are a fraction of manual searches.

WHAT ESL INFORMATION SERVICES HAS TO OFFER YOU

- Fast precise searches of the Engineering Literature
- Immediate access to engineering journals, numerous conference proceedings, reports, and books
- Over 65 databases covering engineering, physics, computers, energy, materials, patents, and chemistry
- Flexible and extensive search terms - authors, title words, subject categories, chemical abstracts register numbers
- More for your money and time... save hours of library research over manual techniques
- Document delivery... tap the vast resources of the Engineering Societies Library's engineering and technological literature... over 5000 serials from some 50 countries in 25 languages

For more information on this indispensable research tool, please call or write:

ESL Information Services

Engineering Societies Library

345 East 47th Street New York, New York 10017 (212) 705-7610